Hypothalamic Transcriptional Profiling and Quantitative Proteomics of Mice under 24-Hour Fasting

Hao Jiang

Dissertation submitted to the faculty of the Virginia Polytechnic Institute and State University in partial fulfillment of the requirements for the degree of

Doctor of Philosophy

In

Biochemistry

Deborah J. Good, Chair

Bin Xu

Richard F. Helm

Roderick V. Jensen

May 6, 2014

Blacksburg, VA

Keywords: microarray, quantitative proteomics, Nhlh2, hypothalamus, fasting

Hypothalamic Transcriptional Profiling and Quantitative Proteomics of Mice under 24-Hour Fasting

Hao Jiang

Abstract

Energy balance includes energy intake and energy expenditure. Either excessive food intake or insufficient physical activity will increase the body mass and cause obesity, a worldwide health problem. In the US, more than two-thirds of people are obesity or overweight. Conversely, it is well accepted that reducing energy intake can increase the life span and the resistance to age-related diseases. MicroRNAs are highly conserved non-coding RNA molecules with a length of 21-23 nucleotides. Recent studies show that numerous microRNAs are associated with the regulation of oxidative stress, inflammation, insulin signaling, apoptosis, and angiogenesis that relate to obesity. However, the role of microRNAs in the regulation of energy balance in central nervous system remains unknown, especially within the hypothalamus, a primary site of energy balance control. In this project, microRNA, and mRNA were profiled using microarray technology. Furthermore, quantitative proteomics were used to identify differential protein levels during fasting, and in a genetically obese mouse model, Mice were given either a 24-hour fast, or *ad libitum* access to food. Hypothalamic RNA and microRNA samples were analyzed by microarray, using both the Affymetrix and Toray 3D mRNA and microRNA platforms. No microRNAs were found to be differentially expressed between two treatments, whereas numerous mRNAs were significantly regulated by fasting, including 7 cell cycle related genes. Hypothalamic protein samples from WT and N2KO mice treated either to *ad lib* feeding or 24-hour fasting were analyzed by MS^E quantitative proteomics. Over 650 proteins were identified with some proteins showing significantly different abundances between or among the four

groups. Between *ad lib fed* WT and N2KO mice, 53 proteins were differentially expressed, with some of these linked to neurodegeneration, NAD synthesis, and the citrate acid cycle (TCA). Overall, the results of this study suggest that while microRNA-mediated mechanisms are not significant modulators of hypothalamic gene expression upon a 24 hour fast, cell cycle gene expression changes represent a major contributor to the fasting response. Moreover, Nlhl2 might play an important role in the neurodegeneration and mitochondrial metabolism.

Table of Contents

List of Figures

List of Tables

Chapter 1

Introduction

The basic components of energy balance include energy intake, energy expenditure, and energy storage. Either excessive food intake or insufficient physical activity will cause a state of positive energy balance, which can increase the body mass and finally cause obesity, a major global epidemic. In the United States, with more than two-thirds of Americans now overweight, with obesity constituting a leading cause of mortality, morbidity, disability, healthcare utilization and healthcare costs (Hammond & Levine 2010). It is generally accepted that energy restriction is a common strategy for treating obesity (Hill et al 2012). Studies also show that reduced energy intake has profound positive effects on the health and longevity of laboratory animals (Mattson 2005).

Over 70 years ago, McCay and colleagues reported that reducing energy intake can increase the life span of rodents. Since then, the influence of dietary factors on life span and age-related disease has become an active and important field of biological and biomedical research (Moraes et al 2009). A large number of studies suggested that intermittent fasting (IF) and caloric restriction (CR) extend lifespan and increase resistance to age-related diseases in rodents (Levine & Levine 2012, Lopez-Dominguez et al 2013, Sun et al 2013, Urbanski et al 2013), monkeys (Mattson & Wan 2005), and humans (Bodkin et al 2003). This is probably due to the fact that IF and CR can reduce levels of oxidative stress and protect proteins, lipids, and DNA form oxidative damage (Mattison et al 2003), and further contribute to protect against diabetes, cardiovascular disease, cancers (Sohal & Weindruch 1996), and neurodegenerative diseases (Mattson et al 2002). However, the cellular and

molecular mechanisms remain poorly understood. Studies in our laboratory are attempting to elucidate the cellular and molecular mechanisms associated fasting, with emphasis on the energy balance control mechanisms in the hypothalamus, and the possible link of these pathways to obesity.

The hypothalamus is a primary site of energy balance control. Anorexigenic (appetite suppressing) pro-opiomelanocortin (POMC) neurons and orexigenic (appetite promoting) neuropeptide Y (NPY) neurons within the hypothalamus are particularly important in energy balance control, and directly regulate feeding. Other area of the hypothalalmus, such as the paraventricular thyrotropin-releasing hormone (TRH) neurons regulate energy expenditure through the thyroid axis, while the numerous ventral medial hypothalamic apparently regulate hunger and feelings of fullness. What is not yet clear is how the hypothalamus, as a whole responds to IF or CR, and this is of clinical, pharmaceutical, and societal importance. Based on studies showing that IF and CR can prolong the health-span of the nervous system (Mattson & Wan 2005) and conversely that high-fat diet can induce apoptosis of hypothalamic neurons (Martin et al 2006), these findings suggest that balance between neurogenesis and neuron apoptosis in the hypothalamus may play an important role in the energy balance (Kokoeva et al 2005, Martin et al 2006).

Nescient helix-loop-helix 2 (Nhlh2) is a member of the basic helix-loop-helix (bHLH) transcription factor family which has been found in POMC neurons and TRH neurons in the hypothalamus (Jing et al 2004). Nhlh2 binds to E-box sequences (CANNTG) and form heterodimers with other transcription factors to regulate the expression of genes, such as necdin, and prohormone convertase 1/3 (PC1/3) (Fox & Good 2008, Kruger et al 2004).

More importantly, Nhlh2 is one the only two genes that are genetically linked to physical activity levels (Good & Braun 2013). In Nhlh2 knockout mice (N2KO), the deletion of Nhlh2 leads to adult onset obesity due to the reduced physical activity levels (Coyle et al 2002). While levels of the mature neuropeptides, αMSH and ACTH, are reduced due to Nhlh2's regulation of the mRNA for the neuropeptide processing enzyme, PC1/3 (Fox & Good 2008), there is no overt hyperphagia in these animals. It is believed that the lack of these fully processed neuropeptides is at least one cause of adult-onset obesity in these animals, possibly through the PVN axis and melanocortin regulation of physical activity (Good and Braun, 2013). Thus, use of N2KO mice in these experiments allows us to study energy balance through physical activity levels, in the absence of overt food intake changes.

MicroRNAs are highly conserved non-coding RNA molecules with a length of 21-23 nucleotides. These small RNAs bind to the target sequence of their regulated mRNAs and regulate protein translation or mRNA stability. Recent studies show that numerous microRNAs are associated with the regulation of oxidative stress, inflammation, insulin signaling, apoptosis, and angiogenesis that relate to obesity (Hulsmans et al 2011, Xie et al 2009). For example, miRNA-143 inhibits insulin-stimulated AKT activation and impairs glucose metabolism, and therefore contributes to the development of obesity-associated insulin resistance (Jordan et al 2011). In the brain, many microRNAs are expressed in a cell type specific patterns and are believed to be essential for neuronal development, survival, function, and plasticity (Vreugdenhil & Berezikov 2010). In fact, multiple studies have shown that microRNAs in the brain are implicated with many aspects of neural development and function, such as neurogenesis and synaptic plasticity (Chiu et al 2014, Numakawa et al

2011, Schouten et al 2013, Wulczyn et al 2007). In particular, studies suggest that microRNAs can be used as biomarkers for neural development, process of function, and neurological diseases (Rao et al 2013). In support of their possible role in energy balance, microRNAs can regulate brain-derived neurotropic factor (BNDF) (Numakawa et al 2011) which is regulated by energy availability via melanocortin-4 receptor signaling. Furthermore, several studies also suggest that microRNAs can regulate neuronal plasticity (Earls et al 2014, Schouten et al 2013), where neuronal plasticity is considered as a component in the hypothalamic control of energy balance (Dietrich & Horvath 2013). However, no direct evidence has related changes in microRNAs expression to the energy balance control mechanisms within the hypothalamus.

Within the hypothalamus, there are total of 2,630 genes with postnatal expression in multiple neuronal subtypes (http://www.informatics.jax.org/). Accumulated evidence has reported that many of these genes are required for the regulation of energy balance and body weight (Morton et al 2006, Woods & D'Alessio 2008). As discussed previously, the anorexigenic POMC neurons, along with the orexigenic NPY neurons are two neuronal populations which have potent functions on the regulation of energy balance. Over last few decades, genetic approaches have been used to explore these energy balance pathways in the hypothalamus. Genetic studies have reported monogenic changes in POMC, and melanocortin pathway genes that lead to differential regulation of energy balance and obesity (Yeo & Heisler 2012). In addition, using high-throughput transcriptional profiling methods, several studies have identified a large number of genes that respond to differential energy availabilities within the hypothalamus (Jovanovic et al 2010, Yang et al 2004). However,

there is still a need to utilize new technologies and platforms to identify other global changes in the hypothalamic transcriptome.

While multiple studies have examined the hypothalamic transcriptome, only a few have attempted to identify the hypothalamic proteome and its response to fasting. Protein abundance is independent of transcriptional control, due to such issues as post-transcriptional, translational and degradation regulation of amount of proteins (Vogel & Marcotte 2012). MicroRNAs are expected to control more than 60% of all protein-coding genes by base-paring to target mRNAs in mammals (Ebert & Sharp 2012), so an understanding of the proteome, along with the microRNA-ome is a needed contribution to the literature. A meta-analysis combined data from literatures and available databases has collected a total of 1,515 protein-coding genes and 221 microRNAs that are associated with obesity (Kunej 2012). However, the subsets of these that change in the hypothalamus have not been described. Overall, it is expected that there are a multitude of changes that occur in the hypothalamic proteome in response to energy availability, but only very few studies using outdated technologies have contributed to characterization of hypothalamic proteome in response to energy availability (Kuhla, Kuhla et al. 2007). Use of new quantitative proteomic data is needed to fully identify the hypothalamic proteome and its differential expression with fasting.

In this study, the regulation of energy balance in the hypothalamus and its response to short-term fasting was examined using microRNA array, exon array, and mass spectrometry based quantitative proteomics. Hypothalamic microRNA levels, mRNA levels, and protein levels between *ad libitum* (*ad lib*) fed and 24 hour fasting mice, as well as between wild type

and genetically obese (N2KO) mice were identified, and confirmed using secondary analyses. Pathway analysis of the datasets was then used to identify new gene groups and signaling pathways participating in the hypothalamic response to fasting.

Chapter 2

Specific Aims

Energy balance is regulated by food intake and energy expenditure via a homeostatic system in the central nervous system (CNS). Excessive energy intake and meal frequency, as well as insufficient physical activity will lead the increasing of the body mass and result in obesity, a major health problem in the United States with nearly two-thirds of Americans are either obese or overweight (Hammond & Levine 2010). Solid evidences suggest that IF and CR can increase extend lifespan and can increase disease resistance in rodent and monkey (Mattison et al 2003, Mattson et al 2002, Mattson & Wan 2005). It is hypothesized that both IF and CR have potential benefits in the prevention and treatment of many diseases, such as obesity, diabetes, cancer, and neurodegeneration (Longo & Mattson 2014, Speakman & Mitchell 2011, Varady & Hellerstein 2007). In fact, clinical trials on humans indicate that both IF and CR provide some beneficial effects (Speakman & Mitchell 2011, Varady & Hellerstein 2007). However, with possible side effects, such as sleeping disorder, anxiety, and irritability, more research would be needed. To further understanding the precise mechanisms and the role of the hypothalamus in response to fasting, here we test the hypothesis that regulation of hypothalamic microRNA, mRNA, and protein levels occurs under short-term fasting, using the following specific aims:

1. To determine if hypothalamic microRNAs levels are altered in response to short-term fasting.

Many microRNAs are differentially expressed in several brain disorders, including neuronal cancers and neurodegeneration (Fassan et al 2011, Roshan et al 2009). There are

also studies that demonstrate a role for microRNAs in more normal physiological processes, such as learning, synaptic plasticity, and neuroadaptation (McNeill & Van Vactor 2012). Although many differentially-expressed hypothalamic mRNAs have been identified in rodent-based studies using the food deprivation/feeding paradigm (Poplawski et al 2010), the global expression of microRNAs that responses to changes in energy availability has not yet been reported. Therefore, in this specific aim we ask the following question: Are hypothalamic microRNA levels modulated in the response to short-term fasting?

2. To identify potential targets of fasting-regulated microRNAs on gene level using transcriptional profiling analysis.

With the high throughput transcriptional profiling methods, numerous genes have been reported to be involved in the regulation of energy balance and in response to the different energy availabilities (Jovanovic et al 2010, Yang et al 2004). However, no study has been performed on 24 hour short term fasting yet. Furthermore, the cellular and molecular mechanisms of the regulation of the transcription activity are not yet clear. In fact, microRNAs are considered to play roles in gene/protein regulation in the brain. In particular, varieties of computational tools are available for identification of putative microRNA targets. It is possible to use the high throughput transcriptional profiling method and the computational tools to identify the target genes of energy balance regulated microRNAs. In this specific aim, the following questions are asked: What hypothalamic genes are responded to the short-term fasting? Are any of these genes associated with the fasting-regulated microRNAs?

3. To determine the global changes of hypothalamic proteins in response to fasting, and to

compare the hypothalamic proteome between WT and N2KO mice.

It is expected that there are a multitude of changes that occur in the hypothalmic proteome in response to energy availability. With the lack of hypothalamic proteome data, especially quantitative data on different energy state, in this specific aim, quantitative protoemic analysis will be performed in order to identify and quantify the hypothalamic proteins that change in levels due to different energy availiablities. Addtionally, quantitative proteomic analysis of WT and N2KO mice will be also performered in order to understand the role of Nlhlh2 in the hypothalamus.

Chapter 3

Microarray analysis of mRNA and microRNA levels following food deprivation reveals a link to cell cycle genes, with no differential microRNA expression

Hao Jiang[2], Thero Modise[4], Richard Helm[2,4], Roderick V. Jensen[3] and Deborah J. Good[1,2,4]

Departments of Human Nutrition Foods and Exercise[1], Biochemistry[2], and Biological Sciences[3], and Program in Genomics, Bioinformatics and Computational Biology[4], Virginia Tech, Blacksburg, VA, 24061

Abstract

Energy restriction in mammals is associated with improved health and increased lifespan, yet the effects of fasting on global mRNA and microRNA expression are largely unknown within the hypothalamus, a central regulator of energy balance. In this study, mice were given either a 24-hour fast, or *ad libitum* access to food. RNA and microRNA samples were analyzed by microarray, using both the Affymetrix and Toray 3D mRNA and microRNA platforms. Selected mRNAs and microRNA were then assessed using quantitative real-time PCR (QPCR) for confirmation. The Toray arrays detected more differentially expressed mRNAs and microRNAs than the Affymetrix arrays. However, while 88 differentially-expressed independent microRNAs were detected by using both microarray platforms, none of the eight microRNAs, including three microRNAs identified by both platforms, were confirmed to be differentially expressed using QPCR. There were 1733 differentially regulated mRNAs between the two arrays, with enrichment analyses identifying changes in cell cycle genes. Ten cell cycle genes were analyzed using QPCR with six showing significant up-regulation, one showing down regulation, and three showing no change in response to fasting. Overall, the results of this study suggest that while microRNA-mediated mechanisms are not significant modulators of hypothalamic gene expression upon fasting, cell cycle gene expression changes represent a major contributor to the fasting response.

Keywords microRNA, fasting, food intake, neuronal, gene ontology, cell cycle, Affymetrix, Toray

1. Introduction

Over 70 years ago, McCay and colleagues reported that reducing energy intake can increase the life span of rodents (McCay et al 1989). Since then, the influence of dietary factors on life span and age-related disease has become an active and important field of biological and biomedical research. Studies done over the last decade have suggested that intermittent fasting (IF) or caloric restriction (CR) can extend lifespan and increase resistance to age-related diseases in rodents (Weindruch & Sohal 1997), monkeys (Bodkin et al 2003, Mattson & Wan 2005), and humans (Mattison et al 2003). IF and CR can reduce levels of oxidative stress and protect proteins, lipids, and DNA form oxidative damage (Mattson et al 2002), thereby possibly contributing to cellular protection against diabetes, cardiovascular disease, cancers, and neurodegenerative diseases (Mattson 2005, Sohal & Weindruch 1996). However, even today, the cellular and molecular mechanisms underlying the response to food restriction, especially within the nervous system, remain poorly defined.

The hypothalamus integrates central nervous system control of energy balance including responses both to food deprivation and re-feeding. Within the hypothalamus, multiple neuronal subtypes respond with both cellular signaling and gene regulatory responses. According to the Mouse Genomic Informatics Gene Expression Database (http://www.informatics.jax.org/) there are 2,630 genes with postnatal expression in the mid brain region. Of these, up to 588 are transcription factors (Good 2010), potentially mediating a transcriptional response. MicroRNAs also play a role in gene/protein regulation, by repressing gene expression through an interaction with the mRNA transcript that results in either degradation or blocked translation of the mRNA. MicroRNA is differentially

expressed in several brain disorders, including neuronal cancers, and neurodegeneration (Fassan et al 2011, Roshan et al 2009). There are also studies that demonstrate a role for microRNAs in more normal physiological processes, such as learning, synaptic plasticity, and neuroadaptation (McNeill & Van Vactor 2012). Within other tissue types, studies report an association of microRNA levels in adipose tissue, under high-fat diet or obesity, and in brown fat undergoing differentiation (Martinelli et al 2010, Sun et al 2011, Takanabe et al 2008). Together, the evidence from these studies suggests that expression of hypothalamic microRNA may also change in response to normal changes in energy availability. Only 2 hypothalamic-specific microRNAs have been characterized (i.e. microRNAs that are only expressed in the hypothalamus and not in other regions of the brain), miR-7a, and the related microRNA, miR-7b (Bak et al 2008). MiR-7a expression is found in both POMC and NPY neurons (Meister et al 2013). Of 717 currently known mouse microRNAs in midbrain regions, 105 microRNAs appear to be expressed above threshold in the hypothalamus (http://www.microrna.org, searched as "midbrain" in database), with the miR-7a family, the Let-7 family, miR-124a, miR-125a, miR-136, miR-138, miR-212, miR-338, and miR-451 the most highly expressed, according to several accounts (Bak et al 2008, Meister et al 2013, Olsen et al 2009).

Many differentially-expressed hypothalamic mRNAs have been identified in rodent-based studies using the food deprivation/feeding paradigm (for example, (Poplawski et al 2010)). However, the global expression of microRNAs, as measured in response to changes in energy availability, has not yet been reported. The experiments in this study sought to identify whether any microRNAs were differentially-expressed in hypothalamic tissue

following either 24 hours of food deprivation or ad lib feeding. mRNA levels were simultaneously analyzed from the same tissue, in order to potentially identify differentially-expressed transcripts that might be targets of identified microRNAs. However, this study found no microRNA with significant changes, suggesting that global microRNA regulation may not play a significant role in the hypothalamic response to energy availability, and that transcriptional mechanisms may be the main response mechanism to fasting within the hypothalamus.

2. Experimental Procedures

2.1 Animals

The Institutional Animal Care and Use Committee at the Virginia Tech approved all studies. C57Bl/6 mice were purchased from The Jackson Laboratory as matched littermates and only male mice were used in this experiment so that estrous cycles did not have to be taken into account during fasting. All mice were maintained under 12-h light/dark cycle with free access to food and water except as noted during experimentation. At the age of 8 weeks, mice were randomly separated to either a food deprived or *ad lib* group, and food was removed for deprived mice at 9am (Figure 1A). After 24h food deprivation, mice were euthanized and hypothalami were collected and put into *RNAlater*® solution (Ambion, US) for microRNA and mRNA analysis. For a limited number of animals, gastrocnemius was collected to compare the sensitivity of our arrays for detecting tissue-specific microRNAs.

2.2 RNA isolation

The RNA was extracted using the *mir*Vana™ PARIS™ Kit (Ambion, US) according to the manufacturer's procedure without modifications. Enrichment procedure for small RNAs was performed for microRNA study. RNA integrity was tested after extraction using Experion™ system (Bio-Rad, US).

2.3 Microarray analysis

For microRNA analysis, N=3 mice for each treatment group, were analyzed on the Affymetrix GeneChip® microRNA 1.0 array and the Toray Mouse microRNA Oligo chip 16 v1.0.0 array. Affymetrix microRNA array raw data were extracted using the Affymetrix microRNA QC tool. Global normalization was used to normalize the raw data, log2 value was processed and Student's *t*-test was performed between ad lib fed and food deprived groups. To survey for candidate microRNA with differential expression, loose statistical criteria were used with cut off by *P*-value $\leq$0.05 and fold change of $\geq$ 1.3.

For mRNA analysis, a total of N=3 mice for each treatment group, which were the same from those analyzed for microRNAs, were analyzed on the Affymetrix GeneChip® Mouse Exon 1.0 ST array and the Toray 3D-Gene™ Mouse Oligo chip 24k version 1.10 array. Global normalization was used to normalize the raw data, log2 value was processed and Student's *t*-test was performed between ad lib fed and food deprived groups. To survey for candidate microRNA with differential expression, loose statistical criteria were used with cut off by *P*-value $\leq$0.05 and fold change of $\geq$ 1.3.

2.4 microRNA and mRNA Quantitative PCR (QPCR) analysis

New samples of RNA from additional mice were obtained for all confirmatory analyses, with microRNA expression levels utilizing the Taqman microRNA assay (Applied

Biosystems, Foster City, CA). For each microRNA tested, 5 ng of small RNA-enriched samples from N=5-6 mice per assay was used. Reverse transcription and QPCR were performed according to the assay manual. The expression level of sno-202 RNA was used as the normalization control. All QPCR results were compared between groups using Student's *t*-test with *P*-value $\leq$0.05 for statistical significance.

The expression levels of mRNA were measured using designed primers and the iTaq™ SYBR® Green Supermix with Rox (Bio-Rad, Hercules, CA). New total hypothalamic RNA was isolated from N=4-6 mice, and 2 μg of total RNA was subjected to reverse transcription using M-MLV Reverse Transcriptase (Promega, Madison, Wisconsin). A 20 ng aliquot of cDNA was then used for RT-PCR analysis using the ABI 7900 system (Applied Biosystems, Foster City, CA). The expression level of β-actin was used as the normalization control. All RT-PCR results were compared between groups using Student's *t*-test with *P*-value $\leq$0.05 for statistical significance.

2.5 Leptin and Glucose measurement

Whole blood was collected immediately after each mouse was euthanized. Blood glucose level was measured using FreeStyle Freedom Lite® Blood Glucose Monitoring System (Abbott Laboratories, US). The serum was collected from the whole blood sample by centrifuging at 1000 x g for 10 minutes at 4^{o}C. Serum leptin level was measured using the Mouse Leptin Quantikine ELISA kit (R&D System, US) according to the manufacturer's instructions, and using manufacturer-provided standards to produce the standard curve.

2.6 GO and STRING analysis

Gene ontology analysis was performed using GeneCodis3 (Carmona-Saez et al 2007, Nogales-Cadenas et al 2009, Tabas-Madrid et al 2012). Genes passing the cutoff of microarray analysis were used for the GO Biological Process, GO Molecular Function, GO Cellular Component, and KEGG pathways analysis. For the settings of statistical parameters, the minimum number of genes was set to 2, and a hypergeometric statistical test and FDR P-value correction were used. The results were listed with corrected hypergeometric *P*-value.

STRING version 9.1 (Franceschini et al 2013) was used in its online format to generate an interaction network using the Cell Cycle genes tested for QPCR. The confidence view was used with one expansion of the protein interactions network.

3. Results

3.1 Physiological and Comparative Measures

Following 24-hour food deprivation (Figure 1A), serum leptin and blood glucose levels for each treatment group showed a significant reduction (Figure 1B-C). Leptin levels are similar to previous reports from our laboratory for *ad lib* and food deprived mice (e.g. (Vella et al 2007) Ad lib 4378.1$\pm$561.3 pg/ml; Food deprived 2144.6$\pm$274.8 pg/ml), while glucose levels were slightly higher than expected (Ad lib 400.8 $\pm$ 30.3 mg/dl; Food deprived 150.4 $\pm$ 9.0 mg/dl), most likely due to use of frozen rather than fresh blood.

3.2 MicroRNA Microarray Analysis

In order to confirm that differences in microRNA would be detectable using the methods employed, we first used N=2 mice (*ad lib* fed) to compare hypothalamic versus skeletal muscle (gastrocnemius) microRNAs on the Affymetrix platform. The relative

expression levels were plotted revealing an exploded comet form (Figure 2A), suggestive of significant differences in expression levels of specific microRNAs between the two tissue types, as expected. Specific microRNAs were then analyzed by QPCR using tissue-specific total RNA from N=4 mice as the starting material. As shown in Figure 2B, let-7d expression was similar between both tissues, and in both conditions. Expression of the skeletal muscle-specific microRNA, miR-1, is significantly higher in skeletal muscle than in hypothalamus tissue, in both *ad lib* and fasted mice (Figure 2C). Conversely, the nervous system specific microRNA, miR-124a, is highly expressed in hypothalamic RNA isolated from fed and fasted mice, when compared to its detection at a significantly lower level in gastrocnemius RNA isolated from either mice in either treatment group (Figure 2D). These results indicate the systems can be applied to hypothalamus to assess the effects of a 24 h fast.

Three mice for each treatment were then used for microRNA expression analysis on Affymetrix and Toray microRNA microarray platforms. Using the loose statistical criteria of $P \leq 0.05$ and fold change ≥ 1.3, there were 22 differentially-expressed microRNAs identified using the Affymetrix platform with 16 up-regulated and 6 down-regulated, and 69 differentially-expressed microRNAs identified using the Toray platform with 64 up-regulated and 5 down-regulated (Table 1). Scatterplot analysis for both the Affymetrix and Toray arrays show that while there was more sensitivity, and more detectable (or identifiable) microRNAs using the Toray array, the overall expression level differences between food deprived and *ad lib* treatment groups were similar and suggestive of few differentially-regulated microRNAs, especially within the significance criteria (Figure 3). All of the differentially expressed microRNAs detected by Affymetrix and Toray arrays are shown in

Supplemental Tables 1, 2. Only 3 overlapping microRNAs, miR-30a-3p, miR-342-5p and miR-496a, were identified as significantly different between the two treatments on both platforms (Table 1). QPCR analysis was performed using microRNA isolated from N=5-6 new mice for each treatment. However, the QPCR analysis failed to confirm that these 3 microRNA were significantly different between *ad lib* and food deprived treatment groups. Five other microRNAs that had shown significant differences only on one platform, also failed to show significant differences by QPCR (Figure 4A). However, differences could be detected using skeletal muscle versus hypothalamic microRNA QPCR for the three overlapping microRNAs (Figure 4B), indicating that the probe sets used could have detected differences by QPCR had they existed in the hypothalamic samples.

3.3 mRNA Microarray Analysis

Both Toray and Affymetrix arrays were used to identify differentially-expressed hypothalamic mRNAs between *ad lib* fed and food deprived animals. Similar to the results using the microRNA arrays, the Affymetrix platform identified fewer differentially-expressed mRNAs (540) relative to the Toray platform (1308) (Table 2), using the statistical criteria of $P \leq 0.05$, and a fold change of ≥ 1.3. There were 115 overlapping genes between the two arrays. Scatterplot analysis for both array platforms again shows the increased sensitivity of the Toray platform, as well as the increased number of genes within the criteria designations detected using the Toray platform (Figure 5). The top 15 mRNAs up-regulated with fasting, as well as the top 5 mRNAs down-regulated with food deprivation are listed in Supplemental Table 3, but only Cdkn1a is listed for both arrays. Therefore differentially expressed genes were selected for further analysis by QPCR, based on probable role in energy balance

regulation, or brain function, and differential expression on both platforms beyond the top candidates. As shown in Figure 6, most genes chosen using these criteria were significantly differentially-expressed in independent samples isolated from *ad lib* and food deprived animals. Of nine genes selected as up-regulated in fasting, six of these changes were confirmed, with similar fold-expression level, by QPCR. Likewise, of ten genes chosen in the down-regulated category, five of these were confirmed to be down-regulated following a 24-hour food deprivation.

3.4 Gene Ontology Analysis

Gene Ontology (GO) analysis was performed to determine if the top differentially-regulated genes were highly represented in any GO category. Only genes meeting the cut-off criteria were used in this analysis. As shown in Table 3, which displays the top 5 GO categories for each of the major component or process categories, the Affymetrix and Toray platforms identified different top GO candidates with only occasional overlap in the top 5 for each category. However, close examination of the entire dataset revealed that categories related to cell cycle were found multiple times for both platforms with significant *P* values (Table 4). In all, seven categories relating to cell cycle and/or apoptosis were found using the Affymetrix array data, while 15 categories were found using the Toray array data. A subset of genes found in cell cycle categories from both platforms were further analyzed using QPCR. Of 10 cell cycle category genes analyzed, seven were confirmed to be differentially-regulated in new hypothalamic mRNA samples from *ad lib* and food deprived animals (Figure 7A). Of these, five comprise a network of protein products involved in cell cycle

control, and all of the five, except rock1 showed significantly different expression by QPCR (Figure 7B).

4. Discussion

The results of this study yield two major findings. First, after a 24 h fast, the microRNAs response is minimal. Second, there are multiple mRNAs differentially expressed following food deprivation, and of these, mRNAs within the cell cycle categories are prominent. As noted, multiple pathways, including, phosphorylation, stress response and specific enzyme categories are also significantly changed in these conditions. In addition to the two major findings, the study compares two different array platforms and offers perspective on use of each for global microRNA and mRNA analysis.

Several recent reports compare microarray platforms for different systems (both microRNA and mRNA) finding that each array platform has different strengths and weaknesses. In a 2007 article, the Microarray Quality Control (MAQC) Consortium showed that in a comparison of five different mRNA arrays up to 30% of genes were inconsistently expressed between platforms (Clark et al 2007). In another report by Del Vescovo and colleagues, Affymetrix and Agilent microRNA arrays were compared in lung tissue from wild type and lung-cancer prone transgenic rats (Del Vescovo et al 2013). They found a considerable number of discrepancies across platforms, with some differentially regulated microRNAs not detected on one or the other platform. For example, miR-433 was detected on Affymetrix and by QPCR as significantly differentially expressed, but not detected at all by the Agilent platform, while the opposite was true for miR-21 and miR-46b—both significant on Agilent and by QPCR but not on the Affymetrix array (Del Vescovo et al

2013). A study comparing Toray microRNA arrays with four other array platforms (but not Affymetrix) concluded that microRNA platforms generally have high intraplatform repeatability, with Toray and Agilent scoring highest (Sato et al 2009). However, none of the platforms tested by this group showed high interplatform concordance, which appears to be a common finding for the microRNA arrays.

Our study reports a comparison between Affymetrix and Toray arrays for both microRNA and mRNA expression. Like previous comparative reports, we found non-concordance between the total number of differentially-expressed genes and microRNAs identified by both platforms, with Toray generally identifying more differentially expressed probes, and with a higher signal-to-noise intensity, than Affymetrix. For microRNA, the two platforms differed on the total number of microRNA detected, with 503 unique microRNAs for Toray and 536 mature microRNAs for the Affymetrix array. Indeed, more differentially-expressed microRNAs were detectable on the Toray array (69) as compared to the Affymetrix array (22), with only 3 microRNAs overlapping.

For the mRNA analysis, the Affymetrix Exon array was chosen so that eventual probe level (splicing and long noncoding RNA) analysis could be done on these samples, in addition to mRNA analysis. There is coverage of approximately 40 probes per gene with all annotated murine genes present on the array. The Toray 3D-gene chip also contains all annotated murine mRNAs, using 70-mer oligonucleotides as probes, and was chosen based on reports of high sensitivity for low expression genes (Nagino et al 2006). The Toray 3D-gene chip detected more differentially-expressed mRNAs than Affymetrix in our study (1308 Toray, versus 540 Affymetrix), with 115 of these overlapping between the two platforms, and

62% of the 30 mRNAs tested confirmed by QPCR. Based on these results, we feel that use of two platforms may provide more information on true differentially expressed genes, especially when overlapped mRNAs are analyzed in follow-up QPCR analyses. For mRNA analysis, the best concordance between array and QPCR results were for those genes found to be differentially-expressed on both platforms, with 9 of the 18 genes confirmed to be differentially-expressed by QPCR originally found on both platforms.

For microRNA analysis, we found miR-1 was highly expressed in gastrocnemius compared with hypothalamus, where miR-124a showed a significantly higher expression in hypothalamus than gastrocnemius. These indicate a potential "brain-specific" microRNA expression pattern compared with skeletal muscle, which provides us specific microRNAs as markers to unveil the functions of microRNAs in the brain. However, none of the overlapping, or other significantly different microRNAs on either platform, was found by follow-up QPCR, to be differentially expressed in new tissue samples, confirming our conclusion of a lack of a microRNA response. The lack of any confirmed differentially-regulated microRNAs detectable by QPCR between hypothalami isolated from fasting and ad lib fed animals is a surprising finding, as fasting initiates a stress-related response, and microRNAs have been found to be differentially regulated in other stress/metabolic paradigms. For example, freshly isolated human fibroblasts subjected to either reduced glucose or reduced lipid conditions for 7 days showed differential expression of multiple microRNAs, compared to fibroblasts in standard media. In this study, four differentially-expressed microRNAs that were affected by either condition were confirmed by QPCR methods, and their activity in regulating target mRNA expression was further characterized

(Kalman et al 2013). Similarly, in muscle tissue, the let-7 family of microRNAs appears to regulate insulin sensitivity in animals subjected to high fat diet (Zhu et al 2011), although in our hands, let-7d is not differentially expressed in either gastrocnemius or hypothalamus in response to food deprivation of normal chow-fed animals. In addition, up-regulated expression of miR-143 is found in the adipose tissue of high-fat diet mice (Takanabe et al 2008), but our data shows no change for miR-143 in the hypothalamus. The hypothalamus may represent a unique tissue in which mechanisms other than microRNA-mediated mRNA regulation primarily play a role in the response to metabolic challenges. Alternatively, microRNA responses could have occurred as a first, and early change and were not detected at the 24-hour time point. Also, as this study represents one of the first energy-related microRNA microarray analyses focusing on hypothalamus, whole hypothalamus rather than different isolated nuclei of the hypothalamus was used. A more global analysis such as ours could result in under-representation of certain microRNA expression, especially if distinct hypothalamic nuclei have opposite regulatory responses, or if a differentially regulated microRNA is uniquely expressed in only one hypothalamic nucleus. In support of this, mRNA levels for dicer, the microRNA processing enzyme, are elevated when diet-induced obese mice are fasted for 16 hours, but returns to normal with just 4 hours of refeeding, suggesting that under these conditions, microRNA regulation may be involved in some aspects of the response to refeeding in obese mice (Schneeberger et al 2012). Much more work should be done to understanding the timing and conditions which results in a global microRNA response, including analysis at multiple time points, obese and normal weight and/or differences in specific hypothalamic nuclei.

In contrast to the microRNA results, a number of mRNAs were identified on both microarray platforms and confirmed by QPCR. We originally chose genes for QPCR confirmation analysis from the 115 overlapping mRNAs for both platforms, based also on their possible role in body weight or energy balance regulation, with an overall 60% confirmation rate. Consistent with our criteria for choosing targets for further analysis, many of these mRNAs are also differentially expressed in other energy availability paradigms. For example, Sulta1a, p21/Cdkn1a, Mt1 and Pnpla2 all have been identified as mRNAs that are differentially-regulated following calorie restriction in multiple tissue types (Swindell 2008). In our study, Sulta1a mRNA was more than 4-fold up-regulated by fasting represented one of the highest inductions. This gene has also been shown to be up-regulated fasted liver tissue (Gutierrez-Aguilar et al 2012), and was originally identified in a genome-wide screen for body weight/mass index related loci (Thorleifsson et al 2009). The protein product of the Sult1a1 mRNA catalyzes the sulfonation of neurotransmitters, and could play a role in neurotransmitter activity. Other genes that were confirmed were also involved in body weight or energy balance regulation. For example, Ddc or dopa decarboxylase catalyzes the formation of dopamine. Ddc mRNA up-regulation on both platforms was confirmed by QPCR using new samples. Up-regulation of Ddc with fasting is consistent with the role of dopamine in motivated food intake (Salamone & Correa 2013). Similarly, lower levels of mRNA for phospholipid transfer protein (Pltp) with fasting, which was confirmed on both arrays, and by QPCR, is consistent with its role in lipid transport, and the association of Pltp with obesity (Tzotzas et al 2009).

p21/Cdkn1a was one of the most significantly up-regulated genes by fasting on both platforms, and this finding was confirmed by QPCR. p21/Cdkn1a controls progression of cells through the cell cycle, by blocking cyclin-dependent kinase activity, with several published reports linking p21/Cdkn1a activity, obesity and adipose tissue (e.g. (Inoue et al 2008, Nakatsuka et al 2012)). Further examination of the dataset revealed that there were many GO categories referring to cell cycle processes in the lists of top GO categories for both Affymetrix and Toray microarrays. Interestingly, it has been reported that calorie restriction can affect cell cycle protein expression levels in liver (Cuenca et al., 2001). Based on this, we looked into whether differential regulation of other cell cycle related genes could be confirmed by QPCR and were able to confirm 7/10 of these genes in follow-up studies on new tissues. Interestingly, the link between fasting-induced up-regulation of p21/Cdkn1a has previously been made for hypothalamic tissue as well. In a 2010 study of C57Bl/6 mice undergoing a 48-hour food deprivation p21/Cdkna expression was significantly up-regulated (Poplawski et al 2010), and more recently, in a 2013 paper, liver and hypothalamus of mice fasted 24 and 48 hours showed significant induction of a p21/Cdkn1a promoter construct (Tinkum et al 2013). The linkage of fasting and cell cycle regulation by this dataset is an interesting one, given previous data on the role of ciliary neurotrophic factor in hypothalamic adult neurogenesis (Kokoeva et al 2005, McNay et al 2012).

Up-regulation of p21/cdkn1a is consistent with a blockage in cell cycle, and reduced proliferation as might occur with food deprivation. Two microRNAs, which are highly expressed on both platforms, have been shown to play a role in neuron differentiation. On the Toray array, miR-124 was significantly up-regulated by fasting, consistent with several

studies reporting that miR-124 regulates early neurogenesis and neuronal differentiation (Liu et al 2011, Yu et al 2008). However, using secondary QPCR analysis, while a slight trend for increased expression of miR-124 in fasted animals remained, a significant change in expression between treatments could not confirmed. The let-7 family was consistently highly expressed on both platforms, and although expression of the family members was not significant between treatments, it is possible that the high expression level of this family plays an important role in neuron differentiation and specification (Wulczyn et al 2007). At this time, more studies would be needed to determine if differential regulation of the p21/cdkn1a and other cell cycle regulation associated genes result in apoptosis, cell cycle arrest or some other event.

In our study, animals were food deprived for 24 hours, in order to see the maximal effects of food deprivation on gene and microRNA expression. It is known that calorie restriction in several models can increase longevity, and at least one study has examined hypothalamic gene expression in response to diet representing 60% of the calories consumed by a matched cohort (Fu et al 2006). Genes in the biological processes category of "heat" and "stress" were the most significantly changed in the calorie-restricted group (Fu et al 2006). While in our study, biological processes category such as "response to DNA damage stimulus" (GO:0006974), "oxidation-reduction process" (GO:0055114), and "lipid biosynthetic process" (GO:0008610) were found among the top groups, stress-related mRNAs such as SultA1a (Maglich et al 2004), Cirbp (De Leeuw et al 2007), Tsc22d3 (Szklarczyk et al 2012), and Txnip (McClintick et al 2013) were also found to be differentially-regulated by QPCR. As mentioned earlier, IF and CR can reduce levels of

oxidative stress and protect proteins, lipids, and DNA form oxidative damage (Mattson et al 2002), thereby possibly contributing to cellular protection against diabetes, cardiovascular disease, cancers, and neurodegenerative diseases (Mattson 2005, Sohal & Weindruch 1996), our findings represent a potential relationship between the acute and chronic effects of calorie restriction.

In summary, there is little evidence of a global microRNA response following food deprivation of 24 hour in mouse hypothalamic tissue, although the microRNAs were detectable in hypothalamus and those tested were differentially expressed when compared in skeletal muscle. It is possible that physiological stressors other than food deprivation may result in differential microRNA expression, or that the timing or use of whole hypothalamus in our analysis was not appropriate to detect the select, nuclei-specific microRNAs that were differentially-expressed following food deprivation. On the other hand, close to half of the mRNA species on the arrays were also detectable in hypothalamic tissue, and many of these were differentially-regulated in response to food deprivation. Our confirmation of a link of food deprivation to mRNAs within the cell cycle control gene ontology categories now provides new insight into hypothalamic plasticity and adult hypothalamic neurogenesis (Kokoeva et al 2005, Mainardi et al 2013). The data also promise to provide new directions in the fields of obesity, caloric restriction, and nutrigenomics, specifically in identifying possible hypothalamic gene regulatory pathways activated by food deprivation signals.

5. References

Bak M, Silahtaroglu A, Moller M, Christensen M, Rath MF, Skryabin B, Tommerup N, Kauppinen S (2008) MicroRNA expression in the adult mouse central nervous system. Rna 14:432-444.

Bodkin NL, Alexander TM, Ortmeyer HK, Johnson E, Hansen BC (2003) Mortality and morbidity in laboratory-maintained Rhesus monkeys and effects of long-term dietary restriction. The journals of gerontology Series A, Biological sciences and medical sciences 58:212-219.

Carmona-Saez P, Chagoyen M, Tirado F, Carazo JM, Pascual-Montano A (2007) GENECODIS: a web-based tool for finding significant concurrent annotations in gene lists. Genome biology 8:R3.

Chen JJ, Hsueh HM, Delongchamp RR, Lin CJ, Tsai CA (2007) Reproducibility of microarray data: a further analysis of microarray quality control (MAQC) data. BMC bioinformatics 8:412.

De Leeuw F, Zhang T, Wauquier C, Huez G, Kruys V, Gueydan C (2007) The cold-inducible RNA-binding protein migrates from the nucleus to cytoplasmic stress granules by a methylation-dependent mechanism and acts as a translational repressor. Experimental cell research 313:4130-4144.

Del Vescovo V, Meier T, Inga A, Denti MA, Borlak J (2013) A Cross-Platform Comparison of Affymetrix and Agilent Microarrays Reveals Discordant microRNA Expression in Lung Tumors of c-Raf Transgenic Mice. PloS one 8:e78870.

Fassan M, Sachsenmeir K, Rugge M, Baffa R (2011) Role of microRNA in distinguishing primary brain tumors from secondary tumors metastatic to the brain. Frontiers in bioscience 3:970-979.

Franceschini A, Szklarczyk D, Frankild S, Kuhn M, Simonovic M, Roth A, Lin J, Minguez P, Bork P, von Mering C, Jensen LJ (2013) STRING v9.1: protein-protein interaction networks, with increased coverage and integration. Nucleic acids research 41:D808-815.

Fu C, Xi L, McCarter R, Hickey M, Han ES (2006) Early hypothalamic response to age-dependent gene expression by calorie restriction. Neurobiology of aging 27:1315-1325.

Good DJ (2010) Transcriptional Regulation of Sensed Energy Availability Within Hypothalamic Neurons. The Open Neuroendocrinology Journal 3:1-5.

Gutierrez-Aguilar R, Kim DH, Woods SC, Seeley RJ (2012) Expression of new loci associated with obesity in diet-induced obese rats: from genetics to physiology. Obesity 20:306-312.

Inoue N, Yahagi N, Yamamoto T, Ishikawa M, Watanabe K, Matsuzaka T, Nakagawa Y, Takeuchi Y, Kobayashi K, Takahashi A, Suzuki H, Hasty AH, Toyoshima H, Yamada N, Shimano H (2008) Cyclin-dependent kinase inhibitor, p21WAF1/CIP1, is involved in adipocyte differentiation and hypertrophy, linking to obesity, and insulin resistance. The Journal of biological chemistry 283:21220-21229.

Kalman S, Garbett K, Vereczkei A, Shelton RC, Korade Z, Mirnics K (2013) Metabolic stress-induced microRNA and mRNA expression profiles of human fibroblasts. Experimental cell research.

Kokoeva MV, Yin H, Flier JS (2005) Neurogenesis in the hypothalamus of adult mice: potential role in energy balance. Science 310:679-683.

Liu K, Liu Y, Mo W, Qiu R, Wang X, Wu JY, He R (2011) MiR-124 regulates early neurogenesis in the optic vesicle and forebrain, targeting NeuroD1. Nucleic acids research 39:2869-2879.

Maglich JM, Watson J, McMillen PJ, Goodwin B, Willson TM, Moore JT (2004) The nuclear receptor CAR is a regulator of thyroid hormone metabolism during caloric restriction. The Journal of biological chemistry 279:19832-19838.

Mainardi M, Pizzorusso T, Maffei M (2013) Environment, leptin sensitivity, and hypothalamic plasticity. Neural plasticity 2013:438072.

Martinelli R, Nardelli C, Pilone V, Buonomo T, Liguori R, Castano I, Buono P, Masone S, Persico G, Forestieri P, Pastore L, Sacchetti L (2010) miR-519d overexpression is associated with human obesity. Obesity 18:2170-2176.

Mattison JA, Lane MA, Roth GS, Ingram DK (2003) Calorie restriction in rhesus monkeys. Experimental gerontology 38:35-46.

Mattson MP (2005) Energy intake, meal frequency, and health: a neurobiological perspective. Annual review of nutrition 25:237-260.

Mattson MP, Chan SL, Duan W (2002) Modification of brain aging and neurodegenerative disorders by genes, diet, and behavior. Physiological reviews 82:637-672.

Mattson MP, Wan R (2005) Beneficial effects of intermittent fasting and caloric restriction on the cardiovascular and cerebrovascular systems. The Journal of nutritional biochemistry 16:129-137.

McCay CM, Crowell MF, Maynard LA (1989) The effect of retarded growth upon the length of life span and upon the ultimate body size. 1935. Nutrition 5:155-171; discussion 172.

McClintick JN, Xuei X, Tischfield JA, Goate A, Foroud T, Wetherill L, Ehringer MA, Edenberg HJ (2013) Stress-response pathways are altered in the hippocampus of chronic alcoholics. Alcohol 47:505-515.

McNay DE, Briancon N, Kokoeva MV, Maratos-Flier E, Flier JS (2012) Remodeling of the arcuate nucleus energy-balance circuit is inhibited in obese mice. The Journal of clinical investigation 122:142-152.

McNeill E, Van Vactor D (2012) MicroRNAs shape the neuronal landscape. Neuron 75:363-379.

Meister B, Herzer S, Silahtaroglu A (2013) MicroRNAs in the Hypothalamus. Neuroendocrinology.

Nagino K, Nomura O, Takii Y, Myomoto A, Ichikawa M, Nakamura F, Higasa M, Akiyama H, Nobumasa H, Shiojima S, Tsujimoto G (2006) Ultrasensitive DNA chip: gene expression profile analysis without RNA amplification. Journal of biochemistry 139:697-703.

Nakatsuka A, Wada J, Hida K, Hida A, Eguchi J, Teshigawara S, Murakami K, Kanzaki M, Inoue K, Terami T, Katayama A, Ogawa D, Kagechika H, Makino H (2012) RXR

antagonism induces G0 /G1 cell cycle arrest and ameliorates obesity by up-regulating the p53-p21(Cip1) pathway in adipocytes. The Journal of pathology 226:784-795.

Nogales-Cadenas R, Carmona-Saez P, Vazquez M, Vicente C, Yang X, Tirado F, Carazo JM, Pascual-Montano A (2009) GeneCodis: interpreting gene lists through enrichment analysis and integration of diverse biological information. Nucleic acids research 37:W317-322.

Olsen L, Klausen M, Helboe L, Nielsen FC, Werge T (2009) MicroRNAs show mutually exclusive expression patterns in the brain of adult male rats. PloS one 4:e7225.

Poplawski MM, Mastaitis JW, Yang XJ, Mobbs CV (2010) Hypothalamic responses to fasting indicate metabolic reprogramming away from glycolysis toward lipid oxidation. Endocrinology 151:5206-5217.

Roshan R, Ghosh T, Scaria V, Pillai B (2009) MicroRNAs: novel therapeutic targets in neurodegenerative diseases. Drug discovery today 14:1123-1129.

Salamone JD, Correa M (2013) Dopamine and food addiction: lexicon badly needed. Biological psychiatry 73:e15-24.

Sato F, Tsuchiya S, Terasawa K, Tsujimoto G (2009) Intra-platform repeatability and inter-platform comparability of microRNA microarray technology. PloS one 4:e5540.

Schneeberger M, Altirriba J, Garcia A, Esteban Y, Castano C, Garcia-Lavandeira M, Alvarez CV, Gomis R, Claret M (2012) Deletion of microRNA processing enzyme Dicer in POMC-expressing cells leads to pituitary dysfunction, neurodegeneration and development of obesity. Molecular metabolism 2:74-85.

Sohal RS, Weindruch R (1996) Oxidative stress, caloric restriction, and aging. Science 273:59-63.

Sun L, Xie H, Mori MA, Alexander R, Yuan B, Hattangadi SM, Liu Q, Kahn CR, Lodish HF (2011) Mir193b-365 is essential for brown fat differentiation. Nature cell biology 13:958-965.

Swindell WR (2008) Comparative analysis of microarray data identifies common responses to caloric restriction among mouse tissues. Mechanisms of ageing and development 129:138-153.

Szklarczyk K, Korostynski M, Golda S, Solecki W, Przewlocki R (2012) Genotype-dependent consequences of traumatic stress in four inbred mouse strains. Genes, brain, and behavior.

Tabas-Madrid D, Nogales-Cadenas R, Pascual-Montano A (2012) GeneCodis3: a non-redundant and modular enrichment analysis tool for functional genomics. Nucleic acids research 40:W478-483.

Takanabe R, Ono K, Abe Y, Takaya T, Horie T, Wada H, Kita T, Satoh N, Shimatsu A, Hasegawa K (2008) Up-regulated expression of microRNA-143 in association with obesity in adipose tissue of mice fed high-fat diet. Biochemical and biophysical research communications 376:728-732.

Thorleifsson G, Walters GB, Gudbjartsson DF, Steinthorsdottir V, Sulem P, Helgadottir A, Styrkarsdottir U, Gretarsdottir S, Thorlacius S, Jonsdottir I, Jonsdottir T, Olafsdottir EJ, Olafsdottir GH, Jonsson T, Jonsson F, Borch-Johnsen K, Hansen T, Andersen G, Jorgensen T, Lauritzen T, Aben KK, Verbeek AL, Roeleveld N, Kampman E, Yanek LR, Becker LC, Tryggvadottir L, Rafnar T, Becker DM, Gulcher J, Kiemeney LA,

Pedersen O, Kong A, Thorsteinsdottir U, Stefansson K (2009) Genome-wide association yields new sequence variants at seven loci that associate with measures of obesity. Nature genetics 41:18-24.

Tinkum KL, White LS, Marpegan L, Herzog E, Piwnica-Worms D, Piwnica-Worms H (2013) Forkhead box O1 (FOXO1) protein, but not p53, contributes to robust induction of p21 expression in fasted mice. The Journal of biological chemistry 288:27999-28008.

Tzotzas T, Desrumaux C, Lagrost L (2009) Plasma phospholipid transfer protein (PLTP): review of an emerging cardiometabolic risk factor. Obesity reviews : an official journal of the International Association for the Study of Obesity 10:403-411.

Vella KR, Burnside AS, Brennan KM, Good DJ (2007) Expression of the hypothalamic transcription factor Nhlh2 is dependent on energy availability. Journal of neuroendocrinology 19:499-510.

Weindruch R, Sohal RS (1997) Seminars in medicine of the Beth Israel Deaconess Medical Center. Caloric intake and aging. The New England journal of medicine 337:986-994.

Wulczyn FG, Smirnova L, Rybak A, Brandt C, Kwidzinski E, Ninnemann O, Strehle M, Seiler A, Schumacher S, Nitsch R (2007) Post-transcriptional regulation of the let-7 microRNA during neural cell specification. FASEB journal : official publication of the Federation of American Societies for Experimental Biology 21:415-426.

Yu JY, Chung KH, Deo M, Thompson RC, Turner DL (2008) MicroRNA miR-124 regulates neurite outgrowth during neuronal differentiation. Experimental cell research 314:2618-2633.

Zhu H, Shyh-Chang N, Segre AV, Shinoda G, Shah SP, Einhorn WS, Takeuchi A, Engreitz JM, Hagan JP, Kharas MG, Urbach A, Thornton JE, Triboulet R, Gregory RI, Consortium D, Investigators M, Altshuler D, Daley GQ (2011) The Lin28/let-7 axis regulates glucose metabolism. Cell 147:81-94.

6. Figure Legends

Figure 1: Experimental design, and confirmation of food deprivation conditions. A. Experimental design of the experiment, showing the timeline for the *ad lib* and food deprived groups of animals. B. Serum glucose levels, relative to ad lib fed. C. Serum leptin levels, relative to ad lib fed $^{**}P \leq 0.01$.

Figure 2: Confirmation of microRNA detection. A. Scatterplot diagram comparing hypothalamic versus skeletal muscle microRNA expression differences. The relative expression was calculated based on ad lib hypothalamus expression =1, for all three microRNA. Three microRNA were further analyzed by RT-QPCR. B. Let-7d is expressed in both tissue types. C. Skeletal muscle-specific miR-1 D. hypothalamus-specific miR-124a. The insets in C and D more clearly show the food deprived and *ad lib* levels of miR-1 in hypothalamus (C) and miR-124a in skeletal muscle as they are expressed at a low level in these tissues, respectively. $^{**}P \leq 0.01$.

Figure 3: microRNA analysis A. log2 Scatter plot of hypothalamus microRNA array data from Affymetrix array. Data was filtered using a p value < 0.05 and 1.3 fold change. B. Plot showing p-value versus log2 expression level for data from Affymetrix array. Lines indicate where significance cut-off values were made. C. Log2 Scatter plot of hypothalamus microRNA array data from Toray array. Data was cut off using the median of the maximum expression value, and filtered using a p value ≤ 0.05 and 1.3 fold change. D. Plot showing p-value versus log2 expression level for data from Toray array. Lines indicate where significance cut-off values were made.

Figure 4: RT-QPCR analysis of selected microRNAs. microRNAs were selected using the cut-off criteria, and expression level tested in N=4-6 new samples for each group. All microRNA levels are reported relative to levels in *ad lib* fed animals, and normalized to the Sno microRNA. A. microRNA expression in hypothalamic tissue of ad lib versus food deprived mice. B. microRNA expression in skeletal muscle versus hypothalamus. $^{*}P \leq 0.05$, $^{**}P \leq 0.01$.

Figure 5: mRNA analysis A. log2 Scatter plot of hypothalamus mRNA array data from Affymetrix array. Data was filtered using a p value < 0.05 and 1.3 fold change. B. Plot showing p-value versus log2 expression level for data from Affymetrix array. Lines indicate where significance cut-off values were made. C. Log2 Scatter plot of hypothalamus mRNA array data from Toray array. Data was cut off using the median of the maximum expression value, and filtered using a p value ≤ 0.05 and 1.3 fold change. D. Plot showing p-value versus log2 expression level for data from Toray array. Lines indicate where significance cut-off values were made.

Figure 6: RT-QPCR analysis of selected mRNAs. mRNAs were selected using the cut-off criteria and expression level tested in N=4-6 new samples for each group. A. Selected mRNAs that were upregulated on the microarrays. B. Selected mRNAs that were

downregulated on the microarrays. All mRNA levels are reported as relative to levels in *ad lib* fed animals, and normalized to the housekeeping gene β-actin. $^{**}P \leq 0.01$

Figure 7: RT-QPCR and pathway analyses for selected cell cycle mRNAs. A. mRNAs were selected from cell cycle GO categories and their expression levels tested in N=4-6 new samples for each group. All mRNA levels are reported as relative to levels in *ad lib* fed animals, and normalized to the housekeeping gene β-actin.$^{*}P \leq 0.05$, $^{**}P \leq 0.01$. B. String v9.1 was used to generate a network using the proteins tested in 7A as input. The network was expanded by one level. Only the names of the proteins input are shown.

Table 1: Comparison of miRNA Array Results from Toray and Affymetrix. The total number of miRNAs up regulated (i.e. lower in ad lib conditions) versus down regulated (i.e. higher in ad lib conditions), as well as the number of overlapping miRNAs are shown.

	TORAY	AFFYMETRIX
Total Detected miRNAs	503	536
Number of significant up-regulated miRNAs	64	16
Number of significant down-regulated miRNAs	5	6
Overlapped miRNAs	3	

Table 2: Comparison of mRNA Array Results from Toray and Affymetrix. The total number of miRNAs up regulated (i.e. lower in ad lib conditions) versus down regulated (i.e. higher in ad lib conditions), as well as the number of overlapping miRNAs found n the total mRNA that were differentially regulated between the two arrays, are shown.

	TORAY	AFFYMETRIX
Total Detected mRNAs	15830	16294
Number of significant up-regulated mRNAs	705	298
Number of significant down-regulated mRNAs	603	242
Overlapped mRNAs	115	

Table 3: GO analysis (Process categories). GO analysis was compiled using the data from the Affymetrix and Toray mRNA arrays.

Biological Process					
Affymetrix Array Top 5			**Toray Array Top 5**		
GO Term	**Gene Count**	**P-value**	**GO Term**	**Gene Count**	**P-value**
GO:0006810 transport	56	8.73E-07	GO:0006468 protein phosphorylation	58	2.29E-14
GO:0007049 cell cycle	26	3.41E-05	GO:0016310 phosphorylation	59	1.65E-11
GO:0016310 phosphorylation	29	8.99E-05	GO:0006810 transport	96	8.88E-10
GO:0048812 neuron projection morphogenesis	7	0.000192	GO:0008152 metabolic process	93	3.64E-08
GO:0006974 response to DNA damage stimulus	17	0.000447	GO:0055114 oxidation-reduction process	48	5.42E-08
Cellular Component					
Affymetrix Array Top 5			**Toray Array Top 5**		
GO Term	**Gene Count**	**P-value**	**GO Term**	**Gene Count**	**P-value**
GO:0016020 membrane	178	4.76E-24	GO:0005737 cytoplasm	325	1.24E-50
GO:0005886 plasma membrane	103	1.23E-17	GO:0016020 membrane	348	4.84E-49
GO:0005634 nucleus	144	7.00E-17	GO:0005634 nucleus	286	7.64E-36
GO:0005737 cytoplasm	141	1.33E-14	GO:0005886 plasma membrane	184	1.59E-27
GO:0016021 integral to membrane	143	6.95E-13	GO:0016021 integral to membrane	268	1.06E-21
Molecular Function					
Affymetrix Array Top 5			**Toray Array Top 5**		
GO Term	**GO Term**	**GO Term**	**GO Term**	**GO Term**	**GO Term**
GO:0005515 protein binding	100	3.92E-16	GO:0005515 protein binding	192	3.77E-26
GO:0046872 metal ion binding	91	5.08E-14	GO:0000166 nucleotide binding	125	2.20E-15
GO:0000166 nucleotide binding	64	8.20E-10	GO:0016740 transferase activity	95	7.94E-14
GO:0005524	47	6.59E-08	GO:0016301	61	2.64E-13

ATP binding			kinase activity (MF)		
GO:0003677 DNA binding	51	1.10E-07	GO:0004672 protein kinase activity	49	6.69E-15
KEGG Pathways					
Affymetrix Array Top 5			**Toray Array Top 5**		
GO Term	**GO Term**	**GO Term**	**GO Term**	**GO Term**	**GO Term**
Kegg:04670 Leukocyte transendothelial migration	9	4.27E-05	Kegg:05200 Pathways in cancer	27	6.12E-05
Kegg:04724 Glutamatergic synapse	9	6.32E-05	Kegg:00230 Purine metabolism	17	0.000318
Kegg:04010 MAPK signaling pathway	10	0.004306	Kegg:00330 Arginine and proline metabolism	9	0.000488
Kegg:04144 Endocytosis	9	0.003344	Kegg:04510 Focal adhesion	18	0.000518
Kegg:04062 Chemokine signaling pathway	12	8.61E-06	Kegg:04062 Chemokine signaling pathway	17	0.000547

Table 4: Cell cycle category GO Terms. GO analysis was compiled using the data from the Affymetrix and Toray mRNA arrays

Biological Process					
Affymetrix Array Top 5			**Toray Array Top 5**		
GO Term	**Gene Count**	**P-value**	**GO Term**	**Gene Count**	**P-value**
GO:0006810 transport	56	8.73E-07	GO:0006468 protein phosphorylation	58	2.29E-14
GO:0007049 cell cycle	26	3.41E-05	GO:0016310 phosphorylation	59	1.65E-11
GO:0016310 phosphorylation	29	8.99E-05	GO:0006810 transport	96	8.88E-10
GO:0048812 neuron projection morphogenesis	7	0.000192	GO:0008152 metabolic process	93	3.64E-08
GO:0006974 response to DNA damage stimulus	17	0.000447	GO:0055114 oxidation-reduction process	48	5.42E-08
Cellular Component					
Affymetrix Array Top 5			**Toray Array Top 5**		
GO Term	**Gene Count**	**P-value**	**GO Term**	**Gene Count**	**P-value**
GO:0016020 membrane	178	4.76E-24	GO:0005737 cytoplasm	325	1.24E-50
GO:0005886 plasma membrane	103	1.23E-17	GO:0016020 membrane	348	4.84E-49
GO:0005634 nucleus	144	7.00E-17	GO:0005634 nucleus	286	7.64E-36
GO:0005737 cytoplasm	141	1.33E-14	GO:0005886 plasma membrane	184	1.59E-27
GO:0016021 integral to membrane	143	6.95E-13	GO:0016021 integral to membrane	268	1.06E-21
Molecular Function					
Affymetrix Array Top 5			**Toray Array Top 5**		
GO Term	**Gene Count**	**P-value**	**GO Term**	**Gene Count**	**P-value**
GO:0005515 protein binding	100	3.92E-16	GO:0005515 protein binding	192	3.77E-26
GO:0046872 metal ion binding	91	5.08E-14	GO:0000166 nucleotide binding	125	2.20E-15

GO:0000166 nucleotide binding	64	8.20E-10	GO:0016740 transferase activity	95	7.94E-14
GO:0005524 ATP binding	47	6.59E-08	GO:0016301 kinase activity (MF)	61	2.64E-13
GO:0003677 DNA binding	51	1.10E-07	GO:0004672 protein kinase activity	49	6.69E-15
Kegg Pathways					
Affymetrix Array Top 5			**Toray Array Top 5**		
GO Term	**Gene Count**	**P-value**	**GO Term**	**Gene Count**	**P-value**
Kegg:04670 Leukocyte transendothelial migration	9	4.27E-05	Kegg:05200 Pathways in cancer	27	6.12E-05
Kegg:04724 Glutamatergic synapse	9	6.32E-05	Kegg:00230 Purine metabolism	17	0.000318
Kegg:04010 MAPK signaling pathway	10	0.004306	Kegg:00330 Arginine and proline metabolism	9	0.000488
Kegg:04144 Endocytosis	9	0.003344	Kegg:04510 Focal adhesion	18	0.000518
Kegg:04062 Chemokine signaling pathway	12	8.61E-06	Kegg:04062 Chemokine signaling pathway	17	0.000547

Figure 1. Experimental design, and confirmation of food deprivation conditions.

A.

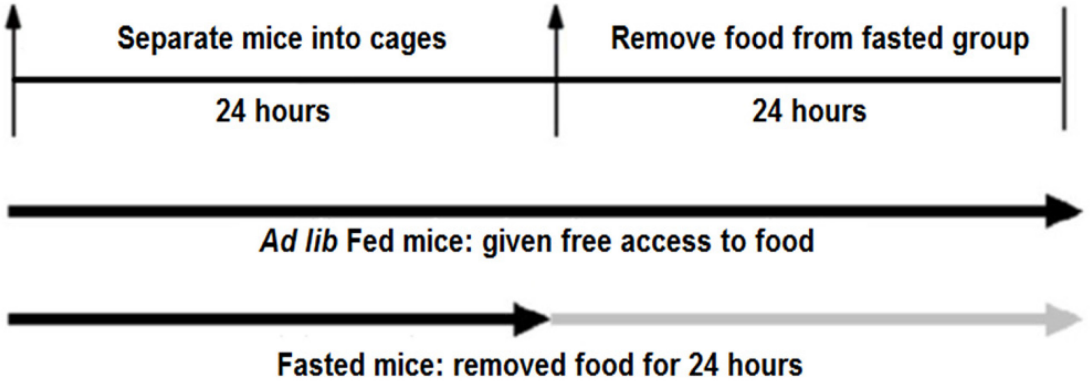

B.

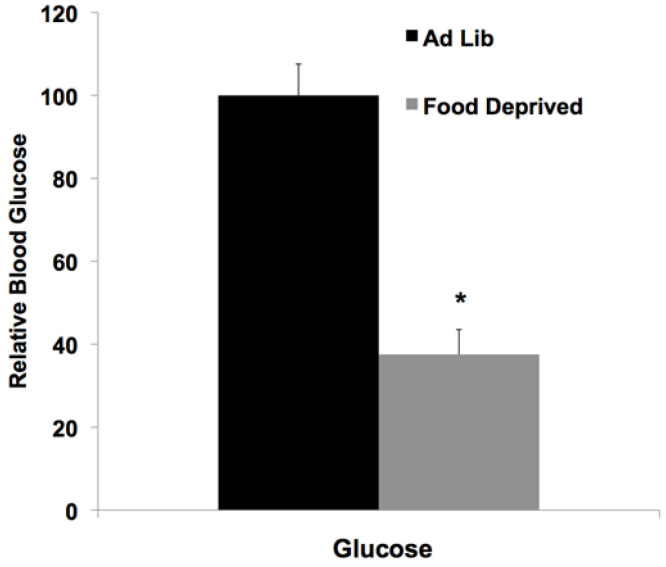

C.

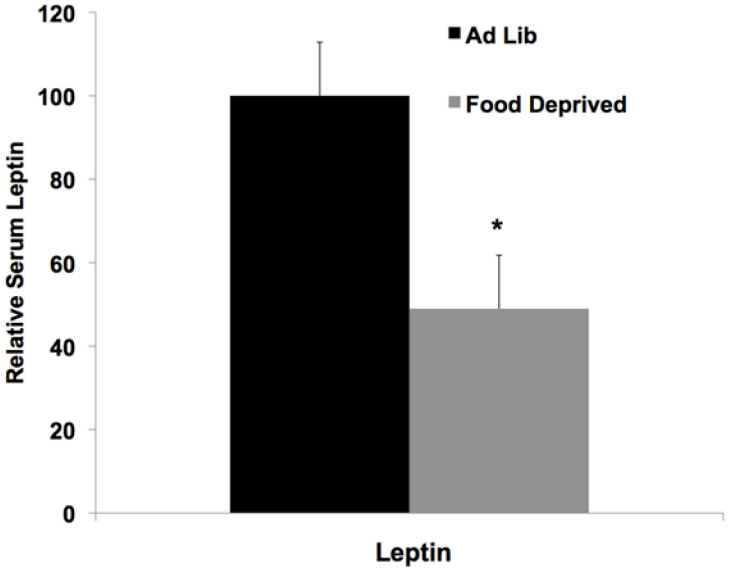

Figure 2. Confirmation of microRNA detection.

A.

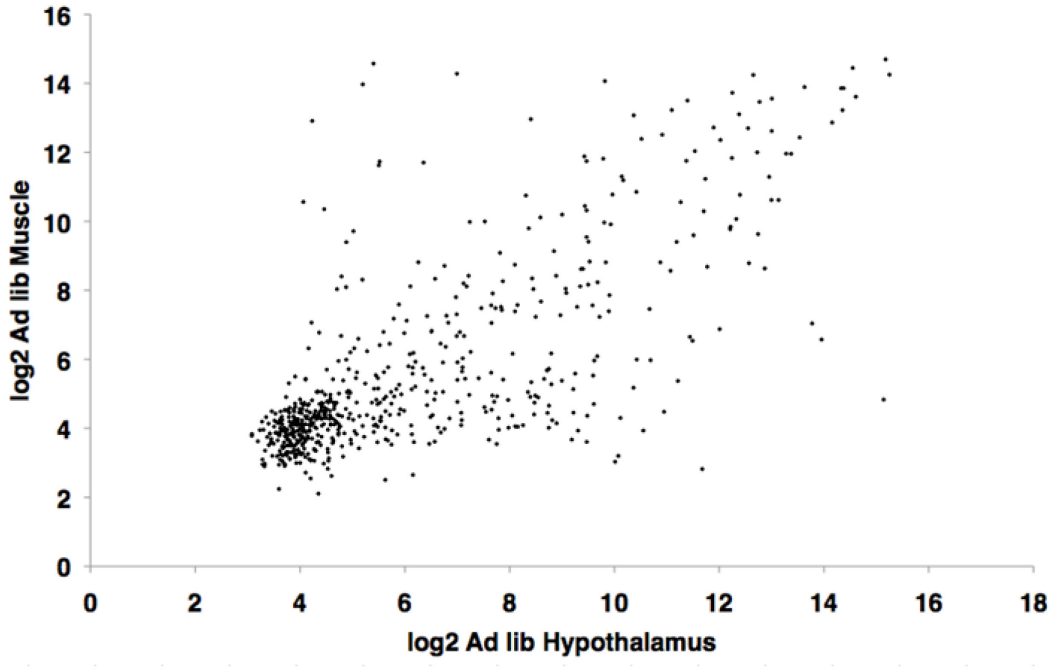

B.

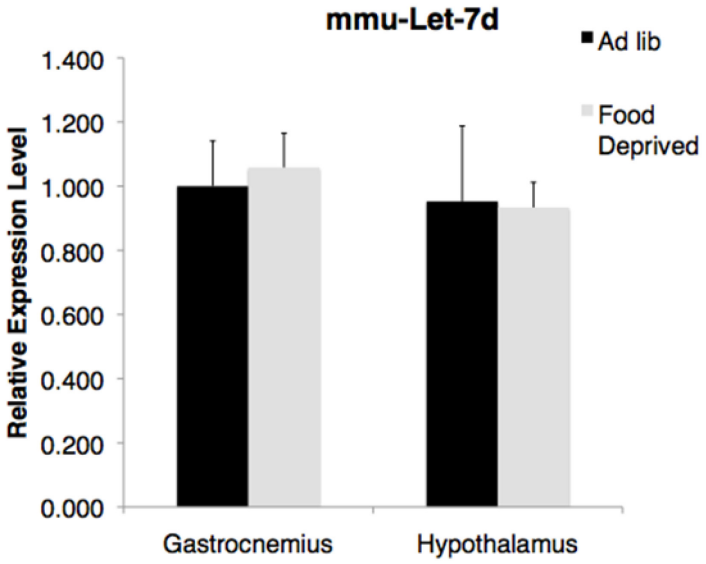

Figure 2. Confirmation of microRNA detection (Con.).

C.

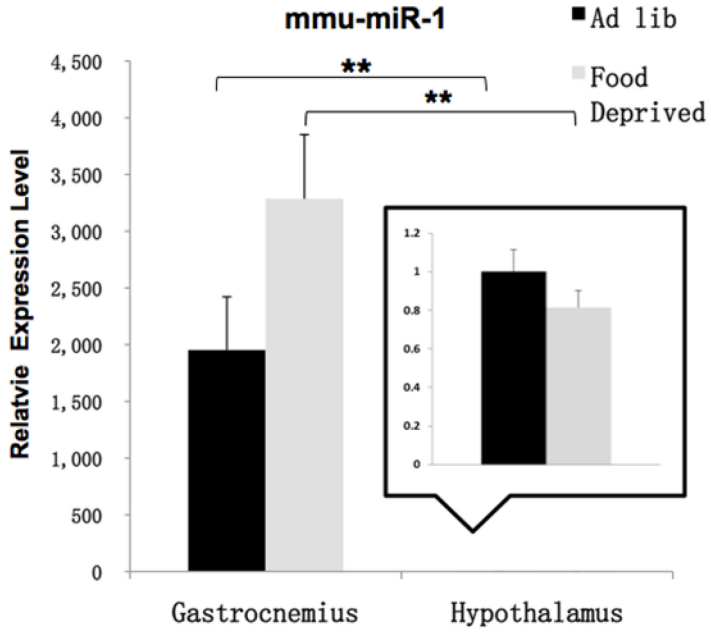

D.

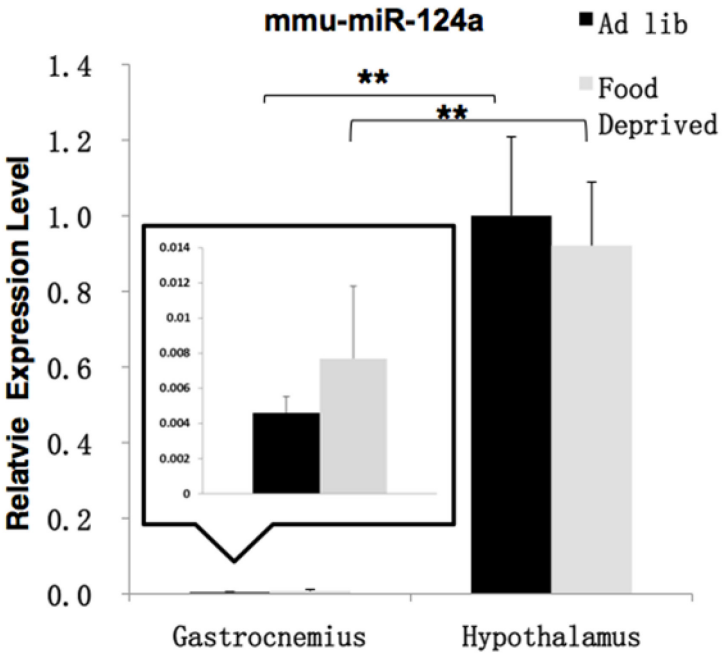

Figure 3. MicroRNA analysis.

A.

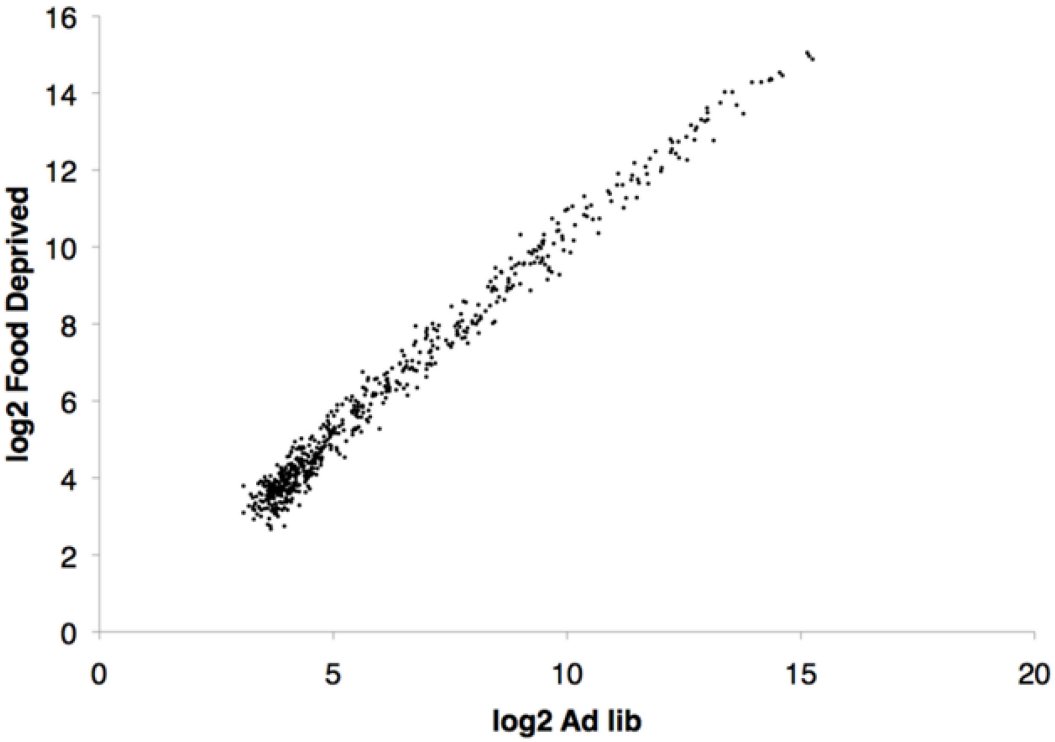

B.

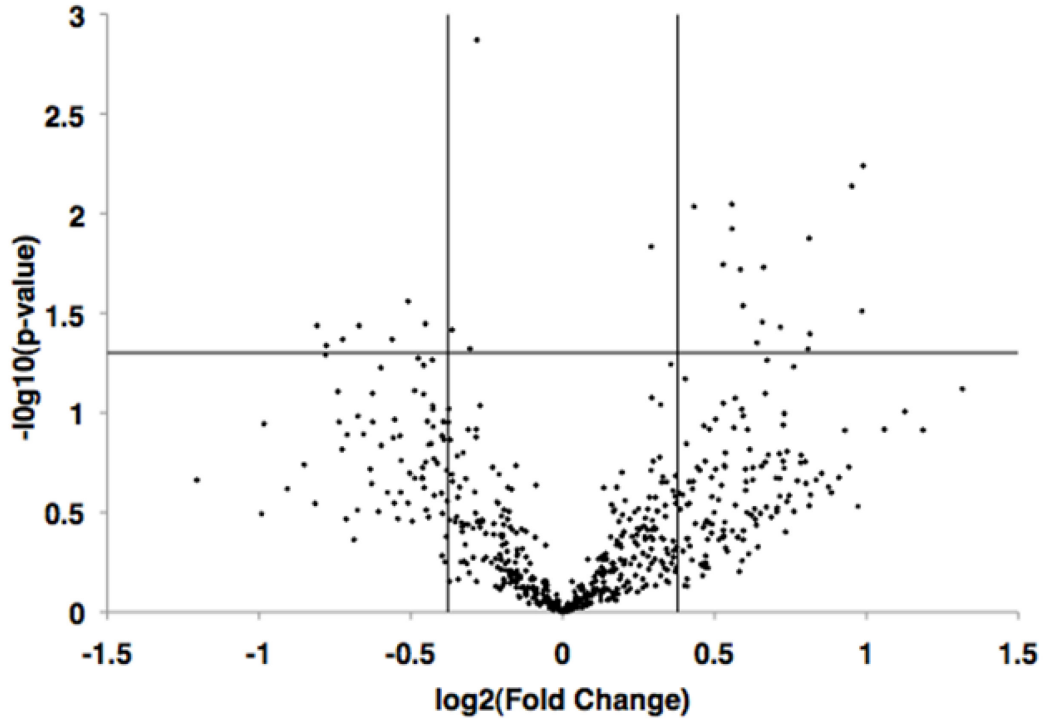

Figure 3. MicroRNA analysis (Con.).

C.

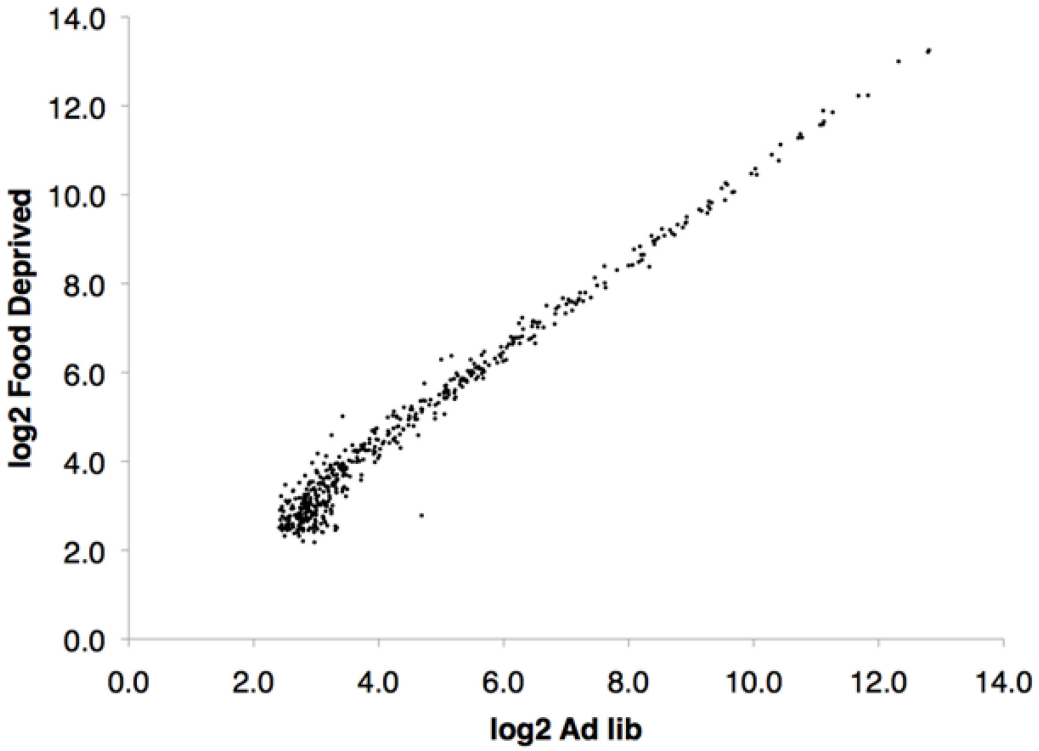

D.

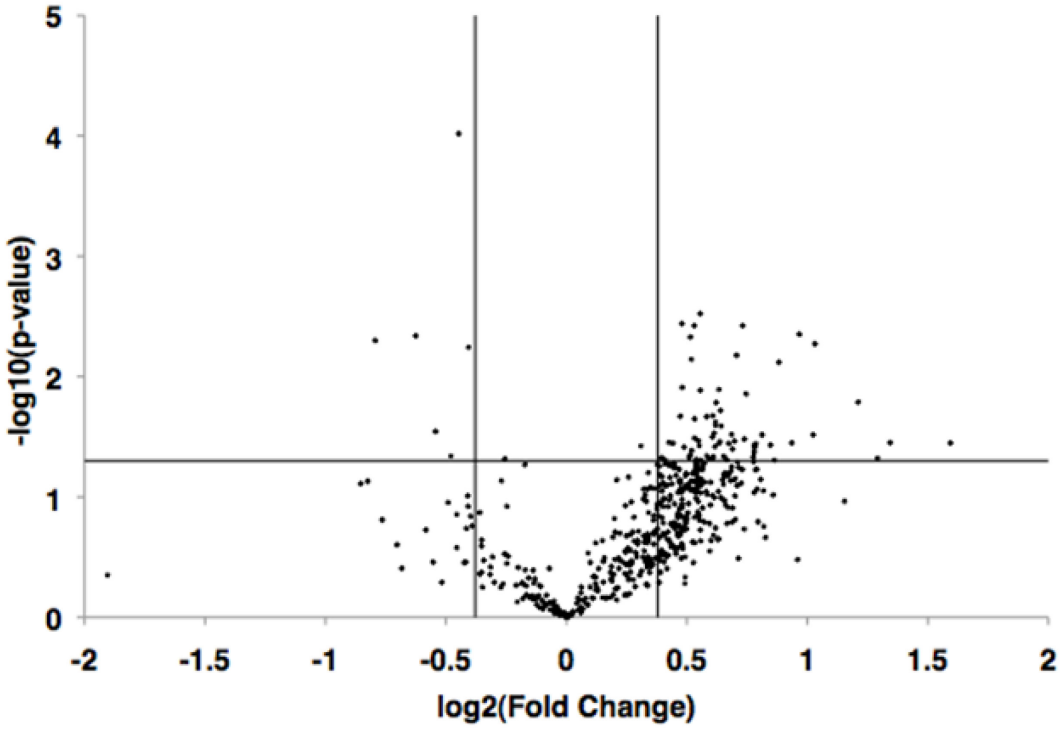

Figure 4. RT-QPCR analysis of selected microRNAs.

A.

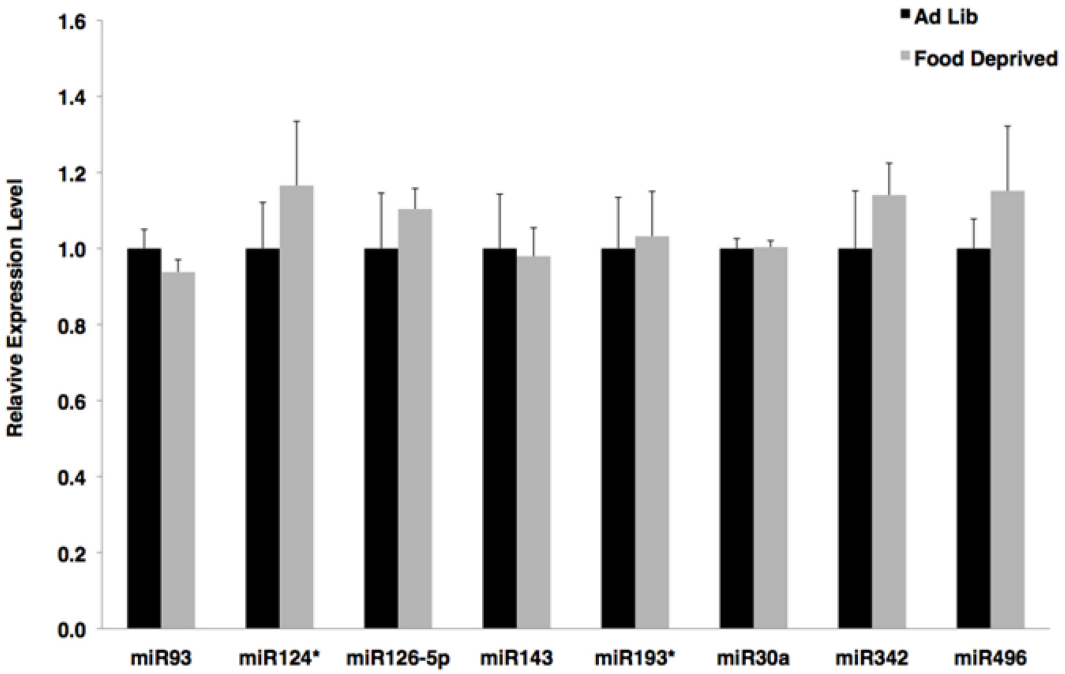

B.

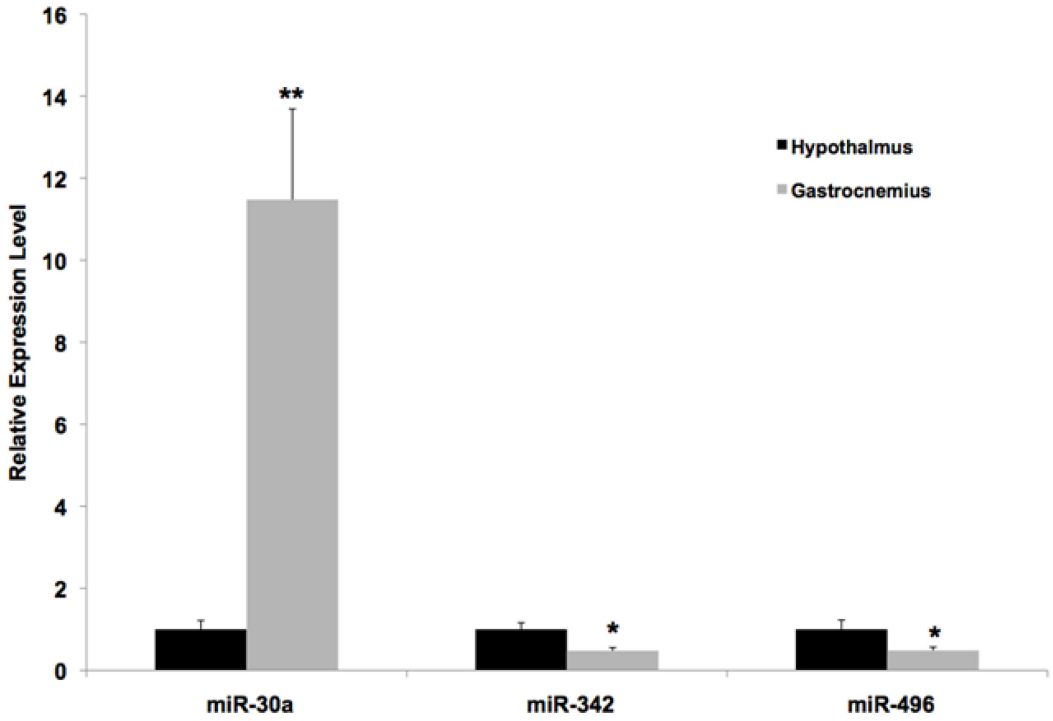

Figure 5. mRNA analysis

A.

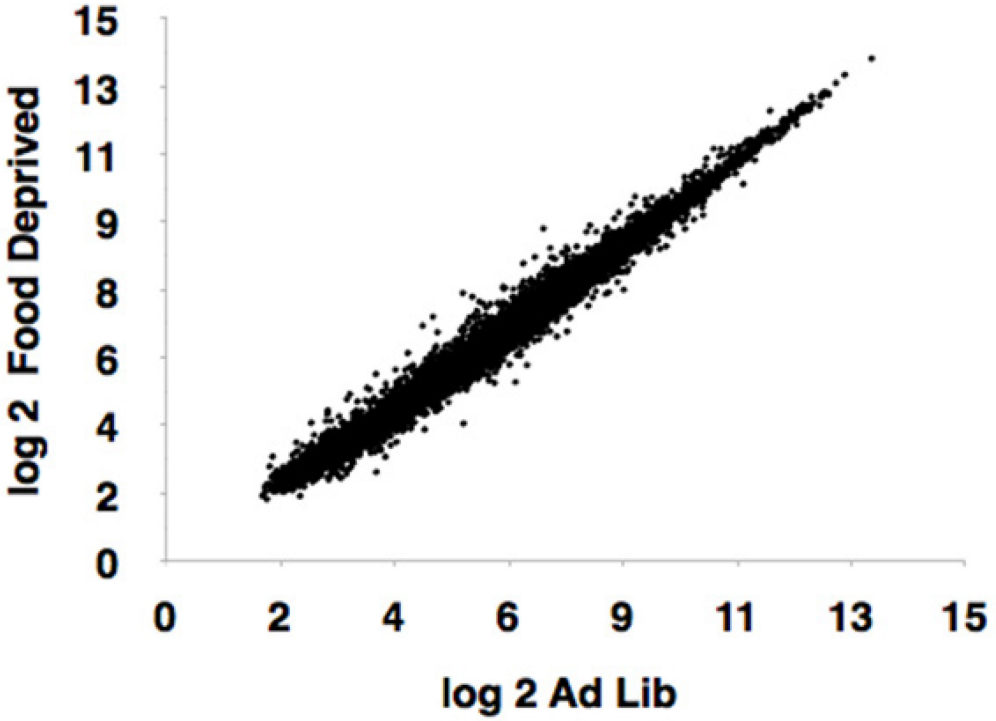

B.

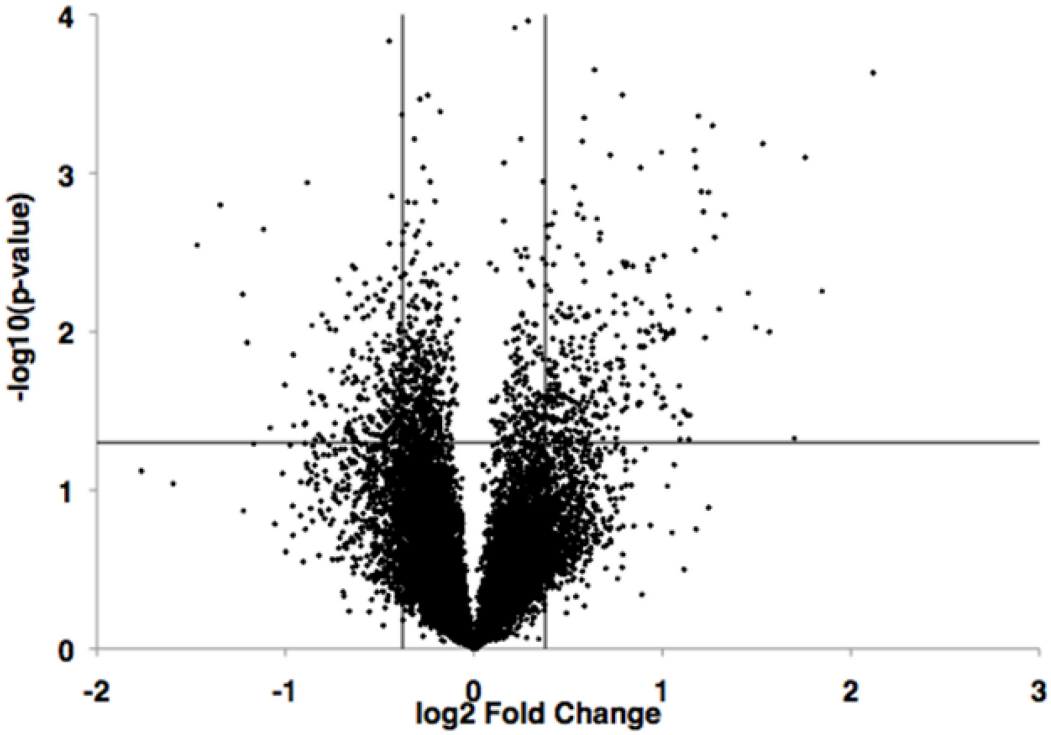

Figure 5. mRNA analysis (Con.).

C.

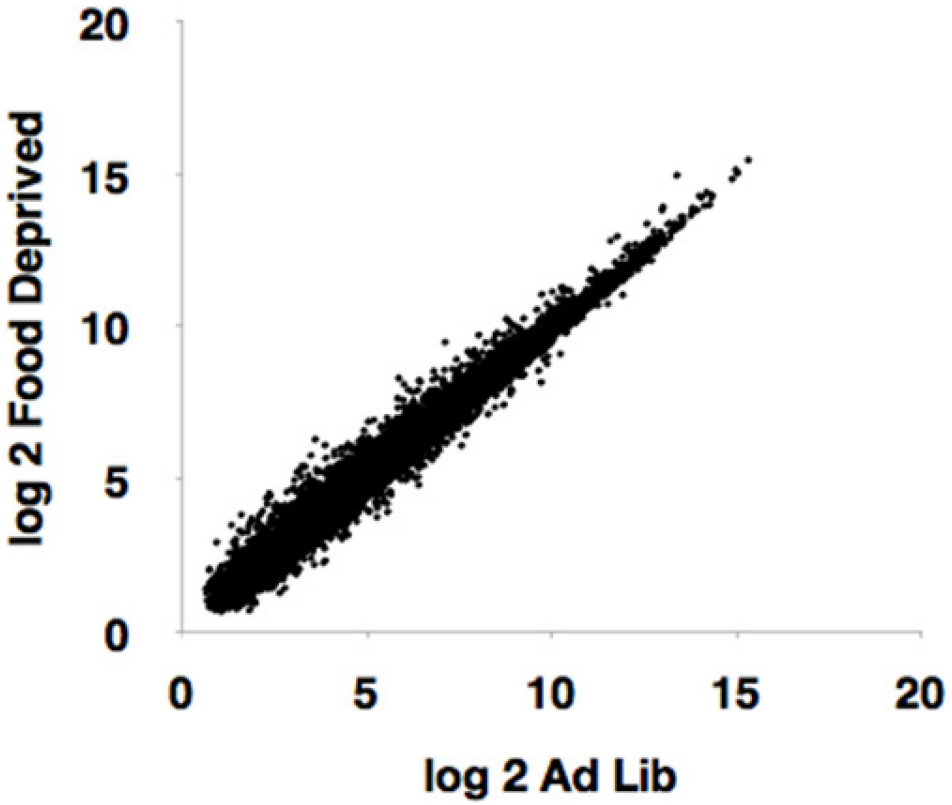

D.

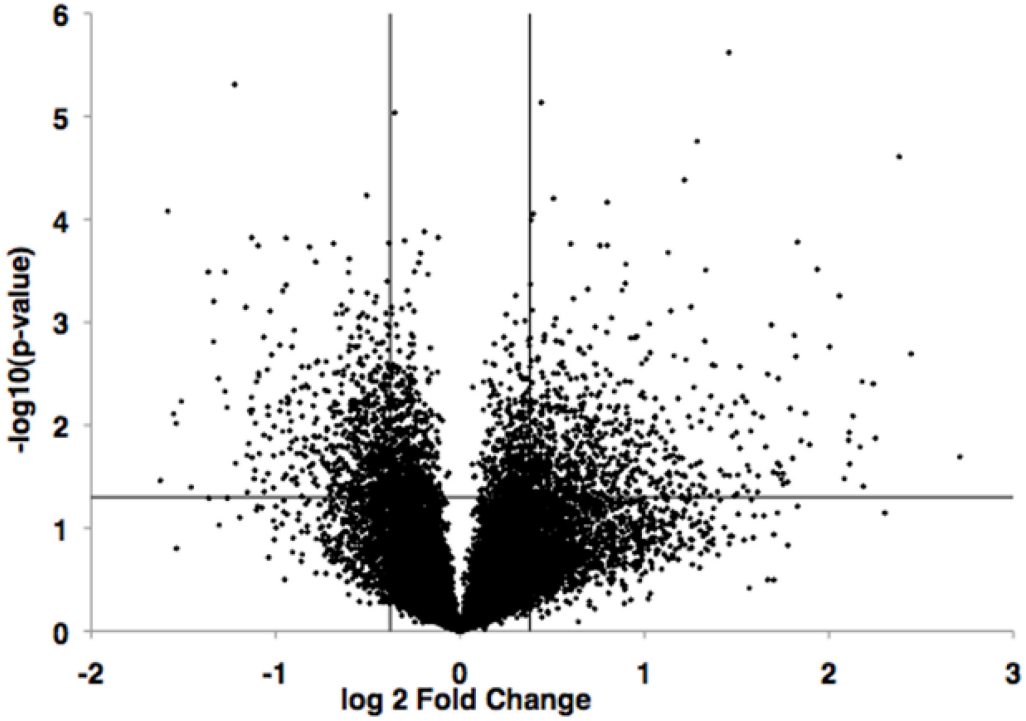

Figure 6. RT-QPCR analysis of selected mRNAs.

A.

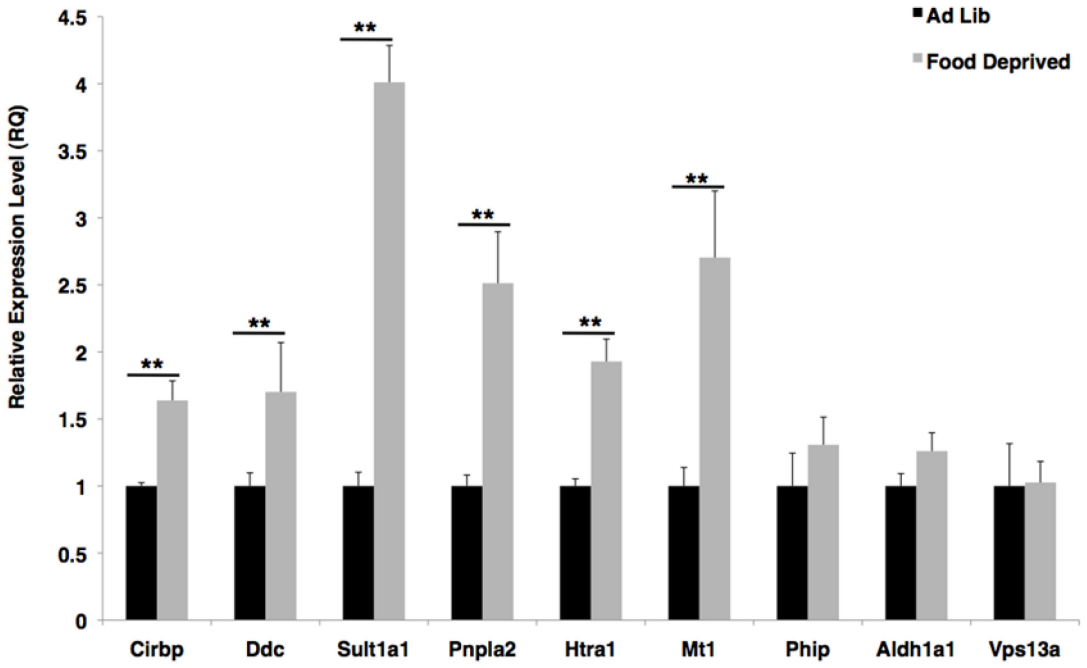

B.

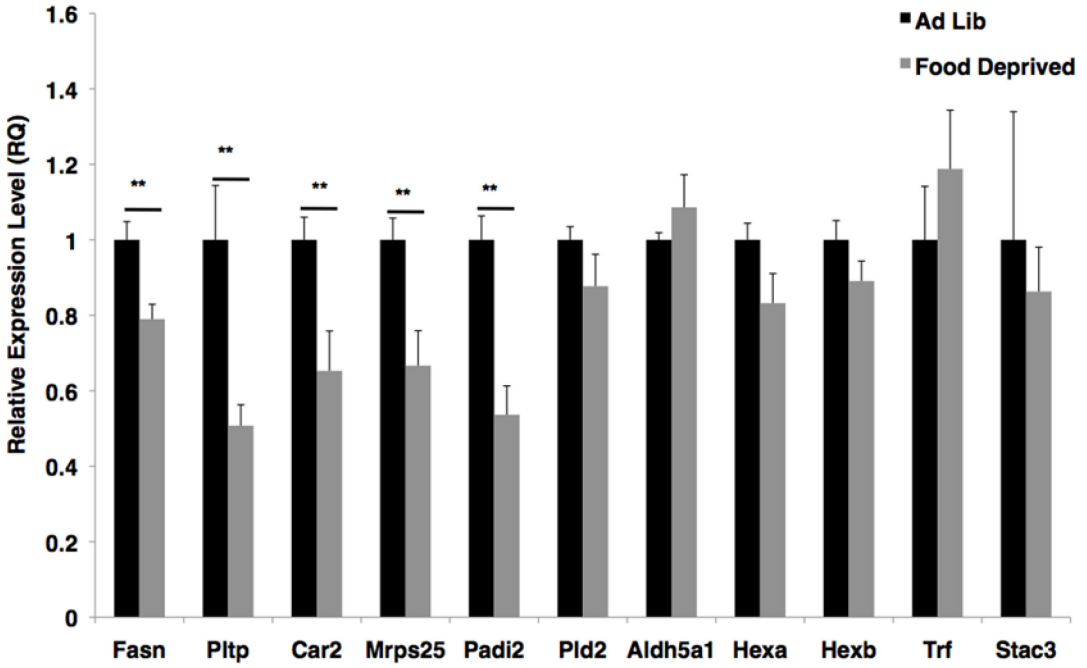

Figure 7. RT-QPCR and pathway analyses for selected cell cycle mRNAs.

A.

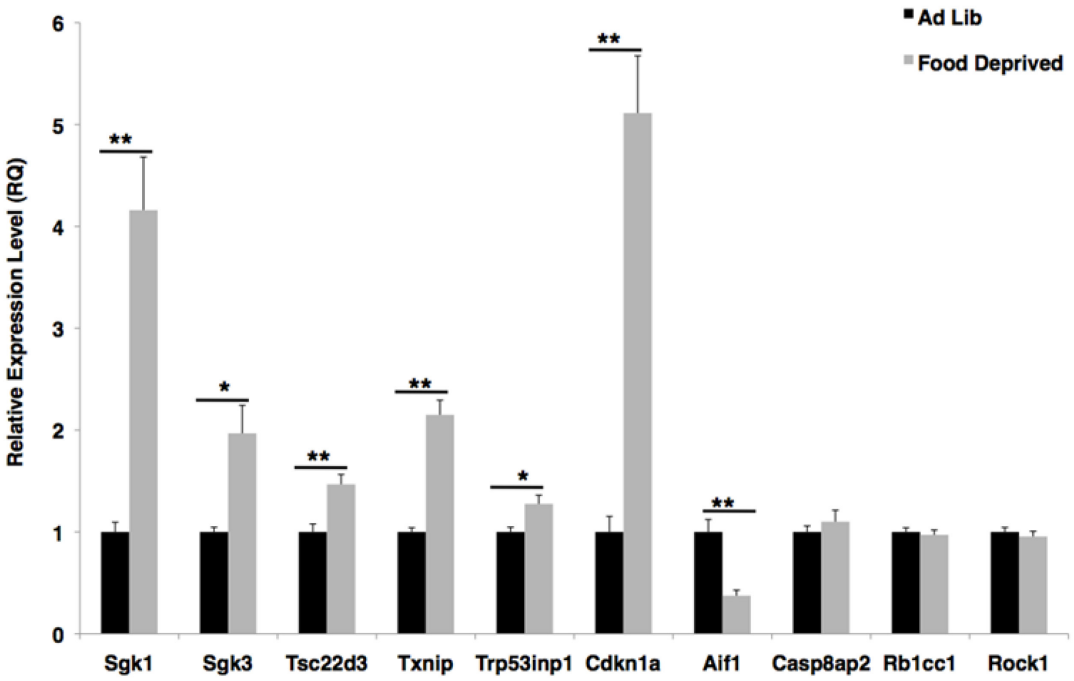

B.

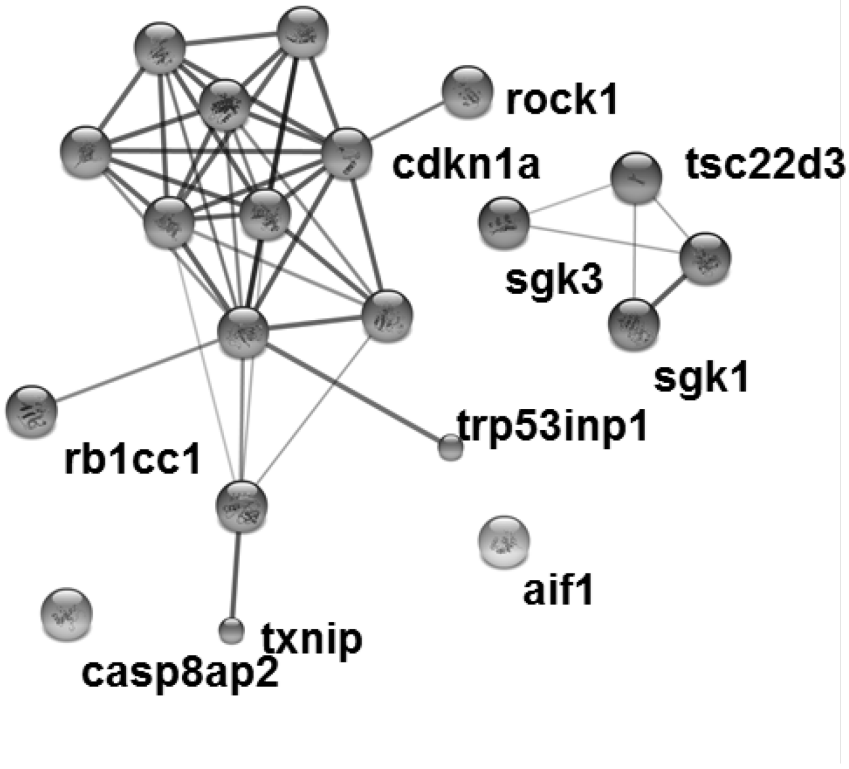

Supplemental Table 1: List of differentially expressed miRNAs identified using the Affymetrix array. The miRNAs down-regulated by food deprivation, compared to ad lib feeding are shown first, and indicated by the negative fold change.

miRBase ID	**Affymetrix ProbeSet Name**	**log2 Fold Change**	***P*-value**
mmu-miR-449c	mmu-miR-449c_st	-0.809	0.037
mmu-miR-470	mmu-miR-470_st	-0.779	0.046
mmu-miR-297c	mmu-miR-297c_st	-0.724	0.043
mmu-miR-875-5p	mmu-miR-875-5p_st	-0.562	0.043
mmu-miR-471	mmu-miR-471_st	-0.510	0.028
mmu-miR-701	mmu-miR-701_st	-0.452	0.036
mmu-miR-496a-3p	mmu-miR-496_st	0.433	0.009
mmu-miR-191-3p	mmu-miR-191-star_st	0.528	0.018
mmu-miR-301a	mmu-miR-301a_st	0.557	0.009
mmu-miR-504	mmu-miR-504_st	0.558	0.012
mmu-miR-322	mmu-miR-322_st	0.585	0.019
mmu-let-7i	mmu-let-7i_st	0.593	0.029
mmu-miR-101b	mmu-miR-101b_st	0.639	0.045
mmu-miR-30a-3p	mmu-miR-30a-star_st	0.657	0.035
mmu-miR-466a-3p	mmu-miR-466a-3p_st	0.662	0.019
mmu-miR-193a-5p	mmu-miR-193-star_st	0.717	0.037
mmu-miR-146b	mmu-miR-146b_st	0.808	0.048
mmu-miR-93	mmu-miR-93_st	0.811	0.013
mmu-miR-126a-3p	mmu-miR-126-3p_st	0.814	0.040
mmu-miR-143	mmu-miR-143_st	0.952	0.007
mmu-let-7g	mmu-let-7g_st	0.985	0.031
mmu-miR-342-5p	mmu-miR-342-5p_st	0.989	0.006

Supplemental Table 2: List of differentially expressed miRNAs identified using the Toray Arrays. The miRNAs downregulated by food deprivation, compared to ad lib feeding are shown first, as indicated by the negative fold change.

miRBase ID	Toray ProbeSet Name	log2 Fold Change	*P*-value
mmu-miR-681	mmu-miR-681	-0.793	0.005
mmu-miR-3113-3p	mmu-miR-3113*	-0.625	0.005
mmu-miR-3083-3p	mmu-miR-3083*	-0.543	0.029
mmu-miR-378a-5p	mmu-miR-378*	-0.480	0.046
mmu-miR-698-3p	mmu-miR-698	-0.406	0.006
mmu-miR-154-5p	mmu-miR-154	0.395	0.047
mmu-miR-132-3p	mmu-miR-132	0.409	0.049
mmu-miR-337-3p	mmu-miR-337-3p	0.425	0.035
mmu-miR-431-5p	mmu-miR-431	0.443	0.036
mmu-miR-484	mmu-miR-484	0.473	0.021
mmu-miR-342-5p	mmu-miR-342-5p	0.479	0.004
mmu-miR-186-5p	mmu-miR-186	0.481	0.012
mmu-miR-1949	mmu-miR-1949	0.489	0.039
mmu-miR-221-3p	mmu-miR-221	0.510	0.047
mmu-miR-677-3p	mmu-miR-677*	0.512	0.045
mmu-miR-3058-3p	mmu-miR-3058*	0.515	0.005
mmu-miR-501-3p	mmu-miR-501-3p	0.518	0.007
mmu-miR-3072-3p	mmu-miR-3072	0.520	0.041
mmu-miR-542-3p	mmu-miR-542-3p	0.531	0.004
mmu-miR-22-5p	mmu-miR-22*	0.532	0.032
mmu-miR-124-5p	mmu-miR-124*	0.533	0.023
mmu-miR-125a-3p	mmu-miR-125a-3p	0.540	0.049
mmu-miR-770-3p	mmu-miR-770-3p	0.548	0.034
mmu-miR-30a-3p	mmu-miR-30a*	0.551	0.038
mmu-miR-138-2-3p	mmu-miR-138-2*	0.555	0.003
mmu-miR-30e-3p	mmu-miR-30e*	0.556	0.013
mmu-miR-30c-5p	mmu-miR-30c	0.557	0.050
mmu-miR-487b-3p	mmu-miR-487b	0.583	0.022
mmu-miR-92a-2-5p	mmu-miR-92a-2*	0.583	0.046
mmu-miR-26b-5p	mmu-miR-26b	0.606	0.047
mmu-miR-126a-5p	mmu-miR-126-5p	0.607	0.032
mmu-miR-34a-5p	mmu-miR-34a	0.607	0.021
mmu-miR-98-5p	mmu-miR-98	0.610	0.046
mmu-let-7f-5p	mmu-let-7f	0.612	0.030
mmu-miR-328-5p	mmu-miR-328*	0.617	0.038
mmu-miR-154-3p	mmu-miR-154*	0.619	0.024
mmu-miR-128-3p	mmu-miR-128	0.619	0.025
mmu-miR-1198-5p	mmu-miR-1198-5p	0.621	0.017
mmu-miR-1927	mmu-miR-1927	0.633	0.013
mmu-miR-296-5p	mmu-miR-296-5p	0.634	0.036
mmu-miR-380-5p	mmu-miR-380-5p	0.636	0.035
mmu-miR-708-5p	mmu-miR-708	0.640	0.019
mmu-miR-151-3p	mmu-miR-151-3p	0.642	0.026
mmu-miR-29c-3p	mmu-miR-29c	0.652	0.046

mmu-miR-218-5p	mmu-miR-218	0.656	0.047
mmu-miR-106b-5p	mmu-miR-106b	0.666	0.049
mmu-miR-2137	mmu-miR-2137	0.685	0.030
mmu-miR-3069-3p	mmu-miR-3069-3p	0.689	0.040
mmu-miR-30b-5p	mmu-miR-30b	0.698	0.035
mmu-miR-652-5p	mmu-miR-652*	0.706	0.007
mmu-miR-711	mmu-miR-711	0.731	0.004
mmu-miR-326-5p	mmu-miR-326*	0.738	0.033
mmu-miR-494-3p	mmu-miR-494	0.745	0.014
mmu-miR-496a-3p	mmu-miR-496	0.776	0.046
mmu-miR-29b-3p	mmu-miR-29b	0.779	0.042
mmu-miR-451a	mmu-miR-451	0.781	0.037
mmu-miR-92a-3p	mmu-miR-92a	0.786	0.036
mmu-miR-3107-3p	mmu-miR-3107*	0.812	0.031
mmu-miR-29b-2-5p	mmu-miR-29b-2*	0.846	0.037
mmu-miR-153-3p	mmu-miR-153	0.862	0.050
mmu-miR-127-5p	mmu-miR-127*	0.882	0.008
mmu-miR-2861	mmu-miR-2861	0.936	0.036
mmu-miR-874-3p	mmu-miR-874	0.967	0.004
mmu-miR-1902	mmu-miR-1902	1.023	0.030
mmu-miR-339-5p	mmu-miR-339-5p	1.031	0.005
mmu-miR-3473a	mmu-miR-3473	1.211	0.016
mmu-miR-3102-5p	mmu-miR-3102*	1.291	0.048
mmu-miR-211-3p	mmu-miR-211*	1.344	0.035
mmu-miR-92b-5p	mmu-miR-92b*	1.593	0.036

Supplemental Table 3: Comparison of top 5 down-regulated mRNAs and the top 15 up-regulated mRNAs identified by the Toray and Affymetrix arrays. The mRNAs listed were either up-regulated or down-regulated by food deprivation, compared to ad lib fed conditions. Only Cdkn1a mRNA is listed for both results.

Toray				Affymetrix			
Toray ID	**Gene Symbol**	**log2 Fold Change**	**p-value**	**ProbeSet ID**	**Gene Symbol**	**log2 Fold Change**	**p-value**
M400004082	Cx3cr1	-1.625	3.45E-02	6960210	Klk1b9	-1.468	2.85E-03
M300001463	Msr2	-1.585	8.32E-05	7018847	Itm2a	-1.345	1.59E-03
M300009616	XP_911710.2	-1.553	7.75E-03	6906652	Fcrls	-1.226	5.82E-03
M300020834	Tmem10	-1.539	9.60E-03	6824216	Gnpnat1	-1.202	1.17E-02
M300008313	Bfsp2	-1.511	5.87E-03	6855084	Aif1	-1.116	2.26E-03
M200012302	4930579C15Rik	2.005	1.73E-03	7018750	Atrx	1.219	1.75E-03
M400000667	Gabrr2	2.058	5.55E-04	6813742	Ctla2b	1.227	1.09E-02
M400004126	2810055G20Rik	2.084	3.31E-02	6770214	Cep290	1.244	1.32E-03
M400002014	Thoc2	2.106	1.40E-02	6779714	Ccdc88a	1.266	5.03E-04
M400002872	Ctla2a	2.110	1.18E-02	6964527	Htra1	1.278	2.54E-03

M200012925	Lrrcc1	2.113	2.37E-02	6854604	Fkbp5	1.302	7.21E-03
M200011815	Lrg1	2.130	8.14E-03	6908350	Amy1	1.330	1.84E-03
M400007614	XP_485832.4	2.170	1.63E-02	6867379	9330132A10Rik	1.455	5.71E-03
M200009277	Omd	2.180	3.77E-03	6982999	1810029B16Rik	1.496	9.39E-03
M400003407	BC005561	2.187	3.94E-02	6920745	Zfp292	1.533	6.54E-04
M200014260	Tmem52	2.241	3.95E-03	6992408	Spink8	1.568	1.00E-02
M300003896	Xdh	2.254	1.33E-02	6985659	Gcsh	1.700	4.71E-02
M300001921	Sgk	2.382	2.47E-05	6971280	Sult1a1	1.757	7.98E-04
M200007578	Cdkn1a	2.446	2.02E-03	6776873	A830054O04Rik	1.848	5.56E-03
M400007180	2810021G02Rik	2.710	2.03E-02	6849595	Cdkn1a	2.117	2.33E-04

Chapter 4

Quantitative proteomic analysis of hypothalamic proteins from wild type and Nhlh2 knockout mice: response to short-term fasting

Hao Jiang[2], W. Keith Ray[2], Roderick V. Jensen[3], Richard Helm[2,4] and Deborah J. Good[1,2,4]

Departments of Human Nutrition Foods and Exercise[1], Biochemistry[2], and Biological Sciences[3], and Program in Genomics, Bioinformatics and Computational Biology[4], Virginia Tech, Blacksburg, VA, 24061

Abstract

Energy balance is regulated by food intake and energy expenditure in the central nervous system (CNS). Accumulated evidence has shown that the hypothalamus plays an important role in the regulation of energy balance. As fasting leads to changes in both glucose availability for neurons, and general stress response, multiple changes in the hypothalamic proteome would be expected in response to reduced energy availability. The nescient helix-loop-helix 2 (Nhlh2) transcription factor regulates energy balance in the hypothalamus, through transcriptional regulation of several genes linked to obesity. Deletion of Nhlh2 in mice results in adult onset obesity. In this study, wild type (WT) and Nhlh2 knockout (N2KO) mice were either fasted for 24 hours, or were *ad libitum* (*ad lib*) fed. MS^E quantitative proteomics on total hypothalamic proteins identified over 650 proteins, including some proteins showing significantly different abundances between or among the four groups. A total of 53 proteins were differentially expressed between ad lib fed WT and N2KO mice, revealing linkages to pathways involving neurodegeneration and the citrate acid cycle (TCA). Overall, our results indicate that Nlhl2 role in the hypothalamic proteomic responses to the energy availability may be in regulating cell death, and mitochondrial energy generation.

Key words: MS^E quantitative proteomics, fasting, hypothalamus, TCA, neurodegeneration

1. Introduction

Energy balance is regulated by food intake and energy expenditure via a homeostatic system in the central nervous system (CNS). Significant evidence has accumulated to show that the hypothalamus plays a key role in the control of energy balance and many other biological processes, such as pituitary hormone secretion, salt and ingestion, body temperature regulation and aspects of behavior (Lightman 1988, Rao et al 2013). In addition, genetic approaches have provided solid evidence that monogenic changes, such as deletion or mutation of the genes for melanocortin-4-receptor, leptin, leptin receptor, and pro-opiomelanocortin (POMC), are linked to the energy balance control. It is expected that there are likely a multitude of changes that occur in the hypothalamic proteome in response to energy availability, but these changes have been characterized in only a few published studies (Kuhla et al 2007, Wang et al 2011). More studies are needed to further understand the mechanism of energy regulation in the hypothalamus, especially, within genetically obese animals.

Mass-spectrometry-based proteomics allows for the large-scale study of proteins in high throughput. It can unveil the complex regulation and relationships of signaling pathways, and therefore has great advantages in the study of brain (Kadakkuzha & Puthanveettil 2013). While several studies have been performed to identify proteins and neuropeptides within the hypothalamus under different treatments in rat (Gao et al 2013, Gasperini et al 2012), cow (Kuhla et al 2007), and mouse (Ihnatko et al 2013, Sarkar et al 2008), there is an apparent lack of follow-up or comparative quantitative studies that serve to provide abundance, distribution, or stoichiometry information for the identified proteins, in addition to the lists of

identified proteins in the system tested (Schulze & Usadel 2010). Although quantitative strategies can be evaluated by genetic approaches, including microarray, RNA sequencing (RNA-seq), and quantitative PCR analysis, several studies reported that protein abundance is independent of transcriptional control, due to such issues as post-transcriptional, translational and degradation regulation of amount of proteins (Vogel & Marcotte 2012). New quantitative proteomic techniques have been recently introduced, including two major approaches: isotope labeling and label-free techniques, with label-free quantitative proteomics considered to be a reliable, versatile, and cost-effective method (Neilson et al 2011). These new quantitative techniques are being widely used for quantitative proteomics including studies identify proteins and neuropeptides in the hypothalamus (Frese et al 2013, Stelzhammer et al 2012, Zhang et al 2012). Of note, these published studies protein information on the hypothalamic proteome, they are lack of information on energy balance. Use of quantitative proteomic techniques to measure diet induced changes in genetically-modified animals may help to answer underlying questions about changes in the proteome following changes in energy availability.

Nescient helix-loop-helix 2 (Nhlh2) is a member of the basic helix-loop-helix (bHLH) transcription factor family which has been found in proopiomelanocortin (POMC) neurons and thyrotropin-releasing hormone (TRH) neurons in the hypothalamus (Jing et al 2004). More importantly, Nhlh2 is one the only two genes that are genetically linked to physical activity levels (Good & Braun 2013). It interacts with signal transducer and activator of transcription 3 (Stat3) which acts to regulate the level of prohormone convertase 1/3 (PC1/3) mRNA, therefore, both αMSH and ACTH neuropeptide levels are reduced in Nhlh2 knockout

mice (N2KO) (Fox & Good 2008). It is believed that the lack of these fully processed neuropeptides is at least one cause of adult onset obesity in these animals (Good and Braun, 2013). While it is not yet clear how reduced physical activity in the N2KO mice is controlled. Recently, a NAD^+-dependent deacetylase protein, sirtuin 1 (Sirt1), was shown to deacetylate Nhlh2 and activate Nhlh2's ability to promote physical activity through modulation of monoamine oxidase levels (Libert et al 2011). As Nhlh2 is a leptin-regulated transcription factor (Al Rayyan et al 2014), with the potential of cause changes in the level of the hypothalamic proteins following changes in food intake or food deprivation, characterization of the hypothalamic proteome in N2KO mice is of crucial importance to further understand the role of Nhlh2 in both obesity and physical activity.

To better understand the role of Nhlh2 in the hypothalamus, here we applied a label-free quantitative proteomics technique to characterize proteins in the mouse hypothalamus with different genotypes (WT and N2KO) and two food availabilities (*ad lib* fed and 24h fasted). Over 650 proteins were identified, with some proteins showing significantly different abundances between or among the four groups, indicating an important role of Nhlh2 in the hypothalamus and the proteomic responses to the energy availability.

2. Experimental Procedures

2.1 Animals

The Institutional Animal Care and Use Committee at the Virginia Tech approved all studies. 129S/Sv wild type and Nhlh2 knockout line of mice were from our own colonies. Only male mice were used in this experiment so that estrous cycles did not have to be taken

into account during fasting. All mice were maintained under 12-h light/dark cycle with free access to food and water except as noted during experimentation. At the age of 8 to 10 weeks, mice were randomly separated to either a food deprived or *ad lib* group, food was removed for deprived mice at 9am. After 24h food deprivation, mice were euthanized using carbon dioxide, hypothalami were collected and frozen in liquid nitrogen immediately, and stored at -80°C until used.

2.2 Sample preparation

Hypothalamic proteins were extracted using the *mir*Vana™PARIS™Kit (Ambion, US) according to the manufacturer's procedure. Tissues were homogenized using ice-cold cell disruption buffer from the kit, the lysate was incubated on ice for 5-10 min and then centrifuged at 12000g for 15min at 4°C, the supernatant was kept at -80°C until use. After the protein extraction, the total protein concentration was determined using Bradford Protein Assay (Pierce, Rockford, IL). Approximately 100µg protein sample were precipitated using 4-fold volume of LC-MS methanol and incubation overnight at -20˚C. The protein pellets would have been resuspended in 100 µl 50 mM Tris-HCl (pH 8.0) containing 8 M urea. Protein reduction was performed with 4.5 mM DTT dissolved in 50 mM Tris-HCl (pH 8.0) at 37˚C for one hour and then alkylated using 50 mM iodoacetamide dissolved in 50 mM Tris-HCl (pH 8.0) for 30 minutes in the dark at room temperature. The reaction was quenched by adding an equimolar amount of DTT followed by dilution of the sample with 50 mM Tris-HCl (pH 8.0) to 1.4 M urea. Proteomics-grade trypsin (Sigma-Aldrich) were then added at 1:50 (w/w), i.e. 2 µg, to each sample and incubated overnight with shaking at 37˚C. Digestions were brought to 0.2% TFA and the pH was adjusted, if needed, to less than 3

using 98% formic acid. Solid-phase extraction was performed utilizing Sep-Pak Vac 1cc 50 mg C18 cartridges (Waters). Basically, the column was wetted with 1 ml LC-MS methanol followed by 1 ml 50:50 LC-MS water: LC-MS acetonitrile containing 0.1% TFA, and then equilibrated with 1 ml 98:2 LC-MS water: LC-MS acetonitrile containing 0.1% TFA, sample was loaded and then washed with 3 x 1 ml 98:2 LC-MS water: LC-MS acetonitrile containing 0.1% TFA. Peptides were eluted using 1 ml 50:50 LC-MS water: LC-MS acetonitrile containing 0.1% TFA and dried in centrifugal vacuum concentrator, and then resuspended in 100 µl 98:2 LC-MS water: LC-MS acetonitrile containing 0.1% TFA and stored at -20°C before usage.

2.3 LC-MS Configuration

N=3 mice for each genotype (WT and N2KO) as well as each food treatment (*ad lib* fed and 24h fasted) were used. Duplicated runs were performed for each sample. Sample equivalent to 1 µg of each desalted and concentrated digestion were injected twice (sample queue randomized) and were separated using an Acquity UPLC I-class system (Waters Corporation; Milford, MA). The mobile phases were 0.1 % formic acid (Sigma-Aldrich Corporation; St. Louis, MO) in LCMS-grade water (solvent A, Spectrum Chemicals & Laboratory Products; New Brunswick, NJ) and 0.1 % formic acid (Sigma-Aldrich Corporation; St. Louis, MO) in LCMS-grade acetonitrile (solvent B, Spectrum Chemicals & Laboratory Products; New Brunswick, NJ). The separation was performed using a CSH130 C18 1.7 µm, 1.0 x 150 mm column (Waters Corporation; Milford, MA) at 50 µL/min flow using a 110 minute gradient from 3-40% solvent B. The column temperature was maintained at 45˚C.

Sample was analyzed using a Synapt G2-S mass spectrometer (Waters Corporation; Milford, MA) using an HDMSe (high-definitionmass spectrometry with alternating scans utilizing low and elevated collision energies) acquisition method in continuum positive ion "resolution" MS mode. Source conditions were as follows: capillary voltage, 3.0 kV; source temperature, 120˚C; sampling cone, 60 V; desolvation temperature, 350˚C; cone gas flow, 50 L/hr; desolvation gas flow, 500 L/hr; nebulizer gas flow, 6 bar. Both low energy (4 V and 2 V in the trap and transfer region, respectively) and elevated energy (4 V in the trap and ramped from 20 to 50 V in the transfer region) scans were 1.2 seconds each for the m/z range of 50 to 1800. For ion mobility separation, the IMS and transfer wave velocities were 600 and 1200 m/sec, respectively. Wave height within the ion mobility cell was ramped from 10 to 40 V.

For lock-mass correction, a 1.2 second low energy scan was acquired every 30 seconds of a 100 fmol/µL [Glu1]-fibrinopeptide B (Waters Corporation; Milford, MA) solution (50:50 acetonitrile: water supplemented with 0.1 % formic acid) infused at 10 µL/min introduced into the mass spectrometer through a different source which was also maintained at a capillary voltage of 3.0 kV.

2.4 Data processing and protein quantification

Each peptide pool was processed using the ProteinLynx Global Server v 3.0 (Waters Corporation; Milford, MA). The complete mouse proteome including protein isoforms was downloaded from Uniprot (version 8/26/2013) and a randomized database consisting of 1 entry for each real entry was appended to the proteome utilizing PLGS 3.0. Apex3D data processing parameters were set to automatic for chromatographic peak width and MS TOF

resolution, ‘Lock Mass for Charge 2’ and ‘Lock Mass Window’ were set to 785.8426 m/z and ±0.25 Da, low energy threshold, elevated energy and bin intensity threshold were set to 250.0, 25.0 and 1000.0 counts. Duplicated runs for each sample were merged after processing. Merged processed data were then searched against mouse UniprotKB Proteomes FASTA database with the search parameter included ‘automatic’ peptide tolerance and fragment tolerance, one minimum fragment matches, 2 allowed missed cleavages, fixed modification of carbamidomethylation of cysteines, variable modifications of oxidation of methionine, acetylation of lysine, and phosphorylation of serine, threonine, or tyrosine, and 100% false discovery rate (required for later import into Scaffold). The identified processed peak list was exported by Scaffold plug-in for PLGS 3.0 and analyzed by Scaffold Q+ (Proteome Software). Data was searched against mouse UniprotKB Proteomes FASTA database with 1:3 non-default forward/decoy ratio and X! Tandem analysis. Legacy PeptideProphet scoring and standard experiment wide protein group were selected. Subset database search (only those previously identified by the searches using PLGS) was chosen for X! Tandem search, the search parameters included same fixed and variable modifications with the search in PLGS. Relative protein quantification was performed using Scaffold Q+, relative intensity values was calculated using top 3 precursor intensity method (i.e. IntensityE).

2.5 GO analysis

Gene ontology analysis was performed using GeneCodis3 (Carmona-Saez et al 2007, Nogales-Cadenas et al 2009, Tabas-Madrid et al 2012). Proteins passing the cutoff ($p \leq 0.05$) were used for the GO Biological Process, GO Molecular Function, GO Cellular Component,

and KEGG pathways analysis. For the settings of statistical parameters, the minimum number of genes was set to 2, and a hypergeometric statistical test and FDR *p*-value correction were used. The results were listed with corrected hypergeometric *p*-value.

2.6 E-box identification

E-box searching was performed with selected proteins based on significant level among the treatments and GO categories. Five hundred base pairs upstream to the transcriptional start site of gene sequences for each protein were used according to the NCBI GenBank database. Putative E-box sequences (CANNTG) were counted and recorded.

3. Results

3.1 Mouse hypothalamic proteome

Proteomic analysis revealed 44799 spectra corresponding to 677 unique proteins, with 1%FDR of protein threshold and each identified by at least two peptides with 99% confidence in Scaffold Q+. These proteins were further analyzed by GO analysis using GeneCodis3. The analysis revealed that 346 identified proteins were localized to the cytoplasm, 184 are mitochondrial-specific proteins. With screening of neural proteins, 33 proteins were localized to neuronal cell body, 29, 25, and 23 proteins are in the axon region, synapse region, and dendrite region, respectively (Figure 1A). Biological process analysis showed that the most abundant proteins were transport proteins, with 91 proteins involved in metabolic processes. Moreover, 59 proteins are associated with oxidation-reduction process, where 35 and 33 identified proteins are related to ATP and GTP catabolic process (Figure

1B). Furthermore, molecular functions analysis identified a total of 174 proteins with nucleotide binding function, and another 174 with a function of protein binding (Figure 1C).

3.2 Protein quantification and comparison among treatments

Among 677 identified proteins, of the 671 total proteins identified in the *ad lib* fed mice, only 499 of these proteins were found in both WT and N2KO mice in the fed state, a 74.4% overlap (Figure 2A). On the other hand, when compared the same genotype, 468 proteins were overlapped between WT *ad lib* fed and WT fasted mice (Figure 2B).

Quantification using Scaffold Q+ showed that 53 proteins were differentially expressed ($p \leq 0.05$) between WT and N2KO mice with *ad lib* feeding, whereas only 15 proteins were differentially expressed between two genotypes under fasted condition (Supplemental Table 1 & 2). On the other hand, total of 13 proteins are differentially expressed between WT and N2KO mice with *ad lib* fed, whereas 14 proteins were differentially expressed between fasted WT and N2KO mice (Supplemental Table 3 & 4).

With the comparison of all four groups of mice (Figure 3), several proteins, including as an example aldehyde dehydrogenase 2 mitochondrial (Aldh2) showed a similar trend across *ad lib* fed and fasted mice, but only had a significant lower abundance in N2KO mice compared with WT mice with *ad lib* fed. Conversely, significant *p*-value were found in eukaryotic translation elongation factor 2 (Eef2), electro transfer flavoprotein alpha polypeptide (Etfa), and glycerol-3-phosphate dehydrogenase 2 (Gpd2) in different genotypes with *ad lib* fed as well as WT mice with different food availabilities.

3.3 GO analysis of differentially expressed proteins

To further understand the differences in the hypothalamic proteome between WT and N2KO mice, a GO analysis was performed using all proteins showing significant changes proteins with *ad lib* feeding (Supplemental Table 1). In *ad lib* fed mice, a total of 53 proteins showed significantly differential expression between WT and N2KO mice. Among these proteins (Table 1), 27 proteins are localized in the mitochondrion (GO:0005739). Categories related to tricarboxylic acid cycle (TCA cycle) and NADH metabolic process were found in GO biological process analysis (GO:0006734, GO:0006099) and KEGG pathways analysis (KEGG:00020). Protein level differences for proteins involved in the TCA cycle (Kegg:00020) are shown in Figure 4. Interestingly, based on the KEGG pathway analysis, several proteins are involved in neurological disorders, such as Parkinson's (KEGG:05012), Huntington's (KEGG:05016), and Alzheimer's (KEGG:05010) diseases. Proteins in neurological disorder categories are shown in Figure 5.

3.4 E-box search for selected proteins

As Nhlh2 is a neuronal transcription factor that binds E-box regions (CANNTG) (Fox & Good 2008, Kruger et al 2004, Wankhade & Good 2011), 500 bp of the proximal promoter region of the genes encoding differentially-expressed proteins were screened for the presence of an E-box sequence. All selected proteins had at least one (Atp5c1) and up to six (Atp5o) putative E-box sequence within the selected region, with several of them (Atp5o, Cyc1, Ogdh, Sucla2, Aldh2, and eEF2) having at least one putative exact match E-box sequence to those previously identified in the proximal promoters of Nhlh2 target genes (Table 2).

4. Discussion

This study is the first to describe the label-free quantitative proteomic analysis of mouse hypothalamus with different food availabilities (*ad lib* fed and 24h fasted), as well as the first to describe the proteome in N2KO mouse hypothalamus. Data-independent analysis (DIA or MS^E) is a new quantitative label-free MS-based method. It is growing in popularity and driven the traditional identical proteomics to a more accurate and reliable quantitative method (Neilson et al 2011). Instead of protein identification, peptides identified through their MS/MS spectra are compared to the intensities of the MS peaks with MS^E analysis, this allows for not only the relative abundance of proteins, but also the absolute quantitative concentration of more than one protein at a time. Thus, MS^E method can provide quantitative data needed to address important biological questions (Craft et al 2013, Silva et al 2006). As the hypothalamic is extraordinarily complex for high-throughput approaches, the performance of accuracy and sensitivity were maximized using UPLC system and C_{18} column with Charged Surface Hybrid particles in this study, as these theoretically are able to improve loadability and peak capacities, and therefore enhance the resolution and sensitivity of the study (Kumar et al 2012, Lauber et al 2013). Overall, a total of 44799 spectra were obtained to identify 677 proteins from the mouse hypothalamus, which is slightly higher than comparable studies in rat (Gasperini et al 2012, Stelzhammer et al 2012) and mouse (Taraslia et al 2013). The higher rate of protein identification is probably due to the species specificity, and the use of the newly introduced method, combined with the new version of analysis software from Waters Corporation (Milford, MA) and Scaffold Q+ (Proteome Software, http://www.proteomesoftware.com/).

Among the identified proteins, 346 are cytoplasmatic proteins and 181 are nuclear proteins. In addition to the many structural proteins, proteins involved metabolic processes, such as oxidation-reduction process, ATP and GTP catabolic process, protein and proton transport, or cell cycle, were abundantly found. In KEGG pathways analysis, over 50 identified proteins have been associated with neurological disorders such as Huntington's disease and Alzheimer's disease, and another 17 proteins are linked to neurotrophin signaling pathways. These findings are similar to another label-free proteomic analysis in the rat hypothalamus (Stelzhammer et al 2012). However, instead of characterizing only the hypothalamus proteome, our study also reports comparisons between the mice with different genotypes and food availabilities.

More than 50 proteins are differentially expressed between WT and N2KO mice during *ad lib* feeding. Interestingly, using KEGG pathway analysis, six proteins, including Cytochrome C-1 (Cyc1), Cytochrome C somatic (Cycs), ATP synthase H+ transporting mitochondrial F1 complex gamma polypeptide 1 (Atp5c1), ATP synthase H+ transporting mitochondrial F1 complex alpha subunit 1 (Atp5a1), ATP synthase H+ transporting mitochondrial F1 complex O subunit (Atp5o), Voltage-dependent anion channel 3 (Vdac3), are linked to neurological disorders including Parkinson's, Huntington's, Alzheimer's disease. Cyc1 is the heme-containing component of the CoQ-cytochrome *c* reductase, which is also called oxidative phosphorylation (OXPHOS) Complex III, where Atp5a1, Atp5c1, and Atp5o are subunits of the ATP synthase, or OXPHOS Complex V. The lower levels of these four proteins in N2KO mice may cause deficiencies of OXPHOS complex III and V in the mitochondria, and therefore cause mitochondrial dysfunction. It has been reported that

mitochondrial dysfunction can alter mitochondrial dynamics and lead to neurodegenerative diseases, such as Parkinson's, Huntington's, and Alzheimer's disease (de Moura et al 2010, Johri & Beal 2012, Witte et al 2014). In addition, Cycs and Vdac3 are found in lower levels in N2KO mice. Cycs, a part of the mitochondrial electron transport chain between OXPHOS complex III and IV, is an intermediate in cellular apoptosis (Cai et al 1998, Goodsell 2004), whereas Vdac3, a channel protein in the mitochondrial outer membrane, is involved in the releasing of Cycs through the mitochondria (Lu et al 2013, Naranmandura et al 2012). Both proteins play a role in the activation of the caspase system, and therefore are involved in cellular apoptosis, possibly leading to neurodegeneration. However, the down-regulation of Cycs and Vdac3 in our case indicates that both proteins may act as rescue proteins and prevent cellular apoptosis from mitochondrial dysfunction. Overall, our study is the first study to describe the potential role of Nhlhl2 in mitochondrial dysfunction. With the increasing evidence that mitochondrial dysfunction contributes to damage and loss of axons and neurons (Witte et al 2014), our finding suggests that N2KO mice may provide a useful model for some neurodegenerative diseases. In support of this, Nhlh2 gene is overexpressed in the likely opposite condition, neuroblastoma tumors (Aoyama et al 2005)

In our study, five proteins, with low expression levels in N2KO mice compared with WT mice, are related to citrate cycle (TCA cycle), including Malate dehydrogenase 1 (Mdh1), Succinate-CoA ligase ADP-forming beta subunit (Sucla2), isocitrate dehydrogenase 3 gamma (Idh3g), oxoglutarate dehydrogenase (Ogdh), and isocitrate dehydrogenase 3 beta (Idh3b). In TCA cycle, Mdh1 catalyzes the reversible oxidation of malate to oxaloacetate, where Sucla2, the beta subunit of the ADP-forming succinyl-CoA synthetase, catalyzes the reversible ATP-

dependent synthesis from succinyl-CoA to succinate and CoA. Idh3b and Idh3g are subunits of isocitrate dehydrogenase 3, which functions in the oxidative decarboxylation of isocitrate to 2-oxoglutarate. Moreover, Ogdh, a subunit of the 2-oxoglutarate dehydrogenase complex, converts 2-oxoglutarate to succinyl-CoA and CO_2 via NAD^+/NADH system. All of these major enzymes of TCA cycle have a lower expression level in N2KO mice, indicating a potential lower oxidative capacity of TCA cycle in the hypothalamus of N2KO mice. In fact, under fasting condition, lower glucose level will reduce the glycolysis and result in lower level of acetyl-CoA, which is required to promote TCA cycle. Moreover, low capacity of TCA cycle could result in a low level of glutamate (from alpha-ketoglutarate) in the hypothalamic neurons ultimately affecting the synthesis of neurotransmitters in the brain (Mergenthaler et al 2013).

Other pathways involved in cellular energetics, namely through NAD+ generation, were also modulated in N2KO mice. GPD2 is a mitochondrial enzyme catalyzing the conversion of glycerol-3-phosphate to dihydroxyacetone phosphate via FAD/$FADH_2$ system, where ALDH2 converse aldehyde to carboxylate via NAD^+/NADH system. Both were significantly decreased in N2KO mice, and interestingly, four out of five proteins identified as lower in abundance in N2KO, and as associated with the TCA cycle, tend to increase the level of NAD^+. In fact, low glucose level under fasting condition can decrease glycolytic NAD^+ demand and therefore increase NADH oxidation and NAD^+ regeneration. In the case of N2KO mice, several proteins tend to increase the NAD^+ in N2KO mice. In conclusion, our finding provides a potential linkage between TCA cycle, as well as NAD^+ metabolism, and

the hypothalamic Nhlh2 transcription factor, and has provided us with future studies that can test the linkage and determine the molecular involvement of Nhlh2 in the NAD^+/NADH ratio.

In yet another example of proteins involved in energy generation and availability, ETFA was also significantly decreased under 24 h fasted conditions in both WT and N2KO mice, with the amount of ETFA protein in WT mice significantly higher than N2KO mice under both food availabilities. ETFA is involved in the mitochondrial fatty acid β-oxidation. This protein transfers the electrons from primary flavoprotein dehydrogenases to the main mitochondrial respiratory chain via the electron transfer flavoprotein ubiquinone oxidoreductase. The down-regulation of ETFA leads to a diminished degradation of fatty acids in the mitochondria (Tojo et al 2011). In fact, fatty acid metabolism has been considered to play a role in the regulation of energy balance in the hypothalamus (Ronnett et al 2006). Reduction of ETFA found in fasted and N2KO mice suggests that there could be lower fatty acid degradation via β-oxidation and lower electron transfer ability in the hypothalamus of these animals.

A key protein involved in the translation of proteins, eEF2, a member of the GTP-binding translation elongation factor family, is dramatically decreased to the point of nearly not being detectable in fasted WT mice, and in both fasted and fed N2KO mice, as compared with fed WT mice which show high expression of this protein. eEF2 and its phosphorylation activator, elongation factor 2 kinase (eEF2K), play an important role in the regulation of dendritic mRNA translation, the activation of eEF2 by eEF2K leads to a dramatic reduction of mRNA translation in dendrites (Heise et al 2014). At this time, there have been no published studies that confirm the role of eEF2 in any hypothalamic process. In addition,

differential regulation of the eEF2 gene has not been extensively studied in mammals. Our findings suggest that the eEF2 promoter might be a novel transcriptional target of Nhlh2, but more studies are needed to further define the transcriptional relationship between Nhlh2 and eEF2, and the role of eEF2 in fasted neurons.

When comparing WT and N2KO proteome, the majority of changed proteins are down-regulated in the N2KO mice compared with WT mice, suggesting that Nhlh2 might directly regulate the expression of these proteins. In fact, as a class II member of the bHLH family transcription factors, Nhlh2 is expected to regulate its target genes via an enhancer box region (E-box) (Fox & Good 2008, Kruger et al 2004, Wankhade & Good 2011). All proteins discussed in this study contain E-box motifs within the proximal promoter region of their encoding gene. In particular, the proximal promoters of 6 of the genes encoding for differentially-regulated proteins have at least one E-box region match to the previous identified sequences regulated by Nhlh2 (Fox & Good 2008, Kruger et al 2004, Wankhade & Good 2011), suggesting Nhlh2 could directly regulate their expression.

In conclusion, the new MS^E method has allowed for identification and quantification of over 600 hundred proteins in the mouse hypothalamus under fasting and *ad lib* conditions. In addition, the data has shown new proteins and associated pathways that appear to be differentially N2KO mouse model. Many of those pathways are involved in energy generation which complement and may explain the phenotype of N2KO mice—namely that of adult onset obesity and reduced physical activity. It is expected that these new data point to new possible pathways to explore within the hypothalamic transcriptional control of energy balance.

5. References

Al Rayyan, N., et al. (2014). "Leptin signaling regulates hypothalamic expression of nescient helix-loop-helix 2 (Nhlh2) through signal transducer and activator 3 (Stat3)." Mol Cell Endocrinol 384(1-2): 134-142.

Aoyama, M., et al. (2005). "LMO3 interacts with neuronal transcription factor, HEN2, and acts as an oncogene in neuroblastoma." Cancer Res 65(11): 4587-4597.

Cai, J., et al. (1998). "Mitochondrial control of apoptosis: the role of cytochrome c." Biochimica et Biophysica Acta (BBA) - Bioenergetics 1366(1–2): 139-149.

Carmona-Saez, P., et al. (2007). "GENECODIS: a web-based tool for finding significant concurrent annotations in gene lists." Genome Biol 8(1): R3.

Craft, G. E., et al. (2013). "Recent advances in quantitative neuroproteomics." Methods 61(3): 186-218.

de Moura, M. B., et al. (2010). "Mitochondrial dysfunction in neurodegenerative diseases and cancer." Environ Mol Mutagen 51(5): 391-405.

Fox, D. L. and D. J. Good (2008). "Nescient helix-loop-helix 2 interacts with signal transducer and activator of transcription 3 to regulate transcription of prohormone convertase 1/3." Mol Endocrinol 22(6): 1438-1448.

Frese, C. K., et al. (2013). "Profiling of diet-induced neuropeptide changes in rat brain by quantitative mass spectrometry." Anal Chem 85(9): 4594-4604.

Gao, Y., et al. (2013). "Proteomic analysis of differential proteins related to anti-nociceptive effect of electroacupuncture in the hypothalamus following neuropathic pain in rats." Neurochem Res 38(7): 1467-1478.

Gasperini, L., et al. (2012). "Proteomics of rat hypothalamus, hippocampus and pre-frontal/frontal cortex after central administration of the neuropeptide PACAP." Mol Biol Rep 39(3): 2921-2935.

Good, D. J. and T. Braun (2013). "NHLH2: at the intersection of obesity and fertility." Trends Endocrinol Metab 24(8): 385-390.

Goodsell, D. S. (2004). "The Molecular Perspective: Cytochrome c and Apoptosis." The Oncologist 9(2): 226-227.

Heise, C., et al. (2014). "Elongation factor-2 phosphorylation in dendrites and the regulation of dendritic mRNA translation in neurons." Front Cell Neurosci 8: 35.

Ihnatko, R., et al. (2013). "Proteomic profiling of the hypothalamus in a mouse model of cancer-induced anorexia-cachexia." Br J Cancer 109(7): 1867-1875.

Jing, E., et al. (2004). "Deletion of the Nhlh2 transcription factor decreases the levels of the anorexigenic peptides alpha melanocyte-stimulating hormone and thyrotropin-releasing hormone and implicates prohormone convertases I and II in obesity." Endocrinology 145(4): 1503-1513.

Johri, A. and M. F. Beal (2012). "Mitochondrial dysfunction in neurodegenerative diseases." J Pharmacol Exp Ther 342(3): 619-630.

Kadakkuzha, B. M. and S. V. Puthanveettil (2013). "Genomics and proteomics in solving brain complexity." Mol Biosyst 9(7): 1807-1821.

Kruger, M., et al. (2004). "NSCL-1 and NSCL-2 synergistically determine the fate of GnRH-1 neurons and control necdin gene expression." Embo j 23(21): 4353-4364.

Kuhla, B., et al. (2007). "Proteomics analysis of hypothalamic response to energy restriction in dairy cows." Proteomics 7(19): 3602-3617.

Kumar, A., et al. (2012). "UPLC: a preeminent technique in pharmaceutical analysis." Acta Pol Pharm 69(3): 371-380.

Lauber, M. A., et al. (2013). "High-resolution peptide mapping separations with MS-friendly mobile phases and charge-surface-modified C18." Anal Chem 85(14): 6936-6944.

Libert, S., et al. (2011). "SIRT1 activates MAO-A in the brain to mediate anxiety and exploratory drive." Cell 147(7): 1459-1472.

Lightman, S. L. (1988). "The neuroendocrine paraventricular hypothalamus: receptors, signal transduction, mRNA and neurosecretion." Journal of Experimental Biology 139(1): 31-49.

Lu, L., et al. (2013). "Voltage-dependent anion channel involved in the alpha-synuclein-induced dopaminergic neuron toxicity in rats." Acta Biochim Biophys Sin (Shanghai) 45(3): 170-178.

Mergenthaler, P., et al. (2013). "Sugar for the brain: the role of glucose in physiological and pathological brain function." Trends Neurosci 36(10): 587-597.

Naranmandura, H., et al. (2012). "Release of apoptotic cytochrome C from mitochondria by dimethylarsinous acid occurs through interaction with voltage-dependent anion channel in vitro." Toxicol Sci 128(1): 137-146.

Neilson, K. A., et al. (2011). "Less label, more free: approaches in label-free quantitative mass spectrometry." Proteomics 11(4): 535-553.

Nogales-Cadenas, R., et al. (2009). "GeneCodis: interpreting gene lists through enrichment analysis and integration of diverse biological information." Nucleic Acids Res 37(Web Server issue): W317-322.

Ronnett, G. V., et al. (2006). "Fatty Acid Metabolism, the Central Nervous System, and Feeding." Obesity 14(S8): 201S-207S.

Sarkar, P., et al. (2008). "Proteomic analysis of mouse hypothalamus under simulated microgravity." Neurochem Res 33(11): 2335-2341.

Schulze, W. X. and B. Usadel (2010). "Quantitation in mass-spectrometry-based proteomics." Annu Rev Plant Biol 61: 491-516.

Silva, J. C., et al. (2006). "Absolute quantification of proteins by LCMSE: a virtue of parallel MS acquisition." Mol Cell Proteomics 5(1): 144-156.

Stelzhammer, V., et al. (2012). "Analysis of the rat hypothalamus proteome by data-independent label-free LC-MS/MS." Proteomics 12(22): 3386-3392.

Tabas-Madrid, D., et al. (2012). "GeneCodis3: a non-redundant and modular enrichment analysis tool for functional genomics." Nucleic Acids Res 40(Web Server issue): W478-483.

Taraslia, V. K., et al. (2013). "Proteomic analysis of normal murine brain parts." Cancer Genomics Proteomics 10(3): 125-154.

Tojo, S., et al. (2011). "Catabolite repression of the Bacillus subtilis FadR regulon, which is involved in fatty acid catabolism." J Bacteriol 193(10): 2388-2395.

Vogel, C. and E. M. Marcotte (2012). "Insights into the regulation of protein abundance from proteomic and transcriptomic analyses." Nat Rev Genet 13(4): 227-232.

Wang, Q. M., et al. (2011). "Proteomic analysis of rat hypothalamus revealed the role of

ubiquitin-proteasome system in the genesis of DR or DIO." Neurochem Res 36(6): 939-946.

Wankhade, U. D. and D. J. Good (2011). "Melanocortin 4 receptor is a transcriptional target of nescient helix-loop-helix-2." Mol Cell Endocrinol 341(1-2): 39-47.

Witte, M. E., et al. (2014). "Mitochondrial dysfunction contributes to neurodegeneration in multiple sclerosis." Trends Mol Med 20(3): 179-187.

Zhang, X., et al. (2012). "High identification rates of endogenous neuropeptides from mouse brain." J Proteome Res 11(5): 2819-2827.

6. Figure Legends

Figure 1: Pathway analysis for all identified proteins. A. Top 20 GO categories of cellular component listed by the number of proteins. B. Top 20 GO categories of biological process listed by the number of proteins. C. Top 20 GO categories of molecular function listed by the number of proteins.

Figure 2: Comparison of identified proteins in each experimental group. A. Venn diagram comparing WT versus N2KO with *ad lib* fed. B. Venn diagram comparing WT *ad lib* fed versus 24h fasted mice.

Figure 3: Comparison of quantified relative expression level between selected proteins. Proteins were selected using the cut-off criteria at least between two treatments (* indicating $p \leq 0.05$ between WT AL and KO AL, # indicating $p \leq 0.05$ between both WT AL and KO AL, and WT AL and WT Fasted). Relative quantifications were calculated by Scaffold Q+, N=3 for each group with standard error shown.

Figure 4: Comparison of quantified relative expression levels between selected proteins in TCA cycle (Kegg:00020). Relative quantifications were calculated by Scaffold Q+, N=3 for each group, standard error was shown

Figure 5: Comparison of quantified relative expression levels between selected proteins in neurological disorders. Relative quantifications were calculated by Scaffold Q+, N=3 for each group, standard error was shown.

Table 1: GO analysis of significantly changed proteins between WT *ad lib* fed and N2KO *ad lib* fed animals.

Top 5 Biological Process			
GO Term	**Accession**	**Protein Count**	***p*-value**
NADH metabolic process	GO:0006734	5	3.40E-13
Tricarboxylic acid cycle	GO:0006099	5	7.01E-11
Transport	GO:0006810	14	8.50E-09
ATP catabolic process	GO:0006200	7	2.88E-08
Oxidation-reduction process	GO:0055114	9	7.58E-08
Top 5 Cellular Component			
GO Term	**Accession**	**Gene Count**	***p*-value**
Mitochondrion	GO:0005739	27	1.47E-25
Cytoplasm	GO:0005737	21	2.38E-07
Membrane	GO:0016020	17	0.000442
Plasma membrane	GO:0005886	9	0.007774
Mitochondrial inner membrane	GO:0005743	9	2.57E-10
Top 5 Molecular Function			
GO Term	**Accession**	**Gene Count**	***p*-value**
Oxidoreductase activity	GO:0016491	9	6.69E-08
Hydrogen ion transporting ATP synthase activity, rotational mechanism	GO:0046933	3	3.18E-07
Proton-transporting ATPase activity, rotational mechanism	GO:0046961	3	5.50E-07
Nucleotide binding	GO:0000166	13	8.53E-07
Isocitrate dehydrogenase (NAD+) activity	GO:0004449	2	4.76E-06
Top 5 KEGG pathways			
GO Term	**Accession**	**Gene Count**	***p*-value**
Citrate cycle (TCA cycle)	Kegg:00020	5	4.48E-10
Parkinson's disease	Kegg:05012	6	1.64E-08
Huntington's disease	Kegg:05016	6	1.06E-07
Oxidative phosphorylation	Kegg:00190	5	7.14E-07
Alzheimer's disease	Kegg:05010	5	2.36E-06

Table 2: Putative E-boxes found in promoter regions of selected protein-coding genes in Figure 3-5. Identified CANNTG that matched to the previously identified Nhlh2 targeted E-box sequences are highlighted in gray.

Protein Name	Reference mRNA Sequence	Selected Proximal Promoter Location	Identified CANNTG (E-Box) Sequence within -500 proximal promoter
Atp5a1	NM_007505.2	NC_000084.6: 77773268 – 77773768	CAGGTG; CACGTG
Atp5c1	NM_020615.4	NC_000068.7: 10055528 – 10056028	CATCTG
Atp5o	NM_138597.2	NC_000082.6: 91924721 - 91925221	CACATG; CATCTG; CACCTG; CAACTG; CACTTG; CATGTG
Cyc1	NM_025567.2	NC_000081.6: 76343023 - 76343523	CAAGTG; CAACTG; CAGATG
Cycs	NM_007808.4	NC_000072.6: 50562061 - 50562561	CAGTTG; CAAGTG
ETFA	NM_145615.4	NC_000075.6: 55453934 - 55454434	CACCTG; CACGTG; CAACTG
Gpd2	NM_001145820.1	NC_000068.7: 57237178 - 57237678	CAGGTG; CAATTG; CAAGTG; CAAGTG
Idh3b	NM_130884.4	NC_000068.7: 130278898 - 130279398	CACTTG; CAAGTG
Idh3g	NM_008323.1	NC_000086.7: 73778518 - 73779018	CACCTG; CAACTG
Ogdh	NM_001252282.1	NC_000077.6: 6291097 - 6291597	CAAGTG; CAGATG
Sucla2	NM_011506.3	NC_000080.6: 73552286 - 73552786	CAGCTG; CACTTG; CACATG; CAACTG
Vdac3	NM_001198998.1	NC_000074.6: 22576573 - 22577073	CAACTG; CAGTTG; CAGTTG
Aldh2	NM_009656.3	NC_000071.6: 121566845 - 121567345	CATGTG; CAGCTG; CACCTG; CAAGTG; CAAGTG
Mdh1	NM_008618.3	NC_000077.6: 21556190 - 21556690	CAGGTG; CAATTG
eEF2	NM_007907.2	NC_000076.6: 81176131- 81176631	CAACTG; CAAGTG; CAGCTG; CACGTG

Figure 1. Pathway analysis for all identified proteins.

A.

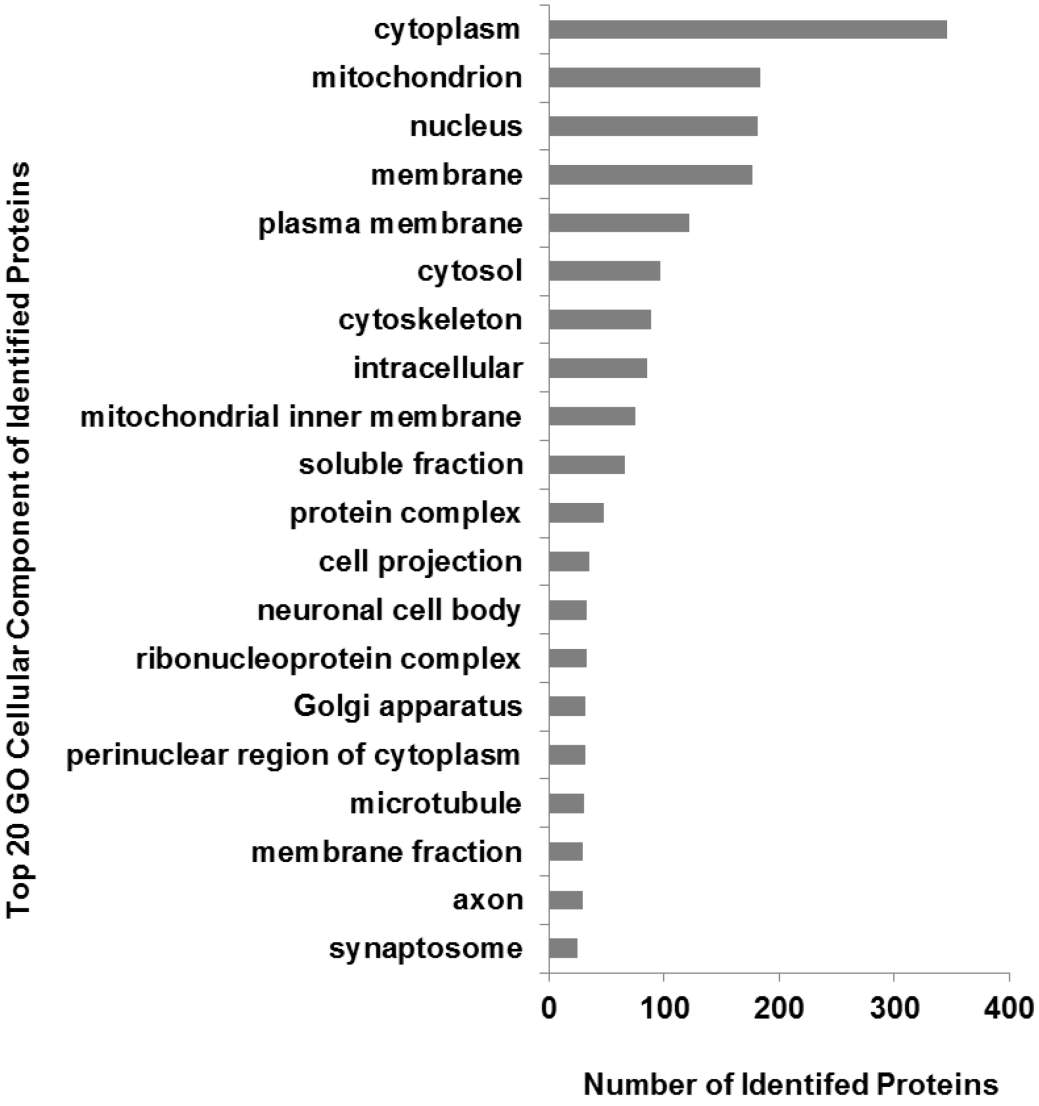

Figure 1. Pathway analysis for all identified proteins (Con.).

B.

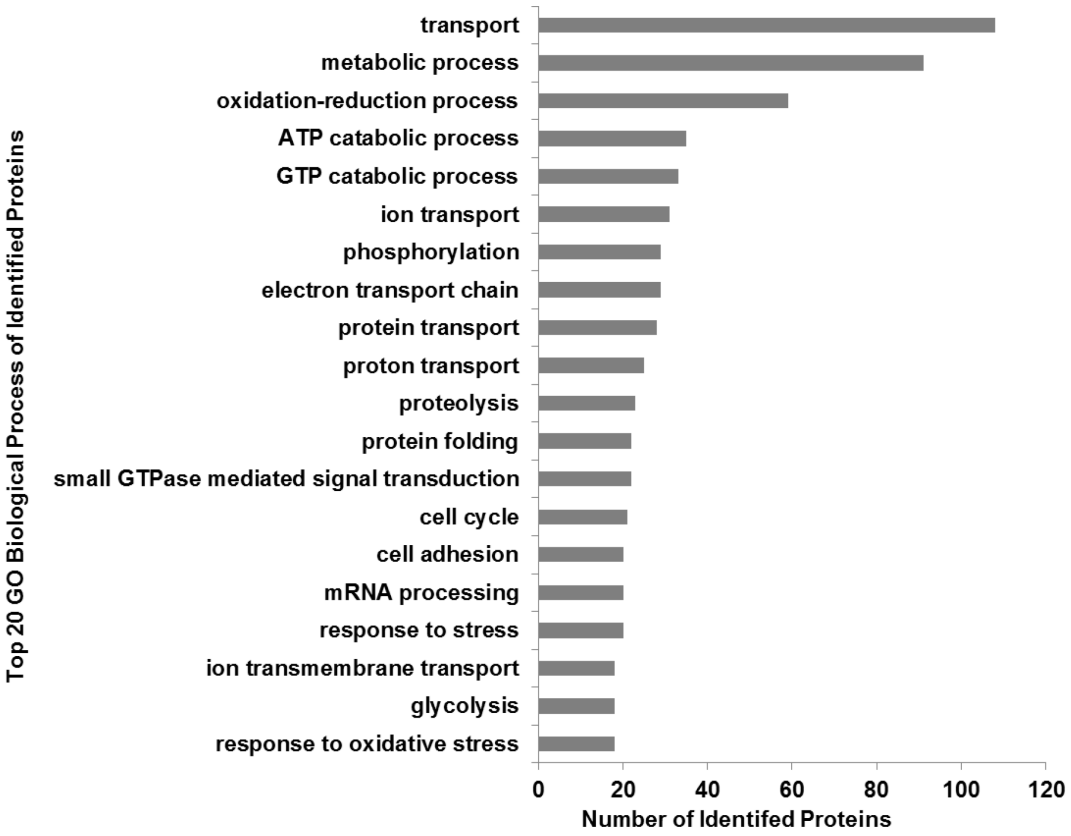

Figure 1. Pathway analysis for all identified proteins (Con.).

C.

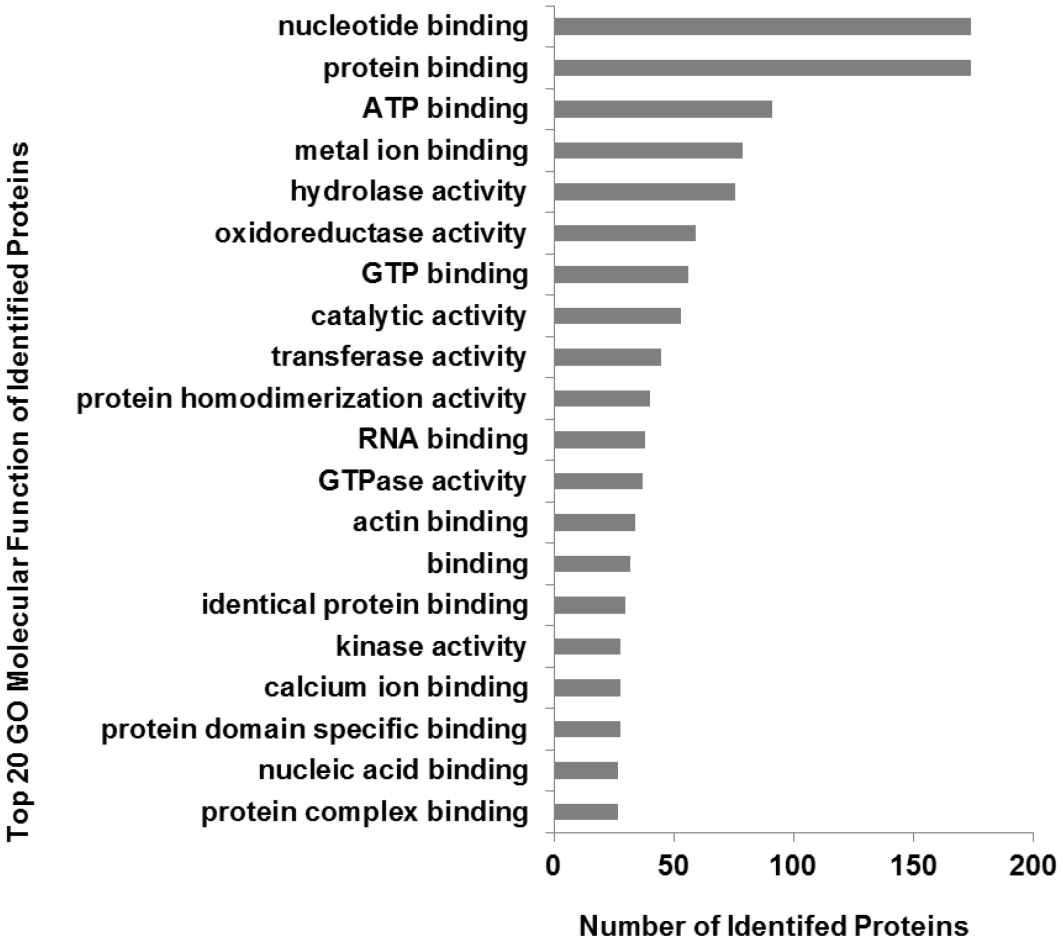

Figure 2. Comparison of identified proteins in each experimental group.

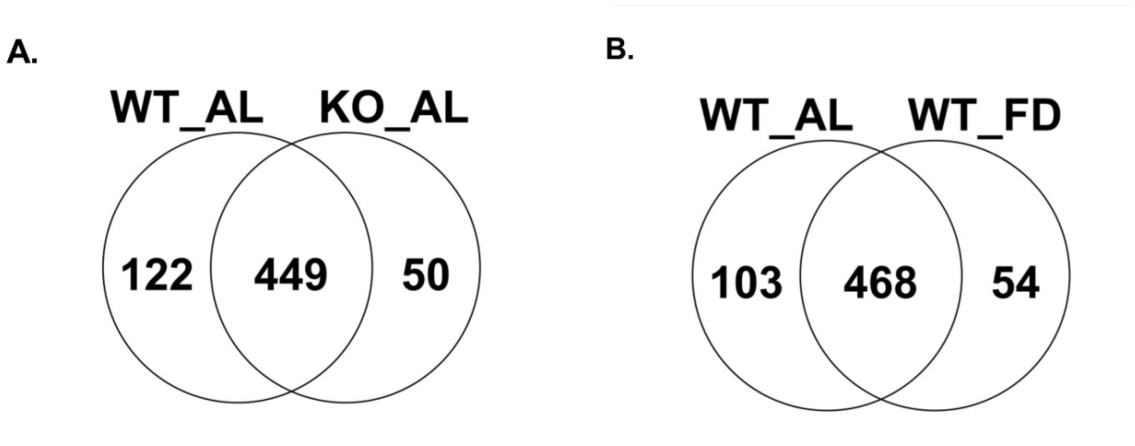

Figure 3. Comparison of quantified relative expression level between selected proteins.

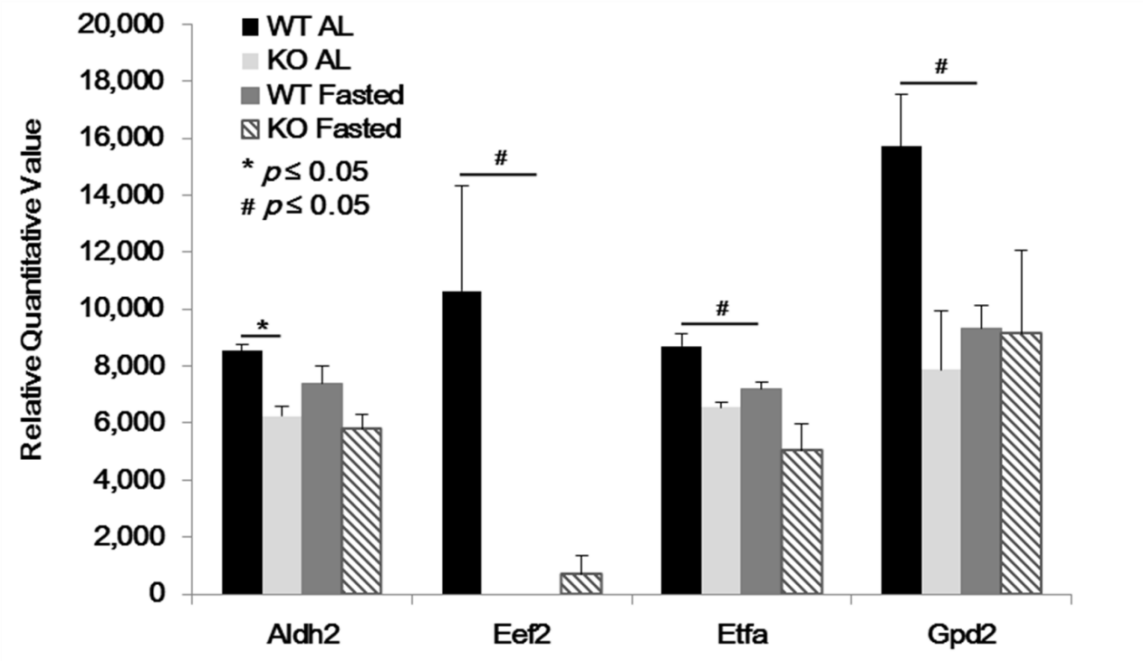

Figure 4. Comparison of quantified relative expression levels between selected proteins in TCA cycle (Kegg:00020).

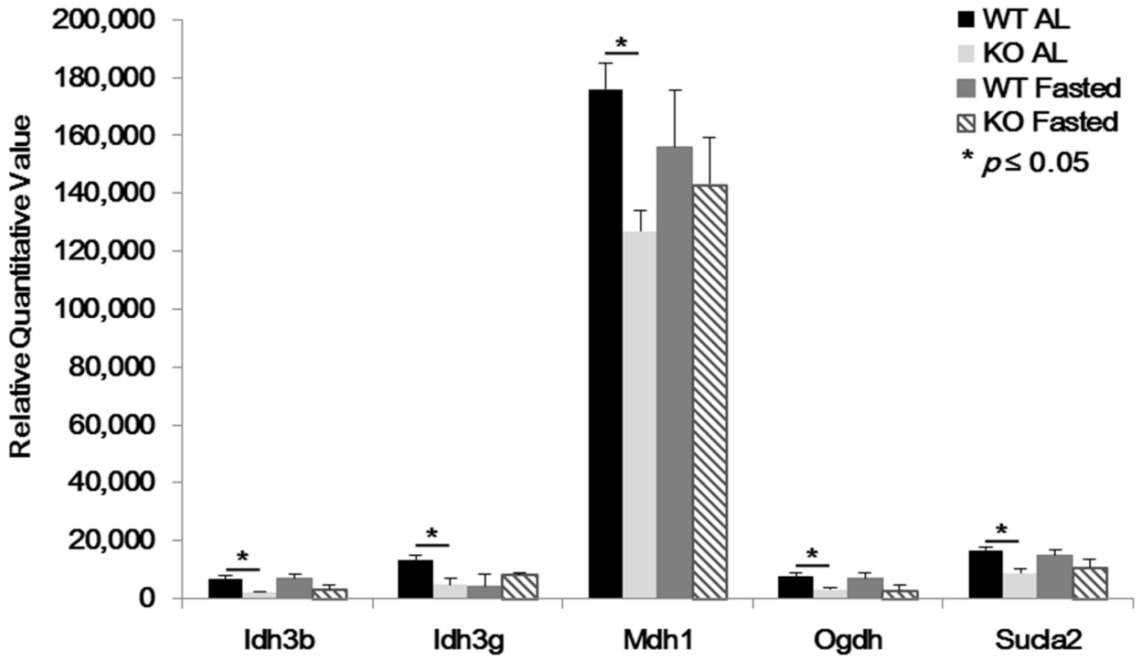

Figure 5. Comparison of quantified relative expression levels between selected proteins in neurological disorders.

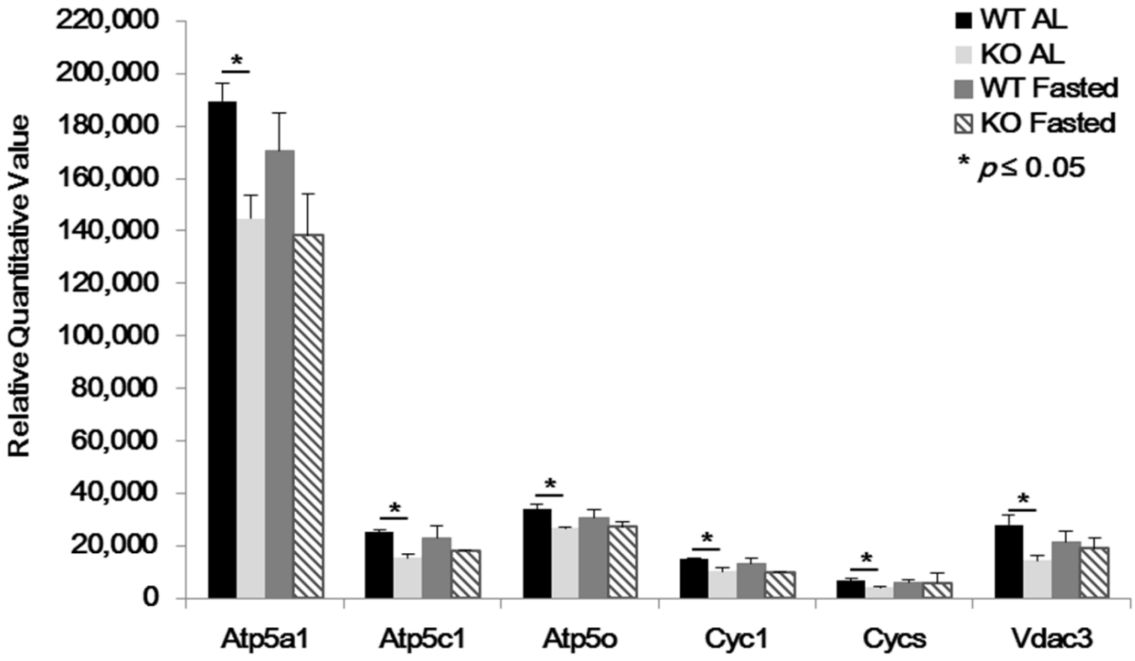

Supplemental Table 1: Proteins with significant expression differences between WT and N2KO, *ad lib* fed animals. Proteins are listed by *p*-value. (INF: infinity)

Protein Symbol	Description	Accession	Relative Quantitative Level		Standard Error		*p*-value	Fold Change (KO/WT)
			WT *Ad lib* fed	N2KO *Ad lib* fed	WT *Ad lib* fed	N2KO *Ad lib* fed		
Coro1c	Coronin-1C	Q9WUM4	6018.1	0	266.8	0	< 0.00010	INF
Pfn2	Profilin-2	Q9JJV2	27966.67	4475.3	2514.26	1389.03	0.0012	0.2
Hbb-b1	Hemoglobin subunit beta-1	P02088	193156.67	0	26162.85	0	0.0018	INF
H3f3a	Histone H3.3	P84244	0	6315.57	0	962.85	0.0028	INF
Aldh2	Aldehyde dehydrogenase 2	Q3U9J7	8545	6243.77	203.15	323.75	0.0038	0.7
Got2	Aspartate aminotransferase, mitochondrial	P05202	110110	67389.67	7130.29	2482.04	0.0048	0.6
Atp5c1	ATP synthase subunit gamma	Q3UD06	25203.33	15306.33	1085.11	1480.22	0.0057	0.6
Plp1	Myelin proteolipid protein	P60202	69547.33	42062.67	4779.02	2251	0.0065	0.6
Acot13	Acyl-coenzyme A thioesterase 13	Q4VA32	8729	910.67	1201.1	910.67	0.0066	0.1
Aldh2	Putative uncharacterized protein	Q3USR5	2123.87	0	421.56	0	0.0073	INF
Gstm1	Glutathione S-transferase Mu 1	P10649	28881.33	15279	2681.58	665.48	0.0079	0.5
Slc25a3	Phosphate carrier protein, mitochondrial	Q8VEM8	6336	819.67	794.42	819.67	0.0084	0.1
Snap91	Clathrin coat assembly protein AP180	Q61548	8823.23	2011.9	1442.65	393.82	0.01	0.2

Etfa	Electron transfer flavoprotein subunit alpha, mitochondrial	Q99LC5	8694.2	6542.8	444.56	192.17	0.011	0.8
Ubqln2	Ubiquilin-2	Q9QZM0	7971.67	5711.67	251.77	435.75	0.011	0.7
Mog	Myelin-oligodendrocyte glycoprotein	Q61885	25061.67	13707.33	1819.87	1849.23	0.012	0.5
Sucla2	Succinyl-CoA ligase [ADP-forming] subunit beta, mitochondrial	Q3U6C7	16669.67	8847.67	1076.51	1455.92	0.012	0.5
Mdh1	Malate dehydrogenase, cytoplasmic	P14152	176020	126960	9075.97	6974.42	0.013	0.7
Phyhipl	Phytanoyl-CoA hydroxylase-interacting protein-like	Q8BGT8	2894.73	0	698.97	0	0.014	0.6
Synj1	Synaptojanin-1	Q8CHC4	5127.47	2007.8	561.45	491.19	0.014	INF
Tkt	Transketolase	P40142	23371.33	14701.33	1302.19	1636.01	0.014	0.4
Atp5a1	ATP synthase subunit alpha, mitochondrial	Q03265	189483.33	144760	6916.85	8842.71	0.016	0.6
Cycs	Cytochrome c, somatic	P62897	6809.33	4113.97	634.22	229.72	0.016	0.8
Atp5o	ATP synthase subunit O, mitochondrial	Q9DB20	33974	26718.67	1813.73	450.77	0.018	0.4
Ogdh	2-oxoglutarate dehydrogenase, mitochondrial	Q60597	7639.1	3193.93	1111.84	302.68	0.018	0.8
Psma4	Proteasome subunit alpha type-4	Q9R1P0	4309.23	3178.97	174.84	242.67	0.019	0.7
Adss	Adenylosuccinate synthetase isozyme 2	P46664	2339.23	0	619.93	0	0.02	INF
Lap3	Cytosol aminopeptidase	Q9CPY7	8553.1	4625.37	1027.05	288.44	0.021	0.5
Atp1b1	Sodium/potassium-transporting ATPase subunit beta-1	P14094	112966.67	89342.67	2833.73	6223.06	0.026	0.8

Cyc1	Cytochrome c1, heme protein, mitochondrial	Q9D0M3	14903	10385.9	414.92	1241.48	0.026	0.3
Idh3b	Isocitrate dehydrogenase 3 (NAD+) beta	Q91VA7	6635.9	2139.8	1276.36	276.79	0.026	0.7
Rab35	RAB35, member RAS oncogene family	Q3U0T9	8078.1	0	2354.23	0	0.027	INF
Abat	4-aminobutyrate aminotransferase, mitochondrial	P61922	21835	9784.33	2878.07	2129.5	0.028	0.4
Nsf	Vesicle-fusing ATPase	P46460	39192.67	25881.33	3769.53	1369.13	0.029	0.7
Prdx3	Thioredoxin-dependent peroxide reductase, mitochondrial	P20108	16634.33	11106.33	1515.9	837.53	0.033	0.7
Slc25a22	Mitochondrial glutamate carrier 1	Q9D6M3	7515.43	3574.87	1160.61	476.69	0.035	0.5
Hsp90aa1	Heat shock protein HSP 90-alpha	P07901	58007.33	38945.33	6166.3	167.91	0.037	0.7
Qdpr	Dihydropteridine reductase	Q8BVI4	22110.67	16056	1770.09	837.77	0.037	0.9
Tubb5	Tubulin beta-5 chain	P99024	82907	72328	3172.67	1338.47	0.037	0.5
Vdac3	Voltage-dependent anion-selective channel protein 3	Q60931	27995.67	14288.67	3821.24	2271.41	0.037	0.7
Arpc4	Actin-related protein 2/3 complex subunit 4	P59999	5650.8	1005.67	1150.44	1005.67	0.038	0.2
Auh	Methylglutaconyl-CoA hydratase, mitochondrial	Q9JLZ3	7993.77	1953.43	287.02	1953.43	0.038	0.3
Idh3g	Isocitrate dehydrogenase [NAD] subunit gamma 1, mitochondrial	P70404	13390	4650.43	1652.13	2339.47	0.038	0.2
Rps7	40S ribosomal protein S7	P62082	5628.7	3494.1	440.91	547.34	0.039	0.6
Rab7a	Ras-related protein Rab-7a	P51150	7139.57	5291.33	552.81	266.54	0.039	0.7

Atp6v1e1	V-type proton ATPase subunit E 1	P50518	14057.67	9729.67	1173.92	861.6	0.041	0.7
Tagln3	Transgelin-3	Q9R1Q8	7758.33	5432.43	737.68	303.73	0.043	0.7
Eef2	Elongation factor 2	P58252	10623.07	0	3696.55	0	0.045	INF
Epb41l1	Band 4.1-like protein 1	Q9Z2H5	3888.87	932.67	419.01	932.67	0.045	0.2
Gpd2	Glycerol-3-phosphate dehydrogenase, mitochondrial	Q64521	15708.33	7874.43	1830.45	2079.74	0.047	INF
Mtpn	Myotrophin	P62774	5612.43	0	1978.54	0	0.047	0.5
Igsf8	Immunoglobulin superfamily member 8	Q8R366	12987.67	7414.87	501.49	1908.93	0.048	0.6
Cox4i1	Cytochrome c oxidase subunit 4 isoform 1, mitochondrial	P19783	21408	16224	357.05	1815.23	0.049	0.8

Supplemental Table 2: Proteins with significant expression differences between WT and N2KO, fasted animals. Proteins are listed by *p*-value**.** (INF: infinity)

Protein Symbol	Description	Accession	Relative Quantitative Level		Standard Error		*p*-value	Fold Change (KO/WT)
			WT Fasted	N2KO Fasted	WT Fasted	N2KO Fasted		
Acyp1	Acylphosphatase-1	P56376	3142.3	0	131.75	0	< 0.00010	INF
Tpd52	Tumor protein D52	Q62393	1973.43	0	224.44	0	0.00092	INF
Uqcrfs1	Cytochrome b-c1 complex subunit Rieske, mitochondrial	Q9CR68	24765.67	18315.33	645.21	492.73	0.0014	0.7
Cox7a2	Cytochrome c oxidase subunit 7A2, mitochondrial	P48771	5143.1	2027.43	478.67	284.6	0.005	0.4
Cntn1	Contactin-1	P12960	11869.67	8820.03	392.06	455.2	0.0071	0.7
Ndrg1	Protein NDRG1	Q62433	3648.37	957.47	300.06	484.99	0.0092	0.3
Hsd17b 10	17beta-hydroxysteroid dehydrogenase type 10/short chain L-3-hydroxyacyl-CoA dehydrogenase	Q99N15	2054.23	306.22	214.73	306.22	0.0095	0.1
Ywhaq	14-3-3 protein theta	P68254	3329.73	427.37	609.85	224.04	0.011	0.1
Cttn	Src substrate cortactin	Q60598	2383.87	0	551.37	0	0.012	INF
Nudt3	Diphosphoinositol polyphosphate phosphohydrolase 1	Q9JI46	2670.53	509.67	369.38	509.67	0.026	0.2
Dmtn	Dematin	Q9WV69	0	3015.77	0	886.04	0.027	INF
Ptms	Ptms protein	Q66JR8	7934.47	4453.67	1052.68	288.22	0.033	0.6
Rps21	40S ribosomal protein S21	Q9CQR2	0	8390.43	0	2681.74	0.035	INF
Napg	Gamma-soluble NSF attachment protein	Q9CWZ7	6079	4458.67	114.64	516.88	0.038	0.7
Lsamp	Limbic system-associated membrane protein	Q8BLK3	2766.43	580	707.23	292.3	0.046	0.2

Supplemental Table 3: Proteins with significant expression differences between *ad lib* fed and fasted WT animals. Proteins are listed by *p*-value. (INF: infinity)

Protein Symbol	Description	Accession	Relative Quantitative Level		Standard Error		*p*-value	Fold Change (Fasted/Ad lib)
			WT *Ad lib* Fed	WT Fasted	WT *Ad lib* Fed	WT Fasted		
Epb41l1	Band 4.1-like protein 1	Q9Z2H5	3888.87	0	419.01	0	0.00075	INF
Nudt3	Diphosphoinositol polyphosphate phosphohydrolase 1	Q9JI46	0	2670.53	0	369.38	0.0019	INF
Ywhaq	14-3-3 protein theta	P68254	642.96	3329.73	172.48	609.85	0.013	5.2
Pkm	Pyruvate kinase PKM	P52480	20534.33	10532.47	1538.63	1743.41	0.013	0.5
Ubqln2	Ubiquilin-2	Q9QZM0	7971.67	5886.23	251.77	434.68	0.014	0.7
Coro1c	Coronin-1C	Q9WUM4	6018.1	2018.77	266.8	1014.61	0.019	0.3
Gpd2	Glycerol-3-phosphate dehydrogenase, mitochondrial	Q64521	15708.33	9336.57	1830.45	794.67	0.033	0.6
Snap91	Clathrin coat assembly protein AP180	Q61548	8823.23	4111.13	1442.65	390.29	0.034	0.5
Etfa	Electron transfer flavoprotein subunit alpha, mitochondrial	Q99LC5	8694.2	7192.23	444.56	236.86	0.041	0.8
Akr1b1	Aldose reductase	P45376	5609.2	3383.47	526.41	559.2	0.044	0.6
Eef2	Elongation factor 2	P58252	10623.07	0	3696.55	0	0.045	INF
Ptms	Ptms protein	Q66JR8	4881.8	7934.47	236.25	1052.68	0.047	1.6

Supplemental Table 4: Proteins with significant expression differences between *ad lib* fed and fasted N2KO animals. Proteins are listed by *p*-value. (INF: infinity)

Protein Symbol	Description	Accession	Relative Quantitative Level		Standard Error		*p*-value	Fold Change (Fasted/ Ad lib)
			N2KO *Ad lib* Fed	N2KO Fasted	N2KO *Ad lib* Fed	N2KO Fasted		
Map4	Microtubule-associated protein 4	P27546	6028.1	0	335.01	0	< 0.00010	INF
Tpd52	Tumor protein D52	Q62393	1699.47	0	65.33	0	< 0.00010	INF
H3f3a	Histone H3.3	P84244	6315.57	0	962.85	0	0.0028	INF
Pkm	Pyruvate kinase PKM	P52480	96775	111970	2707.59	2751.77	0.017	1.2
Kiaa1045	Protein KIAA1045	Q80TL4	5461.53	0	1478.31	0	0.021	INF
Kdr	Vascular endothelial growth factor receptor 2	P35918	3303.3	0	913.4	0	0.022	INF
Anp32a	Acidic leucine-rich nuclear phosphoprotein 32 family member A	O35381	3741.57	2722.53	243.76	162.19	0.025	0.7
Phyhipl	Phytanoyl-CoA hydroxylase-interacting protein-like	Q8BGT8	0	1661.01	0	504.86	0.03	INF
Got2	Aspartate aminotransferase, mitochondrial	P05202	67389.67	79041.67	2482.04	2521.7	0.03	1.2
Mapt	Microtubule-associated protein tau	P10637	33367	23163.67	722.49	3084.93	0.032	0.7
Rab35	RAB35, member RAS oncogene family	Q3U0T9	0	4250.87	0	1334.28	0.033	INF
Plp1	Myelin proteolipid protein	P60202	42062.67	56011.33	2251	3765.41	0.034	1.3
Hsd17b10	17beta-hydroxysteroid dehydrogenase type 10/short chain L-3-hydroxyacyl-CoA dehydrogenase	Q99N15	1348.03	306.22	165.66	306.22	0.04	0.2
Coro1c	Coronin-1C	Q9WUM4	0	1951.23	0	655.42	0.041	INF

Chapter 5

Implications and future directions

The results of our global analysis of the hypothalamic transcriptome and proteome in response to 24 hour fasting have implicated both the control of the cell cycle, and mitochondrial energy generation as targeted pathways. We have also shown that microRNA regulation of the transcriptome and proteome is not a major control point following fasting. Overall, the results have provided a number of avenues for future investigation.

More and more studies have demonstrated the role of microRNAs in the brain, our findings suggest that acute changes in microRNA levels does not occur in response to 24 hour fasting. Although several microRNAs showed significant induction or reduction by fasting using microRNA array analysis, none of the selected microRNAs were confirmed by QPCR in new hypothalamic studies. It is also possible that the differentially-regulated microRNAs were hypothalamic-nuclei-specific changes, that were masked by using whole hypothalamus. Some of those that we detected as changed, may show change if examined using ARC- or PVN-specific RNA samples, and this is an area of possible future study. It is however, possible that microRNAs response to negative energy balance in other situations, involving either IF or CR, rather than 24-hour fasting. For example, one study showing miR-34a, miR-30e, and miR-181a are down-regulated by CR, result in changes of Caspase cleaving levels, could have a putative contribution to the neuronal survival in long-lived CR mice (Khanna et al 2011). Based on this study, and another more recent study of rat hypothalamic microRNAs with 48-hour fasting (Sangiao-Alvarellos et al 2014), a possible future experiment using longer periods of fasting is proposed. Meanwhile, as mentioned earlier, due to the fact that different hypothalamic nuclei might play a different role in the regulation of energy balance, and therefore, might have an

completely opposing expression patterns, it is necessary to work with different nuclei separately in order to explore nuclei-specific microRNA, mRNA, and proteomics changes.

The RNAome or transcriptome is complex with mRNA, microRNA and long non-coding RNA (lncRNA). The long non-coding RNA transcripts, which do not code for protein are poorly studied. In preliminary studies, which will be the basis of future studies in the Good laboratory, different expression patterns for some lncRNA species were found in total hypothalalmic RNA samples isolated from *ad lib* fed, fasting, and leptin retreatment groups (Figure 1 A). This study is based on the re-annotation of over 4 million probes in Affymetrix Mouse Exon 1.0 ST array to make the lncRNA analysis with the exon array capable (Cao et al 2013, Gellert et al 2013). With these methods, using the cut-off criteria of $P \leq 0.05$ and fold change ≥ 1.5, the total of 904 hypothalamic lncRNAs were differently expressed between *ad lib* fed and fasting mouse, whereas 298 lncRNAs were differentially expressed between fasting and leptin retreatment mouse. With n = 3 - 4 per group, the expression of several selected lncRNAs were confirmed with QPCR analysis (Figure 1, B). In fact, it has been reported over half of all lncRNAs identified to date are expressed in the CNS, and as such, these lncRNAs are expected to be important for mediating nervous system development, homeostasis, neurodegenerative, as well as all other CNS functions and processes (Iyengar et al 2014, Qureshi et al 2010, Qureshi & Mehler 2013). Compared with our microRNA results, the study of lncRNAs provides us a new direction of the role of non-coding RNAs in the regulation of gene/protein in the CNS. lncRNA-mediated rather than microRNA-mediated mechanisms might play an important of role of hypothalamic gene expression. At this point, more studies are needed on the molecular and cellular mechanisms on these lncRNAs to further understand their function in the hypothalamus. The work presented here provides a basis for starting these types of studies in the future.

In our microarray analysis, several cell cycle genes were differentially expressed between *ad lib* fed and fasted hypothalamic lysates. With the expression of 7 genes were confirmed by QPCR. p21 was one of the most significantly induced "fasting" genes (Figure 2 A). Interestingly, a recent study reported that the fasting induced p21 expression is driven by forkhead box O1 (FOXO1) protein (Tinkum et al 2013). Moreover, p21 expression is localized to specific regions of the brain, including the paraventricular, arcuate, and dorsomedial nuclei of the hypothalamus (Tinkum et al 2013). The localization of p21 in the hypothalamus implicates a potential role of p21 in the energy balance. Additionally, preliminary data in our lab, using a N29/2 hypothalamic cell line, has confirmed the in vivo changes in p21, and further shown that the fasting-induced p21 mRNA level can be reduced by leptin retreatment (Figure 2 B), but not with insulin level. Therefore, the expression of p21 in the hypothalamus might be regulated by a similar system as AgRP, in other words, the p21 expression is potentially inhibited by leptin-JAK-STAT3 pathway and induced by insulin-Akt-FoxO1 pathway. Whether the fasting-induced p21 expression is associated with the cell cycle progress and the function of p21 in the hypothalamus remain unknown, however these possible mechanisms can be explored.

Fasting induced p21 expression could be result of either cell cycle arrest in response to stress stimuli during fasting (Figure 3, #1); or induction by other down-stream signals of fasting (Figure 3, #2). For example, it has been reported that leptin is associated with the expression of brain-derived neurotropic factor (BDNF) in the hypothalamus (Liao et al 2012). While it is also suggested that BDNF contributes to the hippocampal neurogenesis induced by dietary restriction (Lee et al 2002). These findings indicate a potential relation of BDNF on p21 expression. On the other hand, p21 plays different roles in neuronal cell cycle process. For example, p21 can restrict neuronal proliferation in the hippocampus (Pechnick et al 2011, Pechnick et al 2008, Zonis et al

2013), it can also protects hippocampal neuronal progenitors from apoptosis under inflammation (Zonis et al 2013). Therefore, the function of induced p21 expression in the hypothalamus also has different possibilities. Up-regulated p21 may either arrests neuronal cell cycle and restricts neurogenesis, or protects neuronal apoptosis from stress (Figure 3, #3 and #4). Future studies in this area that may be pursued by the Good laboratory include an investigation of whether these cell cycle related genes promote neuronal cell cycle process in the hypothalamus, Long-term and/or short term fasting protocols could be employed to help us to understand the function of these cell cycle related genes and the mechanisms of neurogenesis and neuronal apoptosis.

Our study is the first to utilize label-free quantitative proteomic analysis of mouse hypothalamus with different food availabilities (*ad lib* fed and 24h fasted), as well as the first to describe the proteome in N2KO mouse hypothalamus. Comparison between WT and N2KO proteome unveiled that protein involved in mitochondria function linked Nhlh2 to the neurodegenerations, neurodegenerative diseases. Based on these findings, one possible future direction for the Good laboratory would be to examine the potential linkage between Nhlh2 and neurodegeneration. No studies have yet looked for any neuroanatomical or neurodegenerative changes in aged N2KO mice. There is some evidence that leptin resistance in obesity can correlate with reduced neuroprotection on aging (Davis et al 2014). With the US population median age increasing, this could be an important area of study.

Interestingly, mitochondrial dysfunction has been reported in individuals with insulin resistance and type 2 diabetes mellitus, and is thought to contribute to the ectopic fat accumulation in muscle and fat (Petersen & Shulman 2006). Therefore, the potential mitochondria dysfunction may be also linked to the adult onset obesity of N2KO mice. In new findings, we also showed that several key enzymes of TCA cycle had lower protein abundance in

N2KO mice, indicated a potential lower oxidative capacity of TCA cycle in the N2KO hypothalamus. Low capacity of TCA cycle may be also associated with the phenotype of N2KO mice. It can cause low level of its intermediate, citrate. Where several studies have been reported that citrate can inhibit hypothalamic AMP-activated protein kinase pathway and lead to a decrease in food intake and diminish weight gain (Cesquini et al 2008, Stoppa et al 2008). Therefore, it is expected that the potential low level of citrate in the N2KO mouse hypothalamus may have a compensation effect and increase the weight gain of N2KO mice. Future investigations into the role of Nlhl2 in controlling TCA cycle genes, and the overall effects of lower TCA cycle on the phenotype of N2KO mice is an important avenue of study. The results of these types of future endeavors could help to build a linkage between genotype and phenotype of N2KO mice, as well as more thoroughly understand the role of Nhlh2 in mitochrondrial metabolism pathways.

The role of Nhlh2 in modulating the hypothalamic proteomic may be explained in Figure 4. As a bHLH transcription factor, Nhhl2 regulates PC1/3 gene transcription resulting in processing of the POMC neuropeptide within hypothalamic neuron (Fox & Good 2008). In N2KO mice, the leptin – POMC signal is blocked or decreased due to the absence of Nhlh2, resulting in low PC1/3 levels, as well as levels of other Nhlh2 target genes (Good & Braun 2013, Wankhade & Good 2011). Interestingly, all select proteins identified by our proteomics study as differentially regulated in N2KO, compared to WT mice, have at least one putative E-box region. These proteins were all found to be lower in abundance in N2KO mice under ad lib feeding conditions. These results suggest that some or all of the genes encoding these proteins may be direct transcriptional targets of Nhlh2, and provide us with new potential Nhlh2 targets and roles for Nhlh2 in mitochondrial and metabolic pathways within the hypotyhalamus.

Overall, these studies have provided us with solid results on the absolute levels of hypothalamic microRNA, mRNA, and protein between *ad lib* fed and fasted mice, as well as WT and N2KO mice. The microRNA study suggests that the role microRNA in response to short-term fasting is not dominant in the mouse hypothalamus. The induction or deduction of numerous RNAs suggests that the expression of hypothalamic mRNAs might play a primary role in the response to short-term fasting. Fasting-induced p21 expression, as well as other cell cycle genes, indicates a potential fasting associated neuronal cell cycle progress. More importantly, the proteomics study gives us a new insight of the role of Nlhlh2 in response to fasting, and its function in neurodegeneration and oxidative metabolic pathway.

1. References:

Al Rayyan N, Zhang J, Burnside AS, Good DJ. 2014. Leptin signaling regulates hypothalamic expression of nescient helix-loop-helix 2 (Nhlh2) through signal transducer and activator 3 (Stat3). *Molecular and cellular endocrinology* 384: 134-42

Aoyama M, Ozaki T, Inuzuka H, Tomotsune D, Hirato J, et al. 2005. LMO3 interacts with neuronal transcription factor, HEN2, and acts as an oncogene in neuroblastoma. *Cancer research* 65: 4587-97

Bak M, Silahtaroglu A, Moller M, Christensen M, Rath MF, et al. 2008. MicroRNA expression in the adult mouse central nervous system. *Rna* 14: 432-44

Bodkin NL, Alexander TM, Ortmeyer HK, Johnson E, Hansen BC. 2003. Mortality and morbidity in laboratory-maintained Rhesus monkeys and effects of long-term dietary restriction. *The journals of gerontology. Series A, Biological sciences and medical sciences* 58: 212-9

Cai J, Yang J, Jones D. 1998. Mitochondrial control of apoptosis: the role of cytochrome c. *Biochimica et Biophysica Acta (BBA) - Bioenergetics* 1366: 139-49

Cao WJ, Wu HL, He BS, Zhang YS, Zhang ZY. 2013. Analysis of long non-coding RNA expression profiles in gastric cancer. *World journal of gastroenterology : WJG* 19: 3658-64

Carmona-Saez P, Chagoyen M, Tirado F, Carazo JM, Pascual-Montano A. 2007. GENECODIS: a web-based tool for finding significant concurrent annotations in gene lists. *Genome biology* 8: R3

Cesquini M, Stoppa GR, Prada PO, Torsoni AS, Romanatto T, et al. 2008. Citrate diminishes hypothalamic acetyl-CoA carboxylase phosphorylation and modulates satiety signals and hepatic mechanisms involved in glucose homeostasis in rats. *Life Sciences* 82: 1262-71

Chiu H, Alqadah A, Chang C. 2014. The role of microRNAs in regulating neuronal connectivity. *Frontiers in cellular neuroscience* 7: 283

Clark TA, Schweitzer AC, Chen TX, Staples MK, Lu G, et al. 2007. Discovery of tissue-specific exons using comprehensive human exon microarrays. *Genome biology* 8: R64

Coyle CA, Jing E, Hosmer T, Powers JB, Wade G, Good DJ. 2002. Reduced voluntary activity precedes adult-onset obesity in Nhlh2 knockout mice. *Physiology & behavior* 77: 387-402

Craft GE, Chen A, Nairn AC. 2013. Recent advances in quantitative neuroproteomics. *Methods* 61: 186-218

Davis C, Mudd J, Hawkins M. 2014. Neuroprotective effects of leptin in the context of obesity and metabolic disorders. *Neurobiology of disease*

De Leeuw F, Zhang T, Wauquier C, Huez G, Kruys V, Gueydan C. 2007. The cold-inducible RNA-binding protein migrates from the nucleus to cytoplasmic stress granules by a methylation-dependent mechanism and acts as a translational repressor. *Experimental cell research* 313: 4130-44

de Moura MB, dos Santos LS, Van Houten B. 2010. Mitochondrial dysfunction in neurodegenerative diseases and cancer. *Environmental and molecular mutagenesis* 51: 391-405

Del Vescovo V, Meier T, Inga A, Denti MA, Borlak J. 2013. A Cross-Platform Comparison of Affymetrix and Agilent Microarrays Reveals Discordant miRNA Expression in Lung Tumors of c-Raf Transgenic Mice. *PloS one* 8: e78870

Dietrich MO, Horvath TL. 2013. Hypothalamic control of energy balance: insights into the role

of synaptic plasticity. *Trends in neurosciences* 36: 65-73
Earls LR, Westmoreland JJ, Zakharenko SS. 2014. Non-coding RNA regulation of synaptic plasticity and memory: Implications for aging. *Ageing research reviews*
Ebert MS, Sharp PA. 2012. Roles for microRNAs in conferring robustness to biological processes. *Cell* 149: 515-24
Fassan M, Sachsenmeir K, Rugge M, Baffa R. 2011. Role of miRNA in distinguishing primary brain tumors from secondary tumors metastatic to the brain. *Frontiers in bioscience* 3: 970-9
Fox DL, Good DJ. 2008. Nescient helix-loop-helix 2 interacts with signal transducer and activator of transcription 3 to regulate transcription of prohormone convertase 1/3. *Molecular endocrinology* 22: 1438-48
Franceschini A, Szklarczyk D, Frankild S, Kuhn M, Simonovic M, et al. 2013. STRING v9.1: protein-protein interaction networks, with increased coverage and integration. *Nucleic acids research* 41: D808-15
Frese CK, Boender AJ, Mohammed S, Heck AJ, Adan RA, Altelaar AF. 2013. Profiling of diet-induced neuropeptide changes in rat brain by quantitative mass spectrometry. *Analytical chemistry* 85: 4594-604
Fu C, Xi L, McCarter R, Hickey M, Han ES. 2006. Early hypothalamic response to age-dependent gene expression by calorie restriction. *Neurobiology of aging* 27: 1315-25
Gao Y, Chen S, Xu Q, Yu K, Wang J, et al. 2013. Proteomic analysis of differential proteins related to anti-nociceptive effect of electroacupuncture in the hypothalamus following neuropathic pain in rats. *Neurochemical research* 38: 1467-78
Gasperini L, Piubelli C, Carboni L. 2012. Proteomics of rat hypothalamus, hippocampus and pre-frontal/frontal cortex after central administration of the neuropeptide PACAP. *Molecular biology reports* 39: 2921-35
Gellert P, Ponomareva Y, Braun T, Uchida S. 2013. Noncoder: a web interface for exon array-based detection of long non-coding RNAs. *Nucleic acids research* 41: e20
Good DJ. 2010. Transcriptional Regulation of Sensed Energy Availability Within Hypothalamic Neurons. *The Open Neuroendocrinology Journal* 3: 1-5
Good DJ, Braun T. 2013. NHLH2: at the intersection of obesity and fertility. *Trends in endocrinology and metabolism: TEM* 24: 385-90
Goodsell DS. 2004. The Molecular Perspective: Cytochrome c and Apoptosis. *The Oncologist* 9: 226-27
Gutierrez-Aguilar R, Kim DH, Woods SC, Seeley RJ. 2012. Expression of new loci associated with obesity in diet-induced obese rats: from genetics to physiology. *Obesity* 20: 306-12
Hammond RA, Levine R. 2010. The economic impact of obesity in the United States. *Diabetes, metabolic syndrome and obesity : targets and therapy* 3: 285-95
Heise C, Gardoni F, Culotta L, di Luca M, Verpelli C, Sala C. 2014. Elongation factor-2 phosphorylation in dendrites and the regulation of dendritic mRNA translation in neurons. *Frontiers in cellular neuroscience* 8: 35
Hill JO, Wyatt HR, Peters JC. 2012. Energy balance and obesity. *Circulation* 126: 126-32
Hulsmans M, De Keyzer D, Holvoet P. 2011. MicroRNAs regulating oxidative stress and inflammation in relation to obesity and atherosclerosis. *FASEB journal : official publication of the Federation of American Societies for Experimental Biology* 25: 2515-27
Ihnatko R, Post C, Blomqvist A. 2013. Proteomic profiling of the hypothalamus in a mouse

model of cancer-induced anorexia-cachexia. *British journal of cancer* 109: 1867-75
Inoue N, Yahagi N, Yamamoto T, Ishikawa M, Watanabe K, et al. 2008. Cyclin-dependent kinase inhibitor, p21WAF1/CIP1, is involved in adipocyte differentiation and hypertrophy, linking to obesity, and insulin resistance. *The Journal of biological chemistry* 283: 21220-9
Iyengar BR, Choudhary A, Sarangdhar MA, Venkatesh KV, Gadgil CJ, Pillai B. 2014. Non-coding RNA interact to regulate neuronal development and function. *Frontiers in cellular neuroscience* 8: 47
Jing E, Nillni EA, Sanchez VC, Stuart RC, Good DJ. 2004. Deletion of the Nhlh2 transcription factor decreases the levels of the anorexigenic peptides alpha melanocyte-stimulating hormone and thyrotropin-releasing hormone and implicates prohormone convertases I and II in obesity. *Endocrinology* 145: 1503-13
Johri A, Beal MF. 2012. Mitochondrial dysfunction in neurodegenerative diseases. *The Journal of pharmacology and experimental therapeutics* 342: 619-30
Jordan SD, Kruger M, Willmes DM, Redemann N, Wunderlich FT, et al. 2011. Obesity-induced overexpression of miRNA-143 inhibits insulin-stimulated AKT activation and impairs glucose metabolism. *Nature cell biology* 13: 434-46
Jovanovic Z, Tung YC, Lam BY, O'Rahilly S, Yeo GS. 2010. Identification of the global transcriptomic response of the hypothalamic arcuate nucleus to fasting and leptin. *Journal of neuroendocrinology* 22: 915-25
Kadakkuzha BM, Puthanveettil SV. 2013. Genomics and proteomics in solving brain complexity. *Molecular bioSystems* 9: 1807-21
Kalman S, Garbett K, Vereczkei A, Shelton RC, Korade Z, Mirnics K. 2013. Metabolic stress-induced microRNA and mRNA expression profiles of human fibroblasts. *Experimental cell research*
Khanna A, Muthusamy S, Liang R, Sarojini H, Wang E. 2011. Gain of survival signaling by down-regulation of three key miRNAs in brain of calorie-restricted mice. *Aging* 3: 223-36
Kokoeva MV, Yin H, Flier JS. 2005. Neurogenesis in the hypothalamus of adult mice: potential role in energy balance. *Science* 310: 679-83
Kruger M, Ruschke K, Braun T. 2004. NSCL-1 and NSCL-2 synergistically determine the fate of GnRH-1 neurons and control necdin gene expression. *The EMBO journal* 23: 4353-64
Kuhla B, Kuhla S, Rudolph PE, Albrecht D, Metges CC. 2007. Proteomics analysis of hypothalamic response to energy restriction in dairy cows. *Proteomics* 7: 3602-17
Kumar A, Saini G, Nair A, Sharma R. 2012. UPLC: a preeminent technique in pharmaceutical analysis. *Acta poloniae pharmaceutica* 69: 371-80
Kunej T. 2012. Obesity Gene Atlas in Mammals. *Journal of Genomics*: 45-55
Lauber MA, Koza SM, McCall SA, Alden BA, Iraneta PC, Fountain KJ. 2013. High-resolution peptide mapping separations with MS-friendly mobile phases and charge-surface-modified C18. *Analytical chemistry* 85: 6936-44
Lee J, Duan W, Mattson MP. 2002. Evidence that brain-derived neurotrophic factor is required for basal neurogenesis and mediates, in part, the enhancement of neurogenesis by dietary restriction in the hippocampus of adult mice. *Journal of neurochemistry* 82: 1367-75
Levine TB, Levine AB. 2012. Weight Loss and Diet In *Metabolic Syndrome and Cardiovascular Disease*, pp. 266-302: Blackwell Publishing Ltd.
Liao GY, An JJ, Gharami K, Waterhouse EG, Vanevski F, et al. 2012. Dendritically targeted Bdnf

mRNA is essential for energy balance and response to leptin. *Nature medicine* 18: 564-71
Libert S, Pointer K, Bell EL, Das A, Cohen DE, et al. 2011. SIRT1 activates MAO-A in the brain to mediate anxiety and exploratory drive. *Cell* 147: 1459-72
Lightman SL. 1988. The neuroendocrine paraventricular hypothalamus: receptors, signal transduction, mRNA and neurosecretion. *Journal of Experimental Biology* 139: 31-49
Liu K, Liu Y, Mo W, Qiu R, Wang X, et al. 2011. MiR-124 regulates early neurogenesis in the optic vesicle and forebrain, targeting NeuroD1. *Nucleic acids research* 39: 2869-79
Longo VD, Mattson MP. 2014. Fasting: molecular mechanisms and clinical applications. *Cell metabolism* 19: 181-92
Lopez-Dominguez JA, Khraiwesh H, Gonzalez-Reyes JA, Lopez-Lluch G, Navas P, et al. 2013. Dietary fat modifies mitochondrial and plasma membrane apoptotic signaling in skeletal muscle of calorie-restricted mice. *Age* 35: 2027-44
Lu L, Zhang C, Cai Q, Lu Q, Duan C, et al. 2013. Voltage-dependent anion channel involved in the alpha-synuclein-induced dopaminergic neuron toxicity in rats. *Acta biochimica et biophysica Sinica* 45: 170-8
Maglich JM, Watson J, McMillen PJ, Goodwin B, Willson TM, Moore JT. 2004. The nuclear receptor CAR is a regulator of thyroid hormone metabolism during caloric restriction. *The Journal of biological chemistry* 279: 19832-8
Mainardi M, Pizzorusso T, Maffei M. 2013. Environment, leptin sensitivity, and hypothalamic plasticity. *Neural plasticity* 2013: 438072
Martin B, Mattson MP, Maudsley S. 2006. Caloric restriction and intermittent fasting: two potential diets for successful brain aging. *Ageing research reviews* 5: 332-53
Martinelli R, Nardelli C, Pilone V, Buonomo T, Liguori R, et al. 2010. miR-519d overexpression is associated with human obesity. *Obesity (Silver Spring)* 18: 2170-6
Mattison JA, Lane MA, Roth GS, Ingram DK. 2003. Calorie restriction in rhesus monkeys. *Experimental gerontology* 38: 35-46
Mattson MP. 2005. Energy intake, meal frequency, and health: a neurobiological perspective. *Annual review of nutrition* 25: 237-60
Mattson MP, Chan SL, Duan W. 2002. Modification of brain aging and neurodegenerative disorders by genes, diet, and behavior. *Physiological reviews* 82: 637-72
Mattson MP, Magnus T. 2006. Ageing and neuronal vulnerability. *Nature reviews. Neuroscience* 7: 278-94
Mattson MP, Wan R. 2005. Beneficial effects of intermittent fasting and caloric restriction on the cardiovascular and cerebrovascular systems. *The Journal of nutritional biochemistry* 16: 129-37
McCay CM, Crowell MF, Maynard LA. 1989. The effect of retarded growth upon the length of life span and upon the ultimate body size. 1935. *Nutrition* 5: 155-71; discussion 72
McClintick JN, Xuei X, Tischfield JA, Goate A, Foroud T, et al. 2013. Stress-response pathways are altered in the hippocampus of chronic alcoholics. *Alcohol* 47: 505-15
McNay DE, Briancon N, Kokoeva MV, Maratos-Flier E, Flier JS. 2012. Remodeling of the arcuate nucleus energy-balance circuit is inhibited in obese mice. *The Journal of clinical investigation* 122: 142-52
McNeill E, Van Vactor D. 2012. MicroRNAs shape the neuronal landscape. *Neuron* 75: 363-79
Meister B, Herzer S, Silahtaroglu A. 2013. MicroRNAs in the Hypothalamus. *Neuroendocrinology*
Mergenthaler P, Lindauer U, Dienel GA, Meisel A. 2013. Sugar for the brain: the role of glucose

in physiological and pathological brain function. *Trends in neurosciences* 36: 587-97
Moraes JC, Coope A, Morari J, Cintra DE, Roman EA, et al. 2009. High-fat diet induces apoptosis of hypothalamic neurons. *PloS one* 4: e5045
Morton GJ, Cummings DE, Baskin DG, Barsh GS, Schwartz MW. 2006. Central nervous system control of food intake and body weight. *Nature* 443: 289-95
Nagino K, Nomura O, Takii Y, Myomoto A, Ichikawa M, et al. 2006. Ultrasensitive DNA chip: gene expression profile analysis without RNA amplification. *Journal of biochemistry* 139: 697-703
Nakatsuka A, Wada J, Hida K, Hida A, Eguchi J, et al. 2012. RXR antagonism induces G0 /G1 cell cycle arrest and ameliorates obesity by up-regulating the p53-p21(Cip1) pathway in adipocytes. *The Journal of pathology* 226: 784-95
Naranmandura H, Chen X, Tanaka M, Wang WW, Rehman K, et al. 2012. Release of apoptotic cytochrome C from mitochondria by dimethylarsinous acid occurs through interaction with voltage-dependent anion channel in vitro. *Toxicological sciences : an official journal of the Society of Toxicology* 128: 137-46
Neilson KA, Ali NA, Muralidharan S, Mirzaei M, Mariani M, et al. 2011. Less label, more free: approaches in label-free quantitative mass spectrometry. *Proteomics* 11: 535-53
Nogales-Cadenas R, Carmona-Saez P, Vazquez M, Vicente C, Yang X, et al. 2009. GeneCodis: interpreting gene lists through enrichment analysis and integration of diverse biological information. *Nucleic acids research* 37: W317-22
Numakawa T, Richards M, Adachi N, Kishi S, Kunugi H, Hashido K. 2011. MicroRNA function and neurotrophin BDNF. *Neurochemistry international* 59: 551-8
Olsen L, Klausen M, Helboe L, Nielsen FC, Werge T. 2009. MicroRNAs show mutually exclusive expression patterns in the brain of adult male rats. *PloS one* 4: e7225
Pechnick RN, Zonis S, Wawrowsky K, Cosgayon R, Farrokhi C, et al. 2011. Antidepressants stimulate hippocampal neurogenesis by inhibiting p21 expression in the subgranular zone of the hipppocampus. *PloS one* 6: e27290
Pechnick RN, Zonis S, Wawrowsky K, Pourmorady J, Chesnokova V. 2008. p21Cip1 restricts neuronal proliferation in the subgranular zone of the dentate gyrus of the hippocampus. *Proceedings of the National Academy of Sciences of the United States of America* 105: 1358-63
Poplawski MM, Mastaitis JW, Yang XJ, Mobbs CV. 2010. Hypothalamic responses to fasting indicate metabolic reprogramming away from glycolysis toward lipid oxidation. *Endocrinology* 151: 5206-17
Qureshi IA, Mattick JS, Mehler MF. 2010. Long non-coding RNAs in nervous system function and disease. *Brain research* 1338: 20-35
Qureshi IA, Mehler MF. 2013. Long non-coding RNAs: novel targets for nervous system disease diagnosis and therapy. *Neurotherapeutics : the journal of the American Society for Experimental NeuroTherapeutics* 10: 632-46
Rao P, Benito E, Fischer A. 2013. MicroRNAs as biomarkers for CNS disease. *Frontiers in molecular neuroscience* 6: 39
Ronnett GV, Kleman AM, Kim E-K, Landree LE, Tu Y. 2006. Fatty Acid Metabolism, the Central Nervous System, and Feeding. *Obesity* 14: 201S-07S
Roshan R, Ghosh T, Scaria V, Pillai B. 2009. MicroRNAs: novel therapeutic targets in neurodegenerative diseases. *Drug discovery today* 14: 1123-9
Rossignol DA, Frye RE. 2012. Mitochondrial dysfunction in autism spectrum disorders: a

systematic review and meta-analysis. *Molecular psychiatry* 17: 290-314
Salamone JD, Correa M. 2013. Dopamine and food addiction: lexicon badly needed. *Biological psychiatry* 73: e15-24
Sangiao-Alvarellos S, Pena-Bello L, Manfredi-Lozano M, Tena-Sempere M, Cordido F. 2014. Perturbation of hypothalamic microRNA expression patterns in male rats following metabolic distress: Impact of obesity and conditions of negative energy balance. *Endocrinology*: en20131770
Sarkar P, Sarkar S, Ramesh V, Kim H, Barnes S, et al. 2008. Proteomic analysis of mouse hypothalamus under simulated microgravity. *Neurochemical research* 33: 2335-41
Sato F, Tsuchiya S, Terasawa K, Tsujimoto G. 2009. Intra-platform repeatability and inter-platform comparability of microRNA microarray technology. *PloS one* 4: e5540
Schneeberger M, Altirriba J, Garcia A, Esteban Y, Castano C, et al. 2012. Deletion of miRNA processing enzyme Dicer in POMC-expressing cells leads to pituitary dysfunction, neurodegeneration and development of obesity. *Molecular metabolism* 2: 74-85
Schouten M, Aschrafi A, Bielefeld P, Doxakis E, Fitzsimons CP. 2013. microRNAs and the regulation of neuronal plasticity under stress conditions. *Neuroscience* 241: 188-205
Schulze WX, Usadel B. 2010. Quantitation in mass-spectrometry-based proteomics. *Annual review of plant biology* 61: 491-516
Silva JC, Gorenstein MV, Li GZ, Vissers JP, Geromanos SJ. 2006. Absolute quantification of proteins by LCMSE: a virtue of parallel MS acquisition. *Molecular & cellular proteomics : MCP* 5: 144-56
Sohal RS, Weindruch R. 1996. Oxidative stress, caloric restriction, and aging. *Science* 273: 59-63
Speakman JR, Mitchell SE. 2011. Caloric restriction. *Molecular aspects of medicine* 32: 159-221
Stelzhammer V, Amess B, Martins-de-Souza D, Levin Y, Ozanne SE, et al. 2012. Analysis of the rat hypothalamus proteome by data-independent label-free LC-MS/MS. *Proteomics* 12: 3386-92
Stoppa GR, Cesquini M, Roman EA, Prada PO, Torsoni AS, et al. 2008. Intracerebroventricular injection of citrate inhibits hypothalamic AMPK and modulates feeding behavior and peripheral insulin signaling. *Journal of Endocrinology* 198: 157-68
Sun L, Xie H, Mori MA, Alexander R, Yuan B, et al. 2011. Mir193b-365 is essential for brown fat differentiation. *Nature cell biology* 13: 958-65
Sun LY, Spong A, Swindell WR, Fang Y, Hill C, et al. 2013. Growth hormone-releasing hormone disruption extends lifespan and regulates response to caloric restriction in mice. *eLife* 2: e01098
Swindell WR. 2008. Comparative analysis of microarray data identifies common responses to caloric restriction among mouse tissues. *Mechanisms of ageing and development* 129: 138-53
Szklarczyk K, Korostynski M, Golda S, Solecki W, Przewlocki R. 2012. Genotype-dependent consequences of traumatic stress in four inbred mouse strains. *Genes, brain, and behavior*
Tabas-Madrid D, Nogales-Cadenas R, Pascual-Montano A. 2012. GeneCodis3: a non-redundant and modular enrichment analysis tool for functional genomics. *Nucleic acids research* 40: W478-83
Takanabe R, Ono K, Abe Y, Takaya T, Horie T, et al. 2008. Up-regulated expression of microRNA-143 in association with obesity in adipose tissue of mice fed high-fat diet.

Biochemical and biophysical research communications 376: 728-32
Taraslia VK, Kouskoukis A, Anagnostopoulos AK, Stravopodis DJ, Margaritis LH, Tsangaris GT. 2013. Proteomic analysis of normal murine brain parts. *Cancer genomics & proteomics* 10: 125-54
Thorleifsson G, Walters GB, Gudbjartsson DF, Steinthorsdottir V, Sulem P, et al. 2009. Genome-wide association yields new sequence variants at seven loci that associate with measures of obesity. *Nature genetics* 41: 18-24
Tinkum KL, White LS, Marpegan L, Herzog E, Piwnica-Worms D, Piwnica-Worms H. 2013. Forkhead box O1 (FOXO1) protein, but not p53, contributes to robust induction of p21 expression in fasted mice. *The Journal of biological chemistry* 288: 27999-8008
Tojo S, Satomura T, Matsuoka H, Hirooka K, Fujita Y. 2011. Catabolite repression of the Bacillus subtilis FadR regulon, which is involved in fatty acid catabolism. *Journal of bacteriology* 193: 2388-95
Tzotzas T, Desrumaux C, Lagrost L. 2009. Plasma phospholipid transfer protein (PLTP): review of an emerging cardiometabolic risk factor. *Obesity reviews : an official journal of the International Association for the Study of Obesity* 10: 403-11
Urbanski HF, Mattison JA, Roth GS, Ingram DK. 2013. Dehydroepiandrosterone sulfate (DHEAS) as an endocrine marker of aging in calorie restriction studies. *Experimental gerontology* 48: 1136-9
Varady KA, Hellerstein MK. 2007. Alternate-day fasting and chronic disease prevention: a review of human and animal trials. *The American journal of clinical nutrition* 86: 7-13
Vella KR, Burnside AS, Brennan KM, Good DJ. 2007. Expression of the hypothalamic transcription factor Nhlh2 is dependent on energy availability. *Journal of neuroendocrinology* 19: 499-510
Vogel C, Marcotte EM. 2012. Insights into the regulation of protein abundance from proteomic and transcriptomic analyses. *Nature reviews. Genetics* 13: 227-32
Vreugdenhil E, Berezikov E. 2010. Fine-tuning the brain: MicroRNAs. *Frontiers in neuroendocrinology* 31: 128-33
Wang QM, Yang H, Tian DR, Cai Y, Wei ZN, et al. 2011. Proteomic analysis of rat hypothalamus revealed the role of ubiquitin-proteasome system in the genesis of DR or DIO. *Neurochemical research* 36: 939-46
Wankhade UD, Good DJ. 2011. Melanocortin 4 receptor is a transcriptional target of nescient helix-loop-helix-2. *Molecular and cellular endocrinology* 341: 39-47
Weindruch R, Sohal RS. 1997. Seminars in medicine of the Beth Israel Deaconess Medical Center. Caloric intake and aging. *The New England journal of medicine* 337: 986-94
Witte ME, Mahad DJ, Lassmann H, van Horssen J. 2014. Mitochondrial dysfunction contributes to neurodegeneration in multiple sclerosis. *Trends in molecular medicine* 20: 179-87
Woods SC, D'Alessio DA. 2008. Central control of body weight and appetite. *The Journal of clinical endocrinology and metabolism* 93: S37-50
Wulczyn FG, Smirnova L, Rybak A, Brandt C, Kwidzinski E, et al. 2007. Post-transcriptional regulation of the let-7 microRNA during neural cell specification. *FASEB journal : official publication of the Federation of American Societies for Experimental Biology* 21: 415-26
Xie H, Lim B, Lodish HF. 2009. MicroRNAs induced during adipogenesis that accelerate fat cell development are downregulated in obesity. *Diabetes* 58: 1050-7
Yang XJ, Kow LM, Pfaff DW, Mobbs CV. 2004. Metabolic pathways that mediate inhibition of

hypothalamic neurons by glucose. *Diabetes* 53: 67-73
Yeo GS, Heisler LK. 2012. Unraveling the brain regulation of appetite: lessons from genetics. *Nature neuroscience* 15: 1343-9
Yu JY, Chung KH, Deo M, Thompson RC, Turner DL. 2008. MicroRNA miR-124 regulates neurite outgrowth during neuronal differentiation. *Experimental cell research* 314: 2618-33
Zhang X, Petruzziello F, Zani F, Fouillen L, Andren PE, et al. 2012. High identification rates of endogenous neuropeptides from mouse brain. *Journal of proteome research* 11: 2819-27
Zhu H, Shyh-Chang N, Segre AV, Shinoda G, Shah SP, et al. 2011. The Lin28/let-7 axis regulates glucose metabolism. *Cell* 147: 81-94
Zonis S, Ljubimov VA, Mahgerefteh M, Pechnick RN, Wawrowsky K, Chesnokova V. 2013. p21Cip restrains hippocampal neurogenesis and protects neuronal progenitors from apoptosis during acute systemic inflammation. *Hippocampus* 23: 1383-94

2. Figure Legends:

Figure 1. Hypothalamic long non-coding RNA analysis. A: log2 Scatter plot of hypothalamus lncRNA data from Affymetrix exon array. B: RT-QPCR analysis of selected lncRNAs. N=3-4 for each group, all lncRNA are reported as relative to levels in *ad lib* fed animals, and normalized to Beta-actin. * $P \leq 0.05$ between Ad lib and fasting mice; # $P \leq 0.05$ between fasting and leptin-treatment mice.

Figure 2. RT-QPCR analysis of p21/Cdkn1a. A. Hypothalamic tissue: N=4-6 C57 Bl/6 mice for each group. Expression levels are reported relative to levels in ad lib fed animals, and normalized to the Beta-actin. B. N29/2 Hypothalamic cell line: N=6 wells of N29/2 hypothalamic neuronal cells for each group. Expression levels are reported relative to levels in normal media, and normalized to the Beta-actin. * $P \leq 0.05$ between *ad lib* fed (normal media) and fasting (serum deprived) samples; # $P \leq 0.05$ between serum deprived and leptin treatment samples.

Figure 3. Hypothetical model of fasting induced p21 expression and its function in the hypothalamus. p21 expression in the hypothalamus is regulated by either (1) cellular stress response to dietary restriction, or (2) the downstream genes that response to the dietary restriction or cellular stress response. The induced p21 expression if then (3) arrests neuronal cell cycle and restricts neurogenesis, or (4) protects neuronal apoptosis from stress. [Modified from Mattson M. P. (Mattson & Magnus 2006)].

Figure 4. Hypothetical model of Nhlh2 regulation of mitochondrial metabolisms in the hypothalamus (1. Gpd2, 2. Etfa, 3. Idh3b & Idh3g, 4. Ogdh, 5. Sucal2, 6. Mdh1, 7.Cyc1, 8. Cycs, 9. Atp5a1, Atp5c1, Atp5o, 10. Vdac3). [Modified from Rossignol D.A. (Rossignol & Frye 2012)].

Figure 1. Hypothalamic long non-coding RNA analysis.
A.

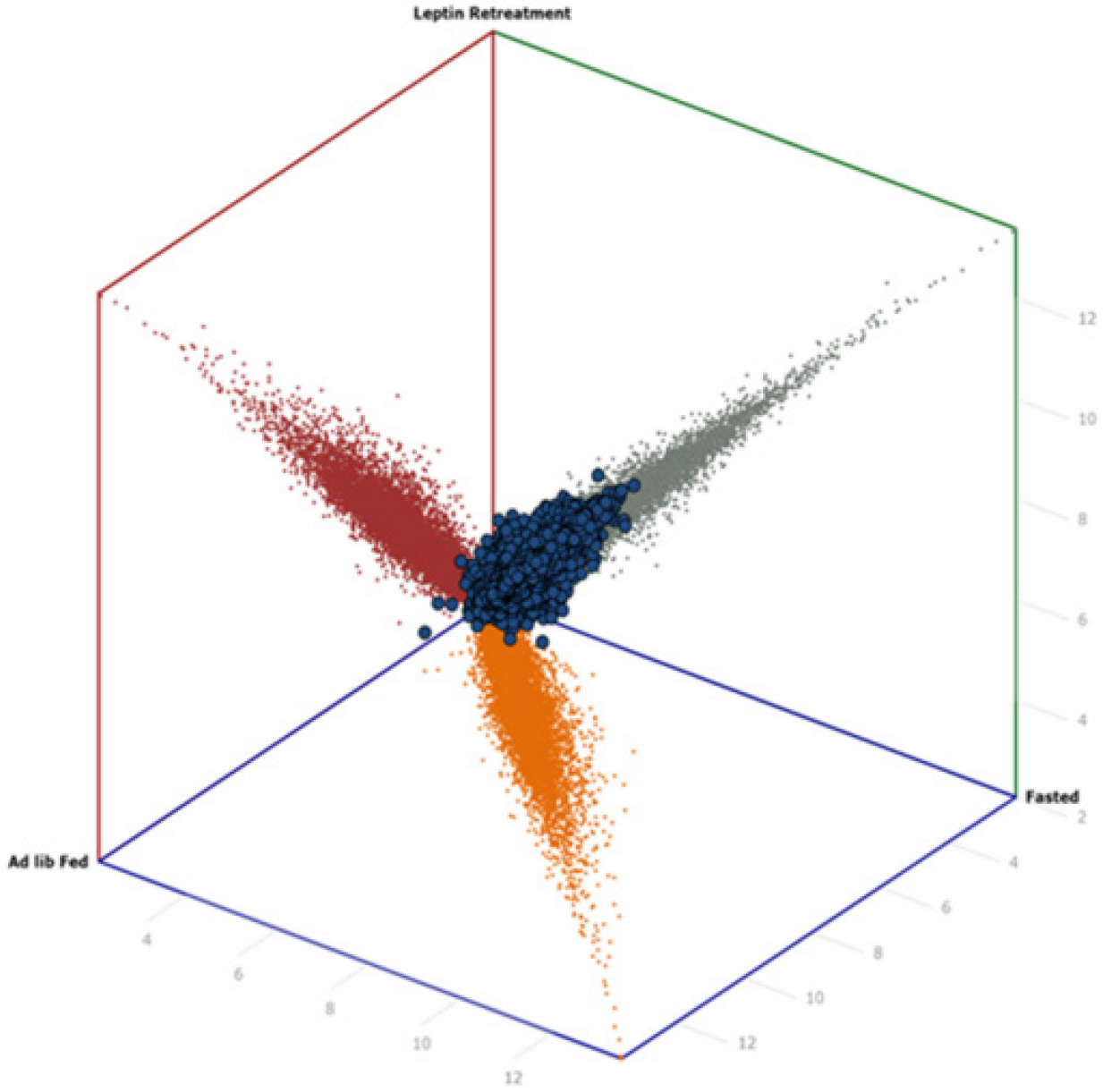

Figure 1. Hypothalamic long non-coding RNA analysis (Con.).
B.

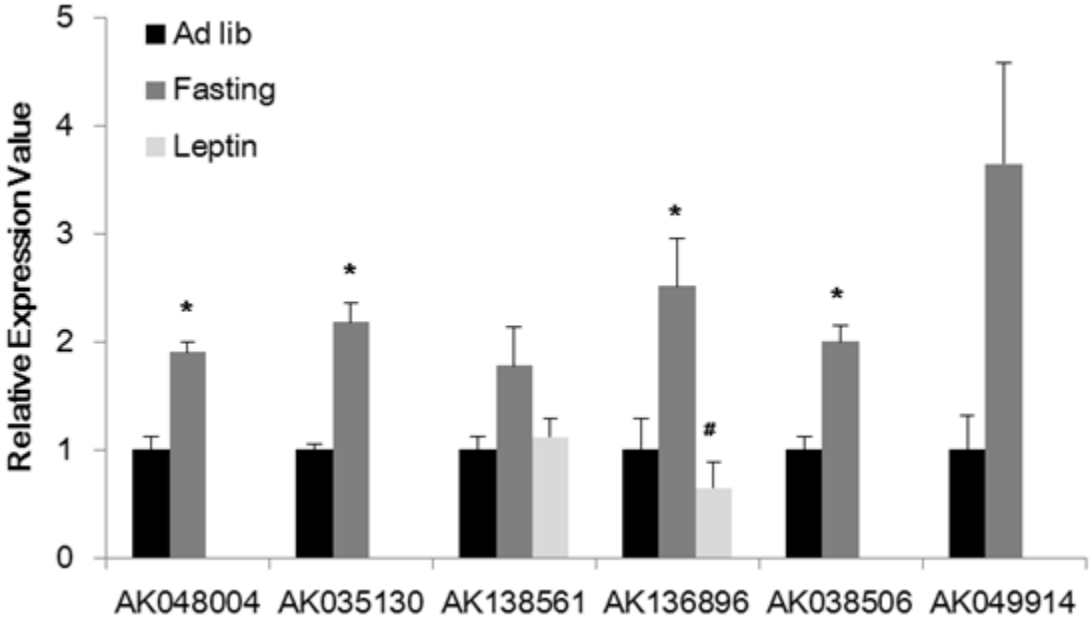

Figure 2. RT-QPCR analysis of p21/Cdkn1a.
A.

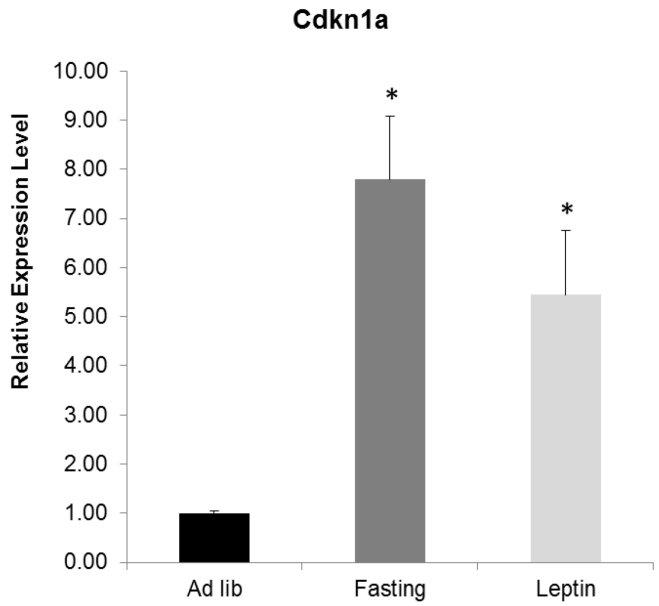

B.

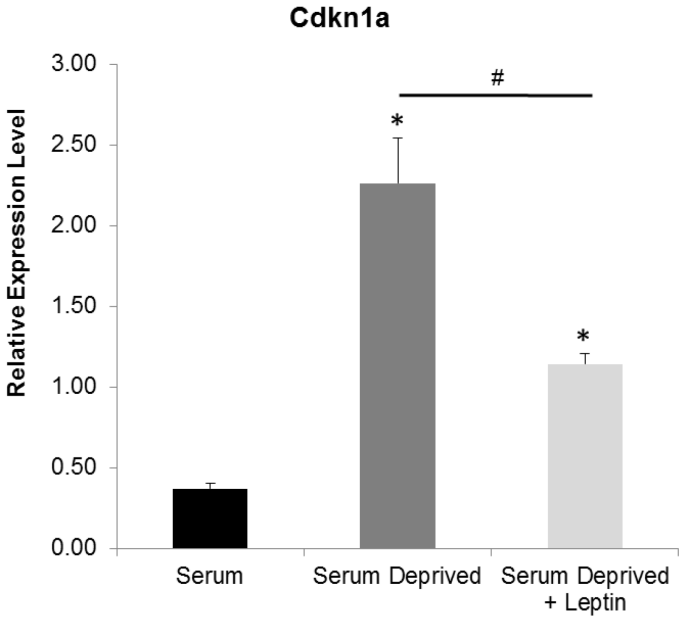

Figure 3. Hypothetical model of fasting induced p21 expression and its function in the hypothalamus.

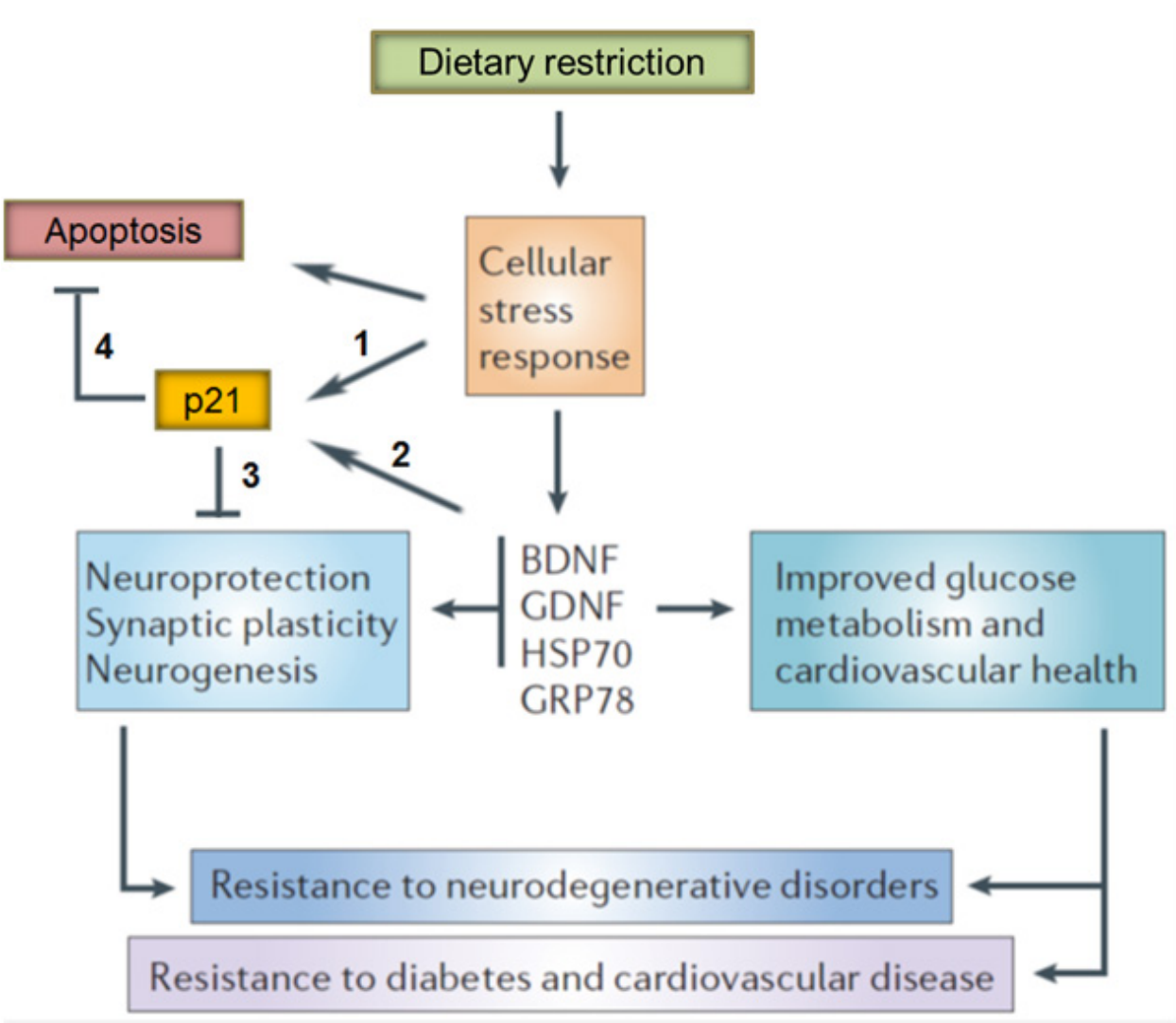

Figure 4. Hypothetical model of Nhlh2 regulation of mitochondrial metabolisms in the hypothalamus.